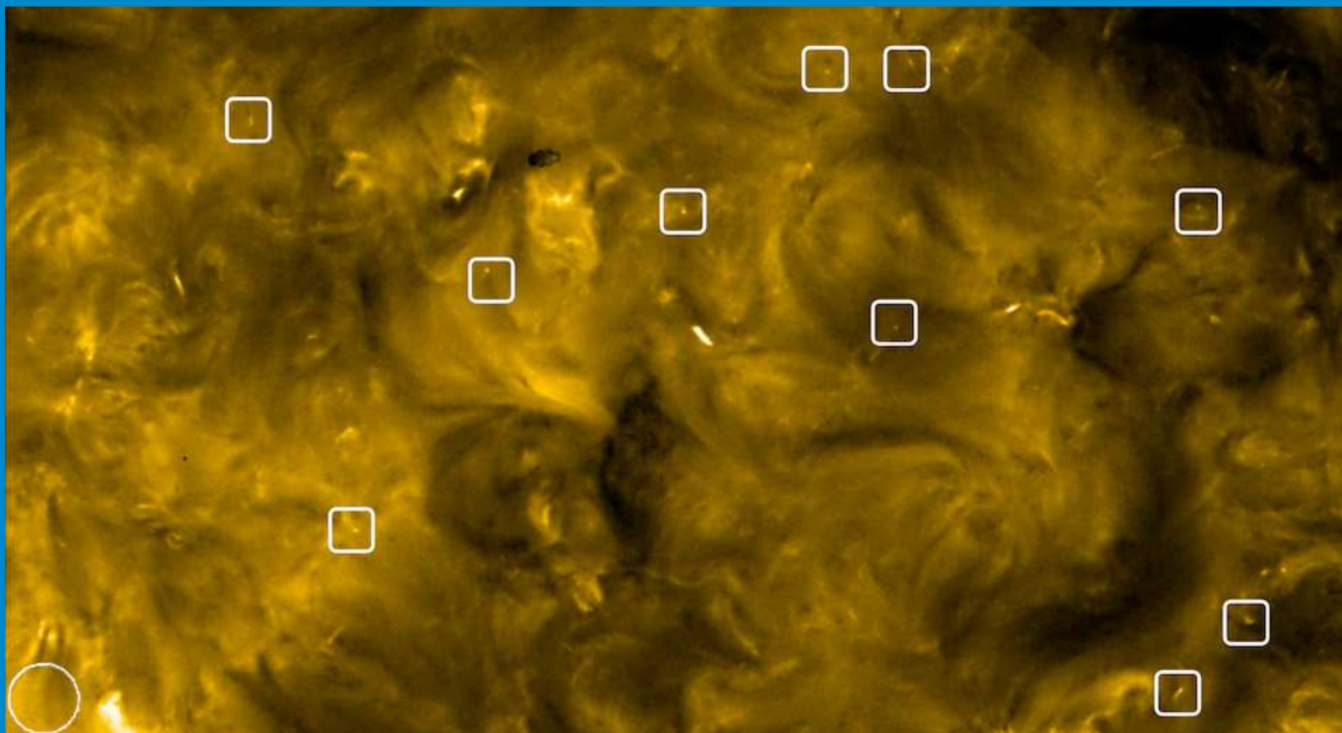

Rapport annuel
Jaarverslag
Annual Report

2020

Observatoire royal de Belgique

Koninklijke Sterrenwacht van België

Royal Observatory of Belgium

ORB - KSB

Cover illustration: Image from the High Resolution EUV Imager of EUI taken on May 30, 2020. The squares indicate examples of little campfires. The circle bottom left illustrates the size of the Earth for comparison. Credit: ESA/Solar Orbiter/EUI Team: CSL, IAS, MPS, PMOD/WRC, ROB, UCL/MSSL.

Foreword

Dear readers,

I am happy to present you with the annual summary report of the Royal Observatory of Belgium (ORB-KSB). As in the previous years, we have decided to only present the highlights of our scientific activities and public services, rather than providing a full, detailed and lengthy overview of all of our work during the year. We hope to provide you, in doing so, with a report that is more interesting to read and gives a taste of life at the ORB-KSB. If you need more or other information on ORB-KSB and/or its activities, contact rob_info@oma.be or visit our website http://www.observatory.be.

A list of publications and staff statistics are included at the end. To also suit our international readers & collaborators and to give it an as wide visibility as possible, the report is written in English.

Ronald Van der Linden

Director General

Table of Contents

Life at the Royal Observatory of Belgium

COVID-19

On March 11, 2020, the World Health Organization declared the COVID-19 crisis as a pandemic. To control it, the Belgian government issued since March 12, 2020, global restrictions impacting Belgian cultural and economic activity and its citizens' life. ORB-KSB and its Planetarium were also impacted by those restrictions. From this date onwards, with periods during which restrictions were eased or reinforced, the majority of ORB-KSB's personnel were advised or mandated to work remotely partially or full time if the nature of their function allowed it. The IT infrastructure and administrative procedures were quickly adapted so that all of the staff could perform their work, research and administrative tasks remotely.

Lockdown periods had prevented scientists from performing activities such as field measurements, astronomical observations on-site, and scientific meetings, in Belgium and abroad. While some conferences and observation missions were later converted into online and remote versions, field measurements became impossible, particularly during the strictest lockdown periods. As a result, a significant number of scientific and field missions were cancelled and postponed in 2020.

Despite those disturbances, the staff quickly adapted to the new ways of working and doing scientific research. All the service activities of ORB-KSB regarding time keeping, seismic and GNSS network monitoring, continuous gravimetric measurements, solar observations, space weather forecasts and PECASUS and astronomical information were maintained to a very high degree.

Planet Mars: First Results of the InSight Mission Published in Nature Geoscience

On February 24, 2020, the journal Nature Geoscience published a series of articles that present results of the NASA InSight (**In**terior exploration using **S**eismic **I**nvestigations, **G**eodesy and **H**eat **T**ransport) mission to Mars, obtained after ten months of observation on the Red Planet. InSight is the first mission dedicated to the study of the deep interior of Mars and is active since November 26, 2018. Scientists from ORB-KSB are implied in the InSight mission. Véronique Dehant from ORB-KSB is CoI (co-investigator) of RISE, a radioscience instrument onboard InSight. Scientists of ORB-KSB are also involved in the analysis of data from the seismometer SEIS and the weather station APSS.

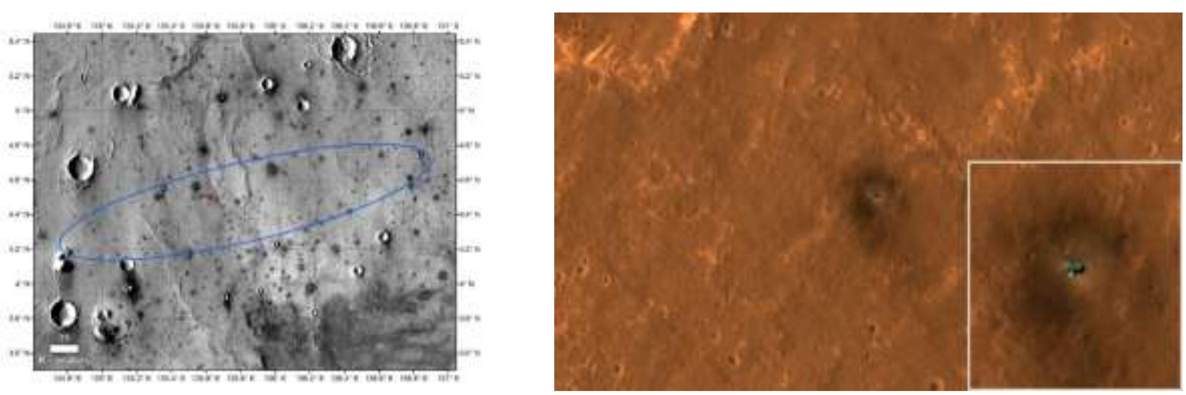

Figure 1: Left: InSight's landing site (red dot) and the ellipse circumscribing its landing zone (in blue). Right: View of the InSight landing site taken by NASA's HiRISE camera on September 23, 2019. Credit: NASA/JPL-Caltech/University of Arizona.

One of their major contributions is the localisation of the landing site. From day one until the end of December 2018, Sébastien Le Maistre of ORB-KSB, with William Folkner of the Jet Propulsion Laboratory, used RISE data to determine the geographical position of the lander. Thanks to their work, the NASA space probe HiRISE (**Hi**gh **R**esolution **I**maging **S**cience **E**xperiment) on NASA Mars Reconnaissance Orbiter was able to photograph the landing site. The precise localisation of the landing site is a prerequisite for the continuation of the mission, particularly for studying the surrounding geological features.

Bart Van Hove and Özgür Karatekin from ORB-KSB reconstructed the landing path of InSight. From this, they deduced the atmospheric temperature profile as a function of altitude, an important aspect for the study of the Martian atmosphere and for the construction of meteorological and climatic models of the Red Planet.

Finally, they were able to locate three of the 174 'Marsquakes'. This would not have been possible without the advanced scientific models of the Red Planet interior provided by a team of researchers which includes Attilio Rivoldini of ORB-KSB. Véronique Dehant also participated in the interpretation of the recorded seismic data.

References:

Golombek et al. (including S. Le Maistre), Geology of the InSight Landing Site on Mars (open access), Nature Communications 11, 1014 (2020). https://doi.org/10.1038/s41467-020-14679-1

Banerdt et al. (including V. Dehant), Initial results from the InSight mission on Mars, Nature Geoscience (2020). https://doi.org/10.1038/s41561-020-0544-y

Banfield et al. (including Ö. Karatekin and B. Van Hove), The Atmosphere of Mars as Observed by InSight, Nature Geoscience (2020). https://doi.org/10.1038/s41561-020-0534-0

Giardini et al. (including A. Rivoldini), The Seismicity of Mars, Nature Geoscience (2020). https://doi.org/10.1038/s41561-020-0539-8

25 Years of Continuous Measurements of Gravity in Membach

Figure 2: The superconducting gravimeter is located at the end of a 132 m – long gallery, 48 metres underneath the surface, in Membach (city of Baelen, eastern Belgium). The instrument sensor is immersed in liquid helium in which the temperature is held at -269°, in other words, 4 degrees above absolute zero, allowing superconductivity. Photo credit: E. Coveliers & B. Frederick. Copy authorised with mention of the source

On August 4, 2020, the superconducting (or cryogenic) gravimeter has been measuring for 25 years the variations of gravity with the precision of one hundredth of a billionth (10^{-11}) of g (g = 9.81 m/s²).

Since September 18, 2017, this instrument holds a double world record, in gravimetry and physics:

1. Record of the cryogenic gravimeter that has operated the longest at a given location;
2. It is also, as far as we know, the longest levitation of a superconducting artefact in a magnetic field. This field is generated by persistent currents, which were injected in 1995 into superconducting coils, where they circulate since then without any resistance and therefore, without ever having been dissipated. Although this record does not contradict what physicists specialising in persistent currents expect – in theory, a superconducting current can flow forever – , it is at least worthy of a place in a 'cabinet of curiosities'.

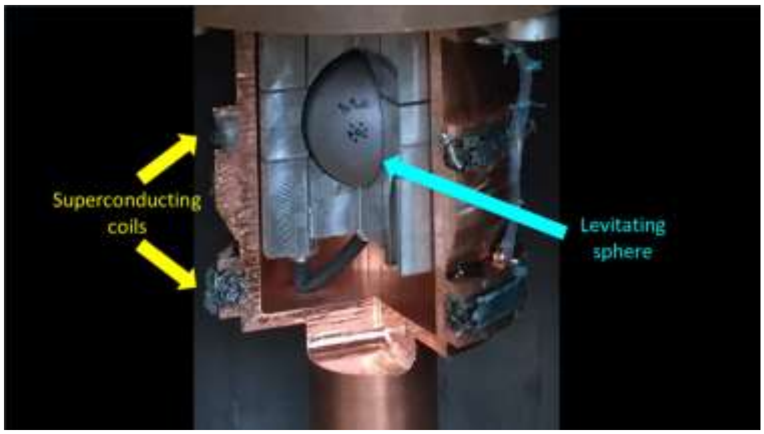

Figure 3: Exploded view of the sensor of a superconducting gravimeter: the 4-gram hollow sphere levitates in a magnetic field generated by currents flowing through the pair of coils. Photo of the sensor from the old instrument of Uccle.

In the field of geophysical research at ORB-KSB, these measurements are important, among other things because they provide insight in long-term variations in gravity, still poorly understood, caused by slow tectonic movements or climatic variations. It is also important for the study of the water cycle, whose varying masses influence gravity.

To date, this gravimeter participates in many research projects and ORB-KSB hopes to be able to perform this type of measurement for many years to come.

Prizes, Awards and Grants

'*Media of the Month*' Award: the ISS Passing Before the Sun

On Saturday, June 6, 2020, at 14:02:16 UTC, the solar telescopes located on the Uccle site (USET, Uccle Solar Equatorial Table), caught a transit of the International Space Station (ISS). ISS is the largest artificial object in space and it flies at low Earth orbit (~400 km), making it visible to the naked eye from Earth.

On the attached image, the ISS appears as three successive black structures taken at around 250 milliseconds interval each. The striking feature of the ISS, its large solar panels, is nicely resolved with the white-light telescope at ROB. As the ISS moves fast (~8 km/s), the total transit duration is very short, being only a fraction of a second (0.8 second for this event); hence it needs a fast recording camera to be caught.

One of the prime goals of USET is to monitor the solar activity by the observation of groups of dark spots covering the solar surface. A nice illustration of such sunspots can be seen on the left side of the solar disk. While being of medium size, this group is very interesting as it is among the first ones of the new solar cycle.

This image won the 'Media of the Month' contest of the European Solar Physics Division in December 2020.

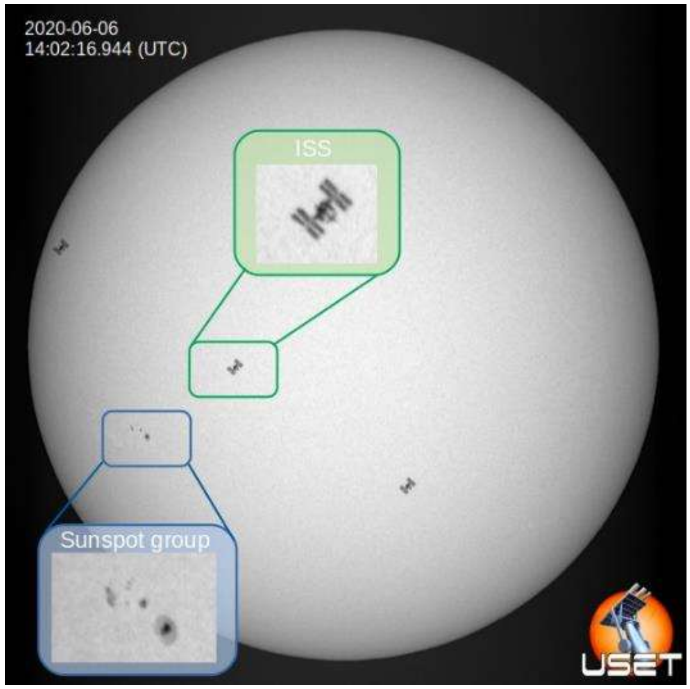

Véronique Dehant, Winner of an FNRS Quinquennial Prize

On 14 September 2020, the Fonds de la Recherche Scientifique (FNRS) awarded Véronique Dehant, researcher at the ORB-KSB, the Dr De Leeuw-Damry-Bourlart Prize in Fundamental Exact Sciences, one of the FNRS Quinquennial Prizes. These prizes reward researchers from the Wallonia-Brussels Federation.

Due to COVID-19 restrictions, the award ceremony for those laureates is postponed to 2021.

Link: https://www.frs-fnrs.be/fr/l-actualite-fnrs/1243-le-fnrs-recompense-l-excellence-de-la-recherche-et-decerne-ses-5-prix-quinquennaux-2020

Space Missions

The Extreme Ultraviolet Imager (EUI) is off to Space onboard Solar Orbiter

On February 10, 2020, the Solar Orbiter satellite was launched on an Atlas V rocket from Cape Canaveral in Florida. Solar Orbiter's mission is to take the closest ever images of the Sun, to observe the solar wind and the Sun's polar regions and to unravel the mysteries of the solar cycle. The Solar Orbiter mission is led by ESA, but has a strong participation from NASA.

Figure 4: Several EUI key consortium members pointing to what they have been working on for nearly a decade.

One of the main instruments onboard is the Extreme Ultraviolet Imager (EUI), developed by an international consortium led by the 'Centre Spatial de Liège' and including ORB-KSB. Both institutes have a longstanding collaboration in the development of solar imagers, including EIT on the SOHO satellite and SWAP on the PROBA2 satellite. EUI consists of three telescopes, a Full Sun Imager and two High Resolution Imagers that are optimised to image in the Lyman-α spectral line and in EUV. The three telescopes will provide coverage from the solar chromosphere up to the corona. EUI is designed to cope with the strong constraints imposed by the Solar Orbiter mission characteristics. Limited telemetry availability is, for example, compensated by state-of-the-art image compression, on board image processing and event selection.

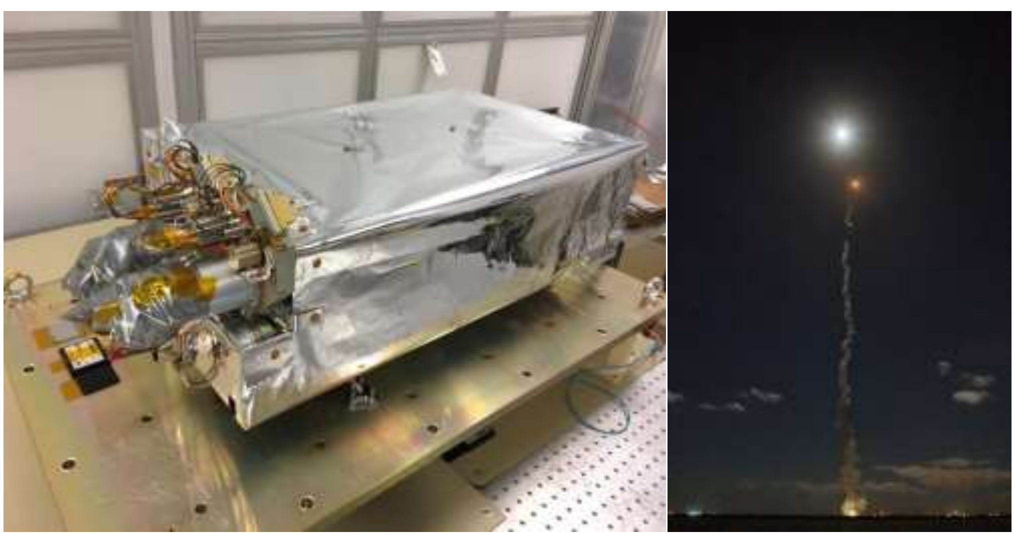

Figure 5: The EUI flight model before integration in the spacecraft (left) and launch of Solar Orbiter towards the Sun (right; Image Courtesy: Emil Kraaikamp).

Solar Orbiter's science mission (nominal and extended phase) is expected to last a decade. By making several Venus flybys in the coming years, the Solar Orbiter spacecraft will use the gravity of the planet to approach the Sun. The EUI high-resolution telescopes are designed for a state-of-the-art spatial resolution but by approaching the Sun, another factor 4 in sharpness will be achieved: it will be possible to study details of only a few hundred kilometres in the solar atmosphere.

Later on, the gravity of Venus will be used to tilt the satellite's orbit and to enable EUI to take images from a polar perspective, something that has never been done before (see Figure 6). Studying the solar poles is of great scientific importance for understanding the Sun's magnetism and the solar activity cycle. The solar cycle lasts about 11 years and takes us from a 'low solar season' with few solar storms to a 'high solar season' with more frequent solar storms. Technology on Earth can be seriously disrupted by these solar storms, which are studied in the context of 'space weather'. By visualising the poles and magnetic forces, the EUI instrument will contribute to unravelling the secrets of the solar cycle.

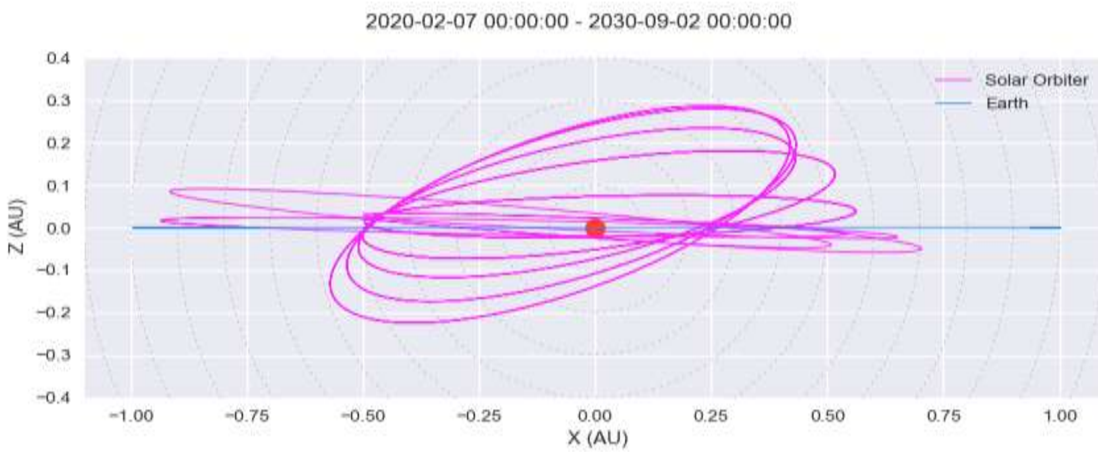

Figure 6: View of the Solar Orbiter trajectory in the X-Z plane close to the end of the extended mission timeframe, by then Solar Orbiter will have an unprecedented view on the Sun with an inclination of 33°.

Solar Orbiter carries ten scientific instruments. After launch, the instrument teams prepared to test their instruments, but suddenly there was the outbreak of the COVID-19 pandemic. Access to the control room in Darmstadt, Germany, had to be restricted and all testing of the instruments was interrupted. But after one week, it was decided to restart operation, with a minimal staff and in a fully COVID-19 proof way. The rest of the commissioning work was performed from people's homes by non-stop teleconferences. Commands to operate EUI were given from living rooms, home offices, bedrooms… Nobody would have dared to plan the commissioning with the instrument experts spread over several continents. Nevertheless, an unexpected advantage was that everybody was only a mouse click away and always immediately available.

Figure 7: The last physical meeting of the Solar Orbiter instrument teams, days before the launch and the start of the Covid19 pandemic.

The test phase ended successfully on June 25, 2020, during an official online 'Mission Commissioning Results Review' meeting with more than 50 participants. The EUI team could look back on a very intense but efficient test period. The EUI instrument was officially cleared for scientific operations.

Hera: the Royal Observatory of Belgium and EMXYS Receive Go for Participation in the Planetary Defence Space Mission

Figure 8: ESA's Hera Mission to the Didymos binary asteroid system will carry two CubeSats: Juventas (the satellite right below) and Milani (the satellite on the top). The GRASS gravimeter of the Observatory and EMXYS will be onboard Juventas.

The Royal Observatory of Belgium (ORB-KSB) and EMXYS (Spain) were selected by the European Space Agency (ESA) to provide a gravimeter for the Juventas spacecraft that will land on asteroid Dimorphos as part of the ESA's planetary defence programme.

They will provide the GRASS instrument (shortcut for **GRA**vimeter for **S**olar system **S**mall bodies) that will make measurements on the gravity field of the asteroid Dimorphos. The gravimeter is part of the Juventas CubeSat, manufactured by GomSpace Luxemburg, that will land on the asteroid in 2027 after travelling onboard the ESA's Hera spacecraft to its vicinity. GRASS will be the first gravimeter ever on an asteroid. Ozgur Karatekin from ORB-KSB is Principal Investigator of the Juventas CubeSat and of the GRASS instrument.

The gravimeter is an instrument proposed, designed and developed by ORB-KSB in cooperation with EMXYS, which will provide the final space version of the instrument for the mission. The gravimeter is expected to send to Earth precious data on the mass distribution, internal structure and dynamics of Dimorphos. This information will improve the knowledge for setting up future diversion strategies on asteroids that may pose a threat of colliding with Earth.

Hera will be the first mission to perform a detailed characterisation of a binary asteroid system. GRASS will monitor surface accelerations to reveal the subsurface structure and to better constrain the spin-orbit dynamics of the binary system. The gravitational forces on such a small body, likely composed of loosely held-together mounds of debris are very small (about six orders of magnitude smaller than the gravity on Earth). The GRASS is designed specifically to operate in such microgravity environment and in harsh surface conditions.

The exploration of solar system bodies to better understand their evolution and origin has been one of the main research areas of ORB-KSB who also has a strong heritage on gravimetry and geophysics.

Due to launch in 2024, Hera is the European contribution to an international double-spacecraft collaboration to a binary asteroid system: The 780 m-diameter main body Didymos is orbited by a 160 m moon, Dimorphos. NASA's DART mission will first perform a kinetic impact on Dimorphos, then Hera will follow up with a detailed post-impact survey that will turn this grand-scale experiment into a well understood and repeatable planetary defence technique.

Service and expertise

Seismic Activity in Belgium in 2020

In 2020, 52 earthquakes and 11 induced earthquakes were located by ORB-KSB in or near Belgium. There were no felt earthquakes on Belgian territory.

The 52 natural earthquakes occurred in a zone between 1° and 8°E longitude and 48° and 52°N latitude (). During the same period, ORB-KSB also measured 11 induced events, 389 quarry blasts, 6 controlled explosions and one sonic boom. The catalogue is complete for natural earthquakes and contains a selection of quarry blasts and earthquakes induced by human activities, e.g. linked to (rock) mass removal in mines or geothermal exploitation. In 2020, there were at least 6 measurable explosions at sea. Most explosions are performed by the Belgian, Dutch or French Army to destroy WW1 and WW2 bombs.

The largest earthquake recorded on Belgian territory in 2020 occurred on 5 May 2020 in Modave. That earthquake had a local magnitude of 1.7. There are nine felt earthquakes in the 2020 ROB catalogue but none of these earthquakes were felt in Belgium. Only one quarry blast (6 May 2020) at the Soignies quarry (ML=1.7) was felt by the local population who spontaneously answered the 'Did You Feel It?' macroseismic questionnaire on the ORB-KSB website.

In comparison, last year in 2019, 45 earthquakes occurred in and around Belgium. The largest earthquake was the induced earthquake in Dessel on 5 December 2019 (magnitude ML=2.1) and which was locally felt.

The monitoring network of ORB-KSB has remained fully operational during the COVID-19 crisis. This results from expertise of technical and scientific staff and from continuous developments allowing the level of excellence to be maintained.

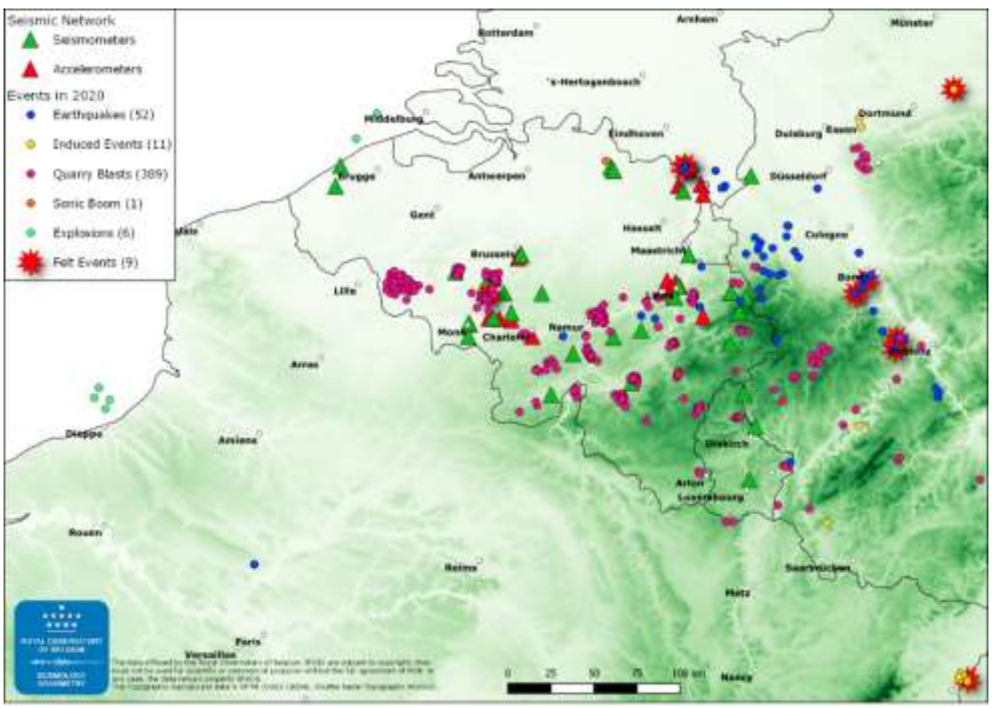

Figure 9 Events recorded in 2020 by the Seismic Network of the Royal Observatory of Belgium.

Research at the Royal Observatory of Belgium

Seismology

The 23 February 1828 Earthquake near Hannut

On 23 February 1828, a moderate-magnitude earthquake shook the central part of Belgium and caused severe damage in the epicentral area. Thierry Camelbeeck and his colleagues from the ORB-KSB published a comprehensive study on the earthquake information provided by scientific studies, newspapers of the Low Countries, and a systematic survey of official, private and religious historical sources. In total, information for 185 localities in the present territory of Belgium, France, Germany, The Netherlands, Grand Duchy of Luxembourg, and Southern England were collected. For each locality, the intensity, i.e. a measure of the shaking strength based on observed effects in a limited area, was determined.

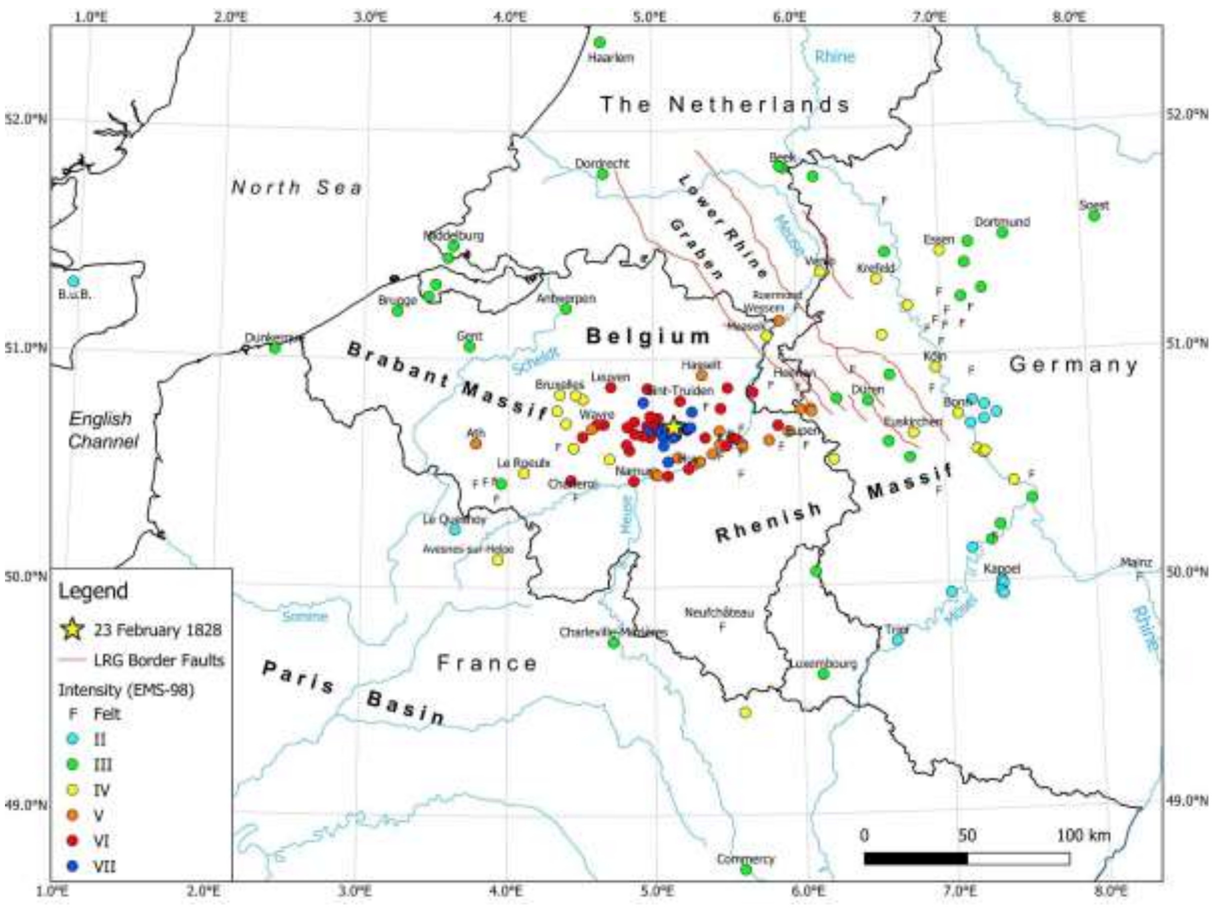

Figure 10: Regional intensity distribution (in the EMS-98 scale) of the 23 February 1828 earthquake in present Belgium and surrounding countries. The epicentre is indicated by the yellow star.

Using the intensity dataset, the earthquake location was determined at 50.70 °N and 5.12 °E, north-east of Hannut, with an uncertainty around 10 km. The magnitude M_w was estimated to be 5.1 ± 0.3 and the earthquake depth was located at 10 km with a possible range between 3 km and 15 km. The distribution of the earthquake testimonies was far from concentric because of the unevenly distributed population density, the various types of historical sources, and differences in the regional geology. This new intensity analysis demonstrates that the shaking strength of the 1828 earthquake diminished more slowly in the WSW-ENE direction in this part of the Brabant Massif and faster towards the surrounding Rhenish Massif and Paris Basin. Towards the north of the epicentre, the increasing thickness of sediments on top of the Brabant Massif caused a fast decrease of the shaking intensity. This observation corroborates the intensity observations from recent earthquakes obtained by the ORB-KSB online survey system. The way intensity varies in different directions in Belgium currently forms the subject of the PhD thesis of Ben Neefs funded by ORB-KSB.

Camelbeeck's study illustrates the benefit of historical seismicity studies to the knowledge of the impact of rare destructive earthquakes in stable continental regions like Western Europe.

Reference:

Camelbeeck, T., Knuts, E., Alexandre, P., Lecocq, T. & Van Noten, K. 2021. The 23 February 1828 Belgian earthquake: a destructive moderate event typical of the seismic activity in Western Europe. Journal of Seismology 25, 369–391. https://doi.org/10.1007/s10950-020-09977-6

Lockdown Noise

The COVID-19 crisis was declared a pandemic on 11 March 2020 by the World Health Organization. In the following days, many countries started enforcing measures to reduce the transmission of the virus within the population. Those measures were mostly based on strict lockdown rules, which had a strong impact on individuals' freedom of movement. Non-essential shops were closed, remote work was enforced. This resulted in an unprecedented global reduction of human activities, especially mobility.

On 20 March 2020, Thomas Lecocq from ORB-KSB posted a figure on the Seismologie.be Facebook page and Twitter account in order to show that

- the ORB-KSB's duties were fulfilled thanks to all the automatic and networking systems in place and the preparation for remote work for more than a decade,
- and that the cumulated effect of individuals following the 'stay home' rules had a significant decreasing effect on the seismic noise recorded by the Uccle seismometer.

This message went viral on Twitter and attracted a lot of interest from the public and the (Belgian) media, mostly because it was 'something different' than the COVID-19 case/casualty numbers and it fascinated many. This message was viewed more than 70,000 times on Facebook and more than 100,000 times on Twitter.

Tweet and Facebook post showing the day-night variation of seismic noise recorded by the Belgian seismic network and its reduction linked to the lockdown measures.

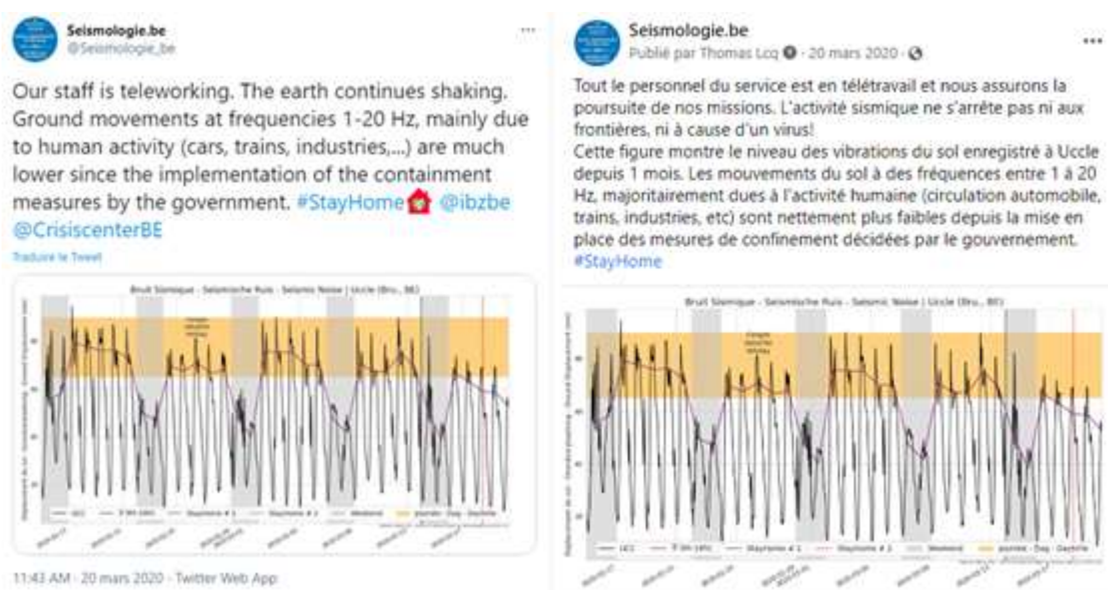

Figure 11: Tweet and Facebook post showing the day-night variation of seismic noise recorded by the Belgian seismic network and its reduction linked to the lockdown measures.

Global Collaboration in Writing a 76-author Science Publication

During more than a month after this initial post, the international (media) interest remained substantial, partly because of the release of a simple, easily reproducible python code on GitHub. This code allowed any individual to download and process any seismic noise data and evaluate the seismic noise in any town worldwide. Following this international interest, Thomas Lecocq launched a call on Twitter and by email to initiate an international collaborative study on the lockdown measures effects on seismic noise. The reaction was fast and numerous and resulted in creating a Slack workspace containing more than 100 users for exchanging ideas, codes and results. This discussion phase resulted into the idea of drafting an 'Article Zero', showing the worldwide impact of COVID-19 restrictions on seismic noise on 150 seismic stations. This preliminary analysis was submitted to Nature and Science editors on 15 May 2020, and Science replied positively to the pre-submission inquiry. The writing of the main manuscript was initially done by a team of six including Thomas Lecocq and Koen Van Noten (ORB-KSB), Stephen Hicks (Imperial College, United Kingdom), Raphael De Plaen (UNAM, Mexico; now ORB-KSB), Paula Koelemeijer (Royal Holloway University of London, United Kingdom) and Kasper van Wijk (University of Auckland, New Zealand) and was reviewed interactively by 76 authors.

The Science Article

Eventually, the community work resulted in a publication in Science entitled 'Global quieting of high-frequency seismic noise due to COVID-19 pandemic lockdown measures' on 23 July 2020. The main results show that the wave of the COVID-19 measures, typically lockdown enforcement, translates into a global wave of high-frequency seismic noise reduction. The study found a near-global reduction in seismic noise, initiated in China in January 2020, followed by Italy, the whole of Europe, and the rest of the world in March to April 2020. This period of reduced seismic noise lasted longer and was often quieter than the Christmas-to-New Year period. In some places high-frequency seismic noise sometimes amounts to more than 50 percent. Eventually it was concluded that the 2020 seismic noise quiet period was the longest and most prominent global anthropogenic seismic noise reduction on record, with seismic quiescence extending for many kilometres radially outside a city and for hundreds of metres in depth!

In the editorial perspective by Denolle and Niessen-Meyer (Science, 2020), the paper was acclaimed as follows: 'Lecocq et al. (2020) exemplify seismological progress through best practices in scientific research: public data, open-access software and hardware, global cooperation, and crowdsourcing of citizen-science projects. […] Although physical borders were closed, the authors demonstrate that, much like the global medical research on SARS-CoV-2, seismological research is and ought to be without borders.'

References:
Lecocq, Thomas, Hicks, Stephen P., Van Noten, Koen, et al. 2020. Global quieting of high-frequency seismic noise due to COVID-19 pandemic lockdown measures. Science 369, 6509, 1338–1343. https://doi.org/10.1126/science.abd2438
T. Lecocq et al., 2020. ThomasLecocq/2020_Science_GlobalQuieting: First Release - v1.0, Zenodo. https://doi.org/10.5281/zenodo.3944739.

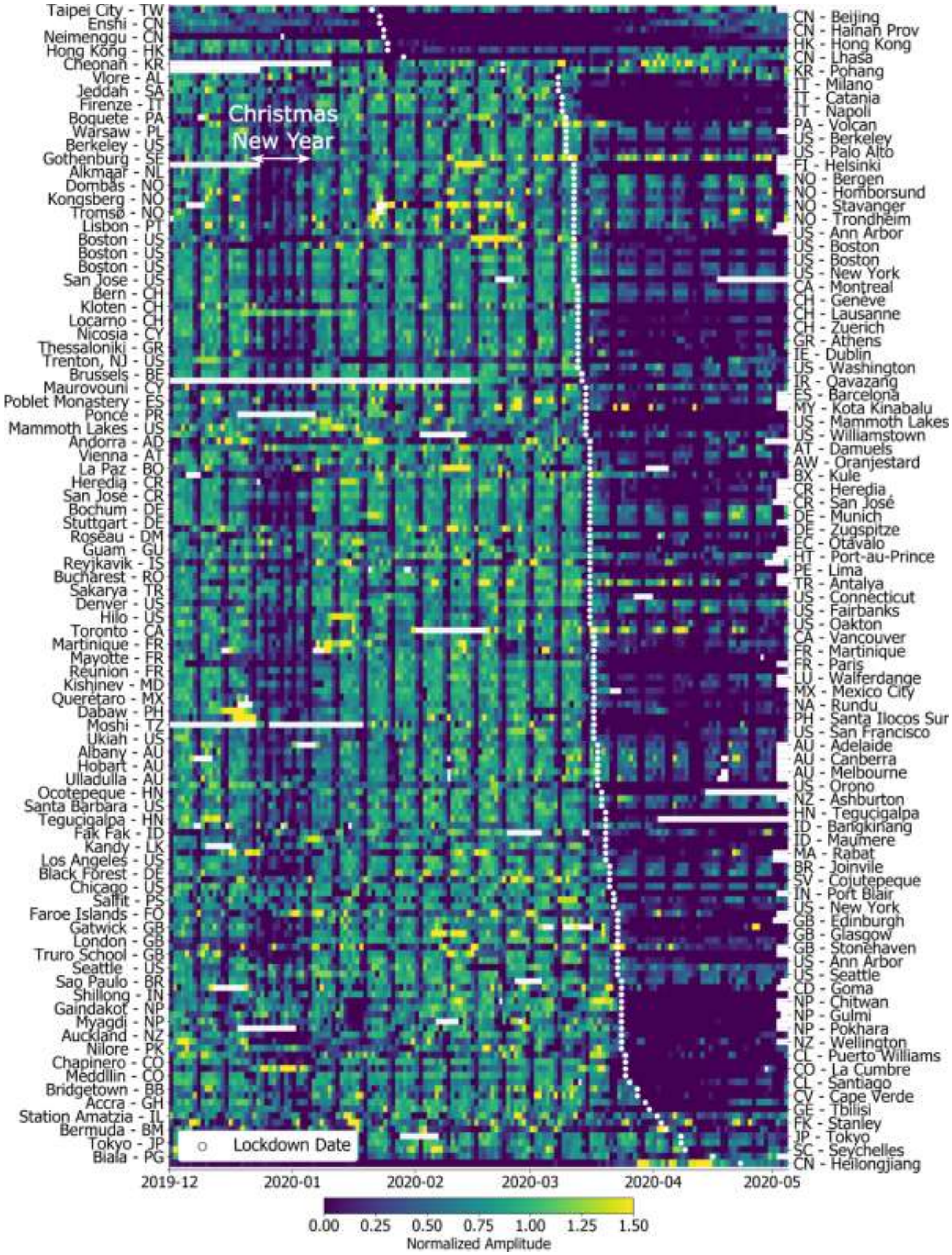

Figure 12: Decrease of Seismic Noise linked to the COVID-19 pandemic. Seismic noise levels for 185 seismic stations worldwide show dramatic changes after lockdown measures (white dots) were enforced. Each line represents the normalised seismic noise of one seismometer recording.

Global Navigation Satellite Systems

M3G: A Unique Catalogue of GNSS Station Information

Because of Earth's constant deformation (e.g. due to plate tectonics), measuring the positions needs accurate points of reference, which are at the foundation of every aspect in collecting and managing geospatial information. For this purpose, in Europe, one can rely on the reference points of the European Terrestrial Reference System 89 (ETRS89). The ETRS89 is the EC-recommended standard frame of reference, included in the 'Infrastructure for Spatial Information in Europe' (INSPIRE) directive. Its reference points are provided by the EUREF Permanent GNSS Network (EPN), a network of permanently tracking GNSS stations installed at fixed locations all over Europe using an open data policy. In addition, thousands of permanently tracking GNSS stations are installed all over the world. The analysis of their observations allows scientists to measure precise ground deformations (e.g. volcano deformations, movements caused by earthquakes, anthropogenic subsidence due to gas extractions), correct sea-level measurements, gather evidence of climate trends, and many more. However, to obtain reliable results, scientists must be able to separate artefacts (notably caused by changes at the GNSS stations) from real (geo)physical signals.

Figure 13: M3G web portal, https://gnss-metadata.eu.

ORB-KSB started in 2018 the development of the 'Metadata Management and Distribution System for Multiple GNSS Networks' (M3G) with the goal to provide open and standardised access to GNSS station information.

Today, M3G consists of a Graphical User Interface (GUI, https://gnss-metadata.eu) and Application Programming Interface (API) used by more than 130 European agencies to maintain and store their GNSS station information. A large majority of these agencies are regional/national authorities providing public georeferencing services. In addition, universities, research agencies, and private companies are using M3G. In Belgium, ~~near~~ besides the ORB-KSB, the National Geographic Institute (https://agn.ngi.be/NL/NL1.jsp), the Agentschap Informatie Vlaanderen (https://flepos.vlaanderen.be/Map/SensorMap.aspx) and the Service public de Wallonie (https://gnss.wallonie.be/walcors.html) also maintain their GNSS station information in M3G.

Although M3G is mainly focusing on Europe, it is not limited to its geographical area. A close collaboration between the Central Bureau of the International GNSS Service (IGS, JPL, US) and ORB-KSB ensures M3G is in-line with international GNSS metadata standards and ready to accept information from GNSS stations installed throughout the globe.

Since its first release, the uptake of M3G by the European GNSS community has been impressive. Currently, EUREF uses M3G to provide its users with information on its EPN stations and it is also used within European Plate Observing System (EPOS), which provides pre-operational access to a first set of Solid Earth data and services to measure how the ground moves and understand the underlying physical processes. Furthermore, with the support of EPOS, M3G has been extended to collect data licenses and Persistent Identifiers (Digital Object Identifiers) in order to better align GNSS data with the FAIR data principles. Today, M3G is working with the SONEL GNSS network managers to add the SONEL GNSS stations in M3G. SONEL (https://www.sonel.org/) aims at providing high-quality continuous measurements of sea- and land levels at the coast from tide gauges (relative sea levels) and from modern geodetic techniques (vertical land motion and absolute sea levels) for studies on long-term sea-level trends.

As a result, M3G currently offers, through a GUI and APIs, access to a unique catalogue of standardised GNSS station information including more than 2700 GNSS stations.

ORB-KSB will continue to develop M3G in the next years to respond to evolving user requirements, the changing GNSS landscape, and improving the FAIRification of the GNSS data. In addition, although station managers can insert the Digital Object identifiers and licence of use of their GNSS station data in M3G, the majority has not done so and needs to be made aware of the importance of attributing DOIs and data licenses to their GNSS data in order to align these data with FAIR data principles.

Acknowledgements:
M3G has been supported EU's H2020 research and innovation programme (GA 676564 & 871121) and Belgian Science Policy Office (GA FSIRI/33/EPI).

More information:
https://gnss-metadata.eu
http://twitter.com/be_GNSS
https://doi.org/10.24414/ROB-GNSS-M3G

Contact: m3g@oma.be

Planetary Science

The Interior of Mars

Introduction

Mars is the most investigated planet by spacecraft, including orbiters as well as rovers and static landers. Over the years, the accumulation of precise tracking data from orbiters and landers improved our knowledge of its gravity field, tides, and rotation, which have been used to probe the planet's interior. These studies have led to the detection of the liquid core, the estimation of the core radius, and knowledge about how Mars deforms at different timescales, among other advances. With the landing of the NASA InSight platform, short for Interior Exploration using Seismic Investigations, Geodesy, and Heat Transport, on 26 November 2018, and its three main instruments, a seismometer, a heat-flow probe, and a radio-science experiment, significant advances about Mars's interior have been obtained. ORB-KSB has contributed at various levels to studies of Mars's interior, from the analysis of the raw data to the planetological interpretation. Three areas of expertise of the ORB-KSB planetary science team have been specifically important in these studies: (1) the determination of geodesy quantities from radio-science data, (2) the modelling of the relation between interior structure and geophysical observations, and (3) the knowledge of material properties about plausible planetary constituent materials.

Observations of the Martian Core from the InSight RISE Experiment

RISE Measurements

Since its landing, InSight (**In**terior exploration using **S**eismic **I**nvestigations, **G**eodesy and **H**eat **T**ransport) communicates with Earth by direct radio transmissions to and from NASA's Deep Space Network (DSN, see Figure 14). InSight instrument Rotation and Interior Structure Experiment (RISE) measures the range rate of the round-trip signal, or the velocity of the lander along the line of sight (LOS) with respect to Earth. These Doppler measurements enable to precisely estimate the rotation and orientation of Mars, which can in turn be used to improve our knowledge of Mars's interior (Folkner et al., 2018).

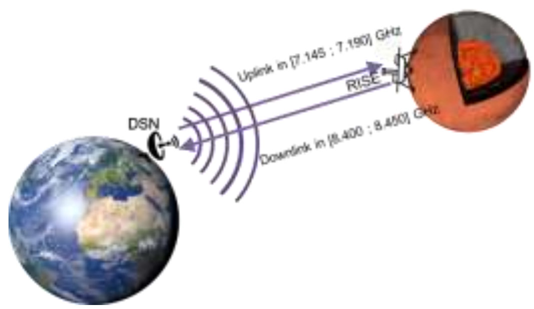

Figure 14: InSight's RISE experiment

The ongoing RISE experiment provides Doppler measurements in X-band (frequency of about 8 GHz) almost daily since day 1 (about 45 min of observation per session on average) by using its two fixed-pointing horn-shape medium-gain antennas. The InSight data set used for this study consists of 21,091 data points, each providing an average over 60s (i.e. 335 hours of tracking), and acquired over one Martian year (687 days) from November 27, 2018, to October 14, 2020. Data between July 16, 2019, and October 18, 2019, were excluded from our analysis since InSight and the Sun as viewed from Earth (the Sun-Earth-Probe, or SEP angle) were separated by less than 15º, inducing significant plasma noise on the measurements. The retained measurements have a very low noise level of about 2 mHz (Figure 15). Nevertheless, it is still more than three times larger than the predicted signature in the Doppler of the liquid core of Mars, one of the main targets of this study (Figure 16 and text below).

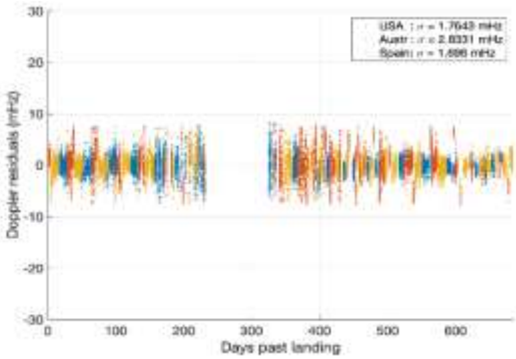

Figure 15: Post-fit Doppler residuals as a function of

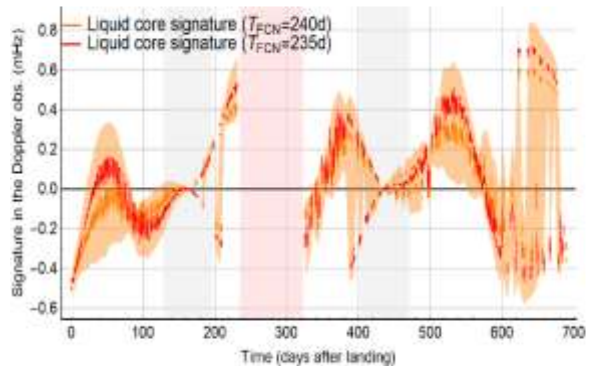

Figure 16: Liquid core predicted signature in RISE Doppler

Determining Mars Precession and Moment of Inertia

The gravitational torque exerted by the Sun on the equatorial bulge of the rotating Mars causes the precession of the rotation axis in space. The spin axis completes one rotation about the normal to the orbit plane in about 171,000 years. Since the precession rate is inversely proportional to the polar moment of inertia, which is a key parameter to constrain interior models, we use RISE measurements to refine its determination. Our latest estimate of -7605±1 mas/year, obtained from almost two years of RISE data (one Martian year), is in very good agreement with the recently published estimates of -7603.9±1.3 mas/year from orbiting spacecraft (Konopliv et al., 2020) and of -7605±3 mas/year from the combination of the InSight first Earth year of data with previous data from the Viking-1 lander, Mars Pathfinder, and Opportunity missions (Kahan et al., 2021). The inferred dimensionless moment of inertia (MOI) equals 0.36394 ± 5e-5, which is a very accurately known value in planetary science. The MOI is an important constraint for the interior structure of the planet and, in particular, for the mass distribution within the crust and upper mantle. When combined with seismic constraints about the structure of the crust, the MOI helps to further refine the global average thickness of the crust inferred from seismic data.

Mars Nutation and Liquid Core Properties

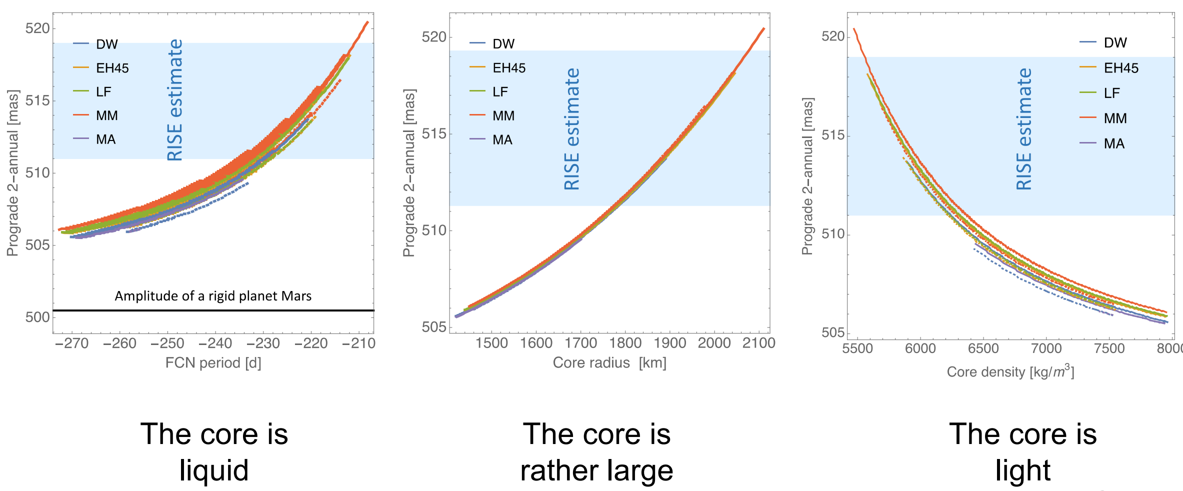

Figure 17: Interior properties from semi-annual nutation amplitude estimates

Periodic variations in the torque due to the orbital motion of Mars lead to periodic variations of the rotation axis in space, the so-called nutations, with periods of one Martian year and harmonics of it. The amplitudes of the nutations depend on the internal structure of Mars, and in particular on whether the core of Mars is liquid or solid. Using RISE Doppler measurements, we were able to detect for the first time the signature of the liquid core in Mars orientation variations using two different approaches: by estimating the amplitudes of nutation as well as by estimating the transfer function parameters (see Le Maistre et al., 2012, for further explanation on the nutation parameters). The estimated amplitude of the semi-annual prograde nutation (p2) confirms that the core is liquid (see Figure 17, left panel). It also indicates that the core of Mars has a radius between 1780 km and 2080 km (see Figure 17, middle panel), which is relatively as large as the core of the Earth, and has quite a low density within 5600 kg/m³ and 6400 kg/m³ (see Figure 17, right panel), indicating that it contains a much larger concentration of light elements than the core of the Earth.

The nutation amplitudes depend on the period of a rotational normal mode of the liquid core, the so-called Free-Core-Nutation (FCN). Its period is still uncertain. Two possible values for the FCN period (TFCN) were found, one on each side of the ter-annual nutation period (229 d): TFCN = -215+/-12 days or TFCN = -255+/-17 days. The latter is our favourite solution because it is obtained along with a core momentum factor estimate of F = 0.078 +/- 0.012 that is considered as realistic unlike the former. The core factor is very sensitive to the core size. Our F estimate indicates that the core radius is within 1870 km and 2030 km. This is in good agreement with the radius range inferred from the nutation amplitudes, but it is slightly larger than independently determined core radius ranges estimated from the tidal Love number and seismic data.

The Chandler wobble of Mars

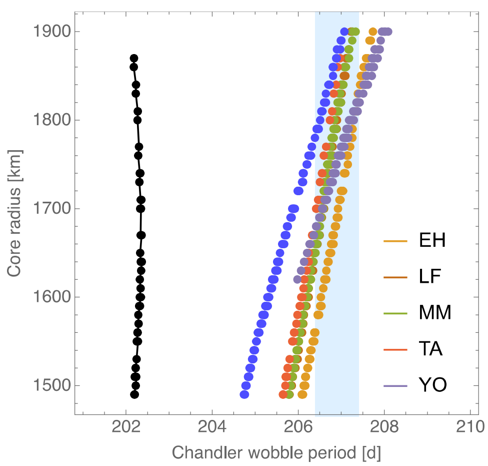

Figure 18: Core radius as a function of the Chandler wobble period for different models for the mantle of Mars, shown by different colours. Black symbols indicate results neglecting dissipation.

The accumulation of more than 30 years of spacecraft tracking data and expertise of the Jet Propulsion Laboratory about the spacecraft orbital evolution enabled us to determine the Chandler Wobble (CW) period of Mars (206.9d). Mars is the second planet after the Earth for which the CW period is known. The wobble exists because the rotation and figure axes of Mars are not aligned. The period of the CW depends on the interior structure of Mars, particularly on the non-elastic behaviour of the mantle at periods close to the CW period (see Figure 18). Compared to the Earth, the CW decays faster, providing further support for the more dissipative behaviour of Mars already evidenced by measuring the long-term orbital evolution of Phobos. In a joint effort, members of ORB-KSB contributed to a study that provided an interpretation of the CW measured by members of the JPL in terms of interior structure. The results were published in Geophysical Research Letters (Konopliv et al. 2020).

The Composition of the Core of Mars

The radius and relatively low density of the core of Mars (e.g. Rivoldini et al. 2011) requires that its iron-rich core incorporates a large amount of light elements. The study of the formation of Mars, as well as analyses of Martian meteorites, surface rocks, and data provided by orbiting spacecraft, are in favour of sulphur as the major candidate light element. Other likely candidate elements are oxygen and hydrogen.

As already evidenced in previous studies that measured the thermo-elastic properties of liquid iron-sulphur alloys (Terasaki et al. 2019), and confirmed by an independent study made within a collaboration with members of ORB-KSB and members of the Sorbonne and Grenoble University, the amount of sulphur required to match the density of its iron-rich core is significantly larger than any predictions made by formation and chemical models (about 17wt%) (see Figure 19). Among the other candidate light elements, oxygen is quite likely present in appreciable amounts, since its capacity to dissolve in liquid iron-sulphur increases with sulphur.

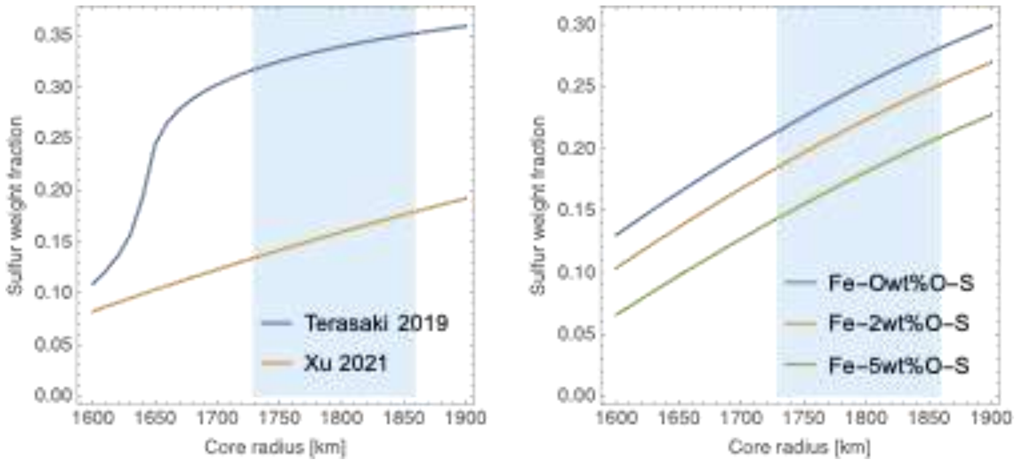

Figure 19: Sulphur concentration in the core of Mars as a function of the core radius.

Published equations of state for liquid iron-oxygen, required to model the core properties, are scarce and not in agreement with more recent data about the melting temperature of solid iron-oxygen. For this reason, members of ORB-KSB have worked together with members of the Sorbonne and Grenoble University to derive an equation of state for liquid iron-oxygen based on thermodynamic modelling as well as on melting data and thermo-elastic data of solid iron-oxygen. The application of those results, together with those obtained for iron-sulphur, indicates that by adding up to 5wt% of oxygen in liquid iron-sulphur the amount of sulphur required to match the core density of Mars can be brought more in line with chemical and formation models (see Figure 19). It is noteworthy to mention that the low core density deduced by measuring tides is confirmed by preliminary results obtained by the RISE and SEIS experiments on InSight. The collaboration of ORB-KSB with experts in experimental work led to a publication in Earth and Planetary Science Letters Letters (Xu et al. 2021).

The Bottom of the Mantle of Mars

Before InSight, the core radius of Mars was inferred from measuring tides induced by the Sun and was based on interior structure models that assume that the whole mantle is solid. It is, however, conceivable that the initial global magma ocean overturned and led to the formation of a stable basal layer that was highly enriched in heat-producing elements. A significant volume of this stable layer could be molten to this day. Such a layer would introduce an appreciable bias in the core radius inferred from tides: the core radius would be smaller than the value inferred from tides assuming a solid mantle down to the core-mantle boundary. If Mars had a smaller core, it could be denser and the amount of light elements required together with iron would be lower and more in agreement with formation and geochemical models. Like for tides, core radius estimates deduced from seismic waves reflected at a solid-liquid interface would associate the depth of that interface to the core-mantle boundary and overestimate the core radius if the presence of the molten layer in the mantle is not taken into account. Core-traversing seismic waves are required to prove the presence of such a layer, as seismic waves propagate differently in liquid iron-rich alloys than in molten silicates. Finally, the Free Core Nutation period (see above), which is sensitive to the density jump between the core and the solid mantle, could be appreciably different if a basal magma ocean were present since the density jump between liquid and solid mantle material is significantly lower than between the core alloy and the solid mantle. Members of

ORB-KSB participated in a study that discussed the occurrence of a basal layer and its consequences on the thermal state of Mars and tidal deformation. The results of this study were submitted to the Journal of Geophysical Research and published in 2021 (Samuel et al. 2021).

The Crust of Mars

One of the primary scientific targets of InSight is the precise determination of the structure of the crust. To this day, the acquired seismic events have revealed the reflection of seismic waves below the lander, which are expected to occur at the depth of the Moho, the transition layer between the crust and the mantle. The data is consistent with a crust thickness of either 20 km or 39 km. The local crust thickness estimate can be used to determine the global average thickness and density of the Martian crust when combined with gravity and topographic data. Both resulting crustal models contradict the thick crust models of basaltic origin that have been proposed in the literature. Moreover, global interior models built with either of the two crustal models cannot match the moment of inertia of Mars if they are based on the standard Mars composition model and agree with the expected thermal state of the mantle. From seismic data alone, both models are equally likely, but other constraints prefer the thick crust model. The thin crust model requires appreciable more heat-producing elements in the crust than what has been deduced by orbital observations with the Gamma Ray Spectrometer on the Odyssey spacecraft. Additionally, the relatively low density required by the thin crust model to explain the observed gravity field, requires a large volume of low-density rocks, which are almost not observed on the surface. The ORB-KSB team has collaborated to that study that is currently under review in Science.

References:

Folkner et al., Space Science Review, 214:100, 2018.

Konopliv, A., Park, R.S., Rivoldini, A., Baland, R.-M., Le Maistre, S., Van Hoolst, T., Yseboodt, M., Dehant, V., Detection of the Mars Chandler Wobble from Mars Orbiting Spacecraft, Geophysical Research Letters 47, e2020GL090568. https://doi.org/10.1029/2020GL090568

Kahan et al., PSS, 199, 2020, 2021.

Le Maistre et al. , PSS, 68, 2012.

Rivoldini, A., Van Hoolst, T., Verhoeven, O., Mocquet, A., Dehant, V., Geodesy constraints on the interior structure and composition of Mars, Icarus 213, 451-472, 2011. doi:10.1016/j.icarus.2011.03.024 (impact factor 2009: 3.340)

H. Samuel, M. D. Ballmer, S. Padovan, N. Tosi, A. Rivoldini, and A.-C. Plesa, The Thermo-Chemical Evolution of Mars With a Strongly Stratified Mantle, Journal of Geophysical Research: Planets, 126(4):e2020JE006613, 2021.

F. Xu, G. Morard, N. Guignot, A. Rivoldini, G. Manthilake, J. Chantel, L. Xie, A. Yoneda, A. King, E. Boulard, S. Pandolfi, F. J. Ryerson, and D. Antonangeli, Thermal expansion of liquid Fe-S alloy at high pressure, Earth and Planetary Science Letters, 563:116884, 2021.

Solar Physics

EUI First Light and Discovery of Campfires on the Sun

On May 12, 2020, only two months after the launch of Solar Orbiter, the doors of its Extreme Ultraviolet Imager (EUI) were opened for the first time, a crucial moment in the mission's life. It is only during this 'First Light' moment that the EUI team found out whether the telescope survived the launch and was working properly. For EUI, this first light was especially challenging as the whole of Europe, including the Mission Operation Centre in Darmstadt, was in lockdown because of the COVID-19 pandemic. In normal circumstances, instrument experts are present in the Operation Room during this procedure so that communication is quick and efficient. Performing this type of operation from home through simultaneous teleconferences was tough for all teams involved, yet very successful: the high-resolution images of EUI (Figure 20) were breathtaking and immediately led to a scientific discovery: campfires on the Sun.

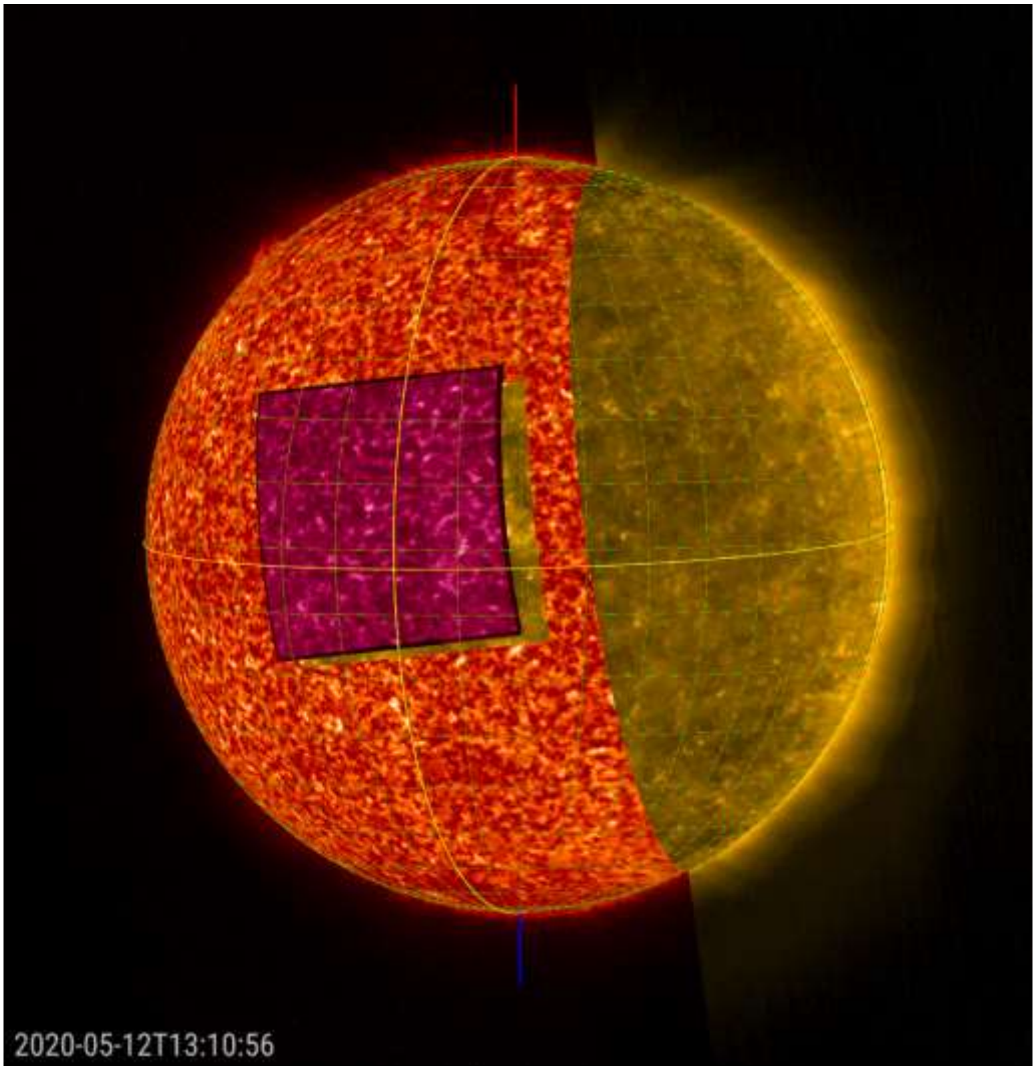

Figure 20: Combination of the first light images of EUI in each of its four channels. The large red area is the FSI 30.4 nm channel imaging the solar transition region. The square violet area is the HRILYA channel imaging in the Lyman-alpha line and showing the solar chromosphere. The yellow/golden coloured areas are taken in the 17.4 nm bandpasss and show the 1 million degree corona by HRIEUV (square area below the HRILYA square) and the FSI (large area on the right).

Solar Orbiter makes one complete orbit around the Sun in 168 days. The point of the orbit that is closest to the Sun is called ‘perihelion’. At perihelion, the speed of the spacecraft approaches the speed with which the Sun rotates around its own axis. While the spacecraft hovers closely above the solar surface, the cameras onboard are in an excellent position to photograph the solar atmosphere. The EUI cameras made images overwhelmingly rich in small detail. David Berghmans, principal investigator of the EUI telescope, explains: ‘It is like zooming in on the iconic blue marble Earth and suddenly you see details which you had never expected: rivers, cows, a road with cars, smoking chimneys. This is exactly what we see with EUI: we can now see the solar corona at work on a micro-level.’

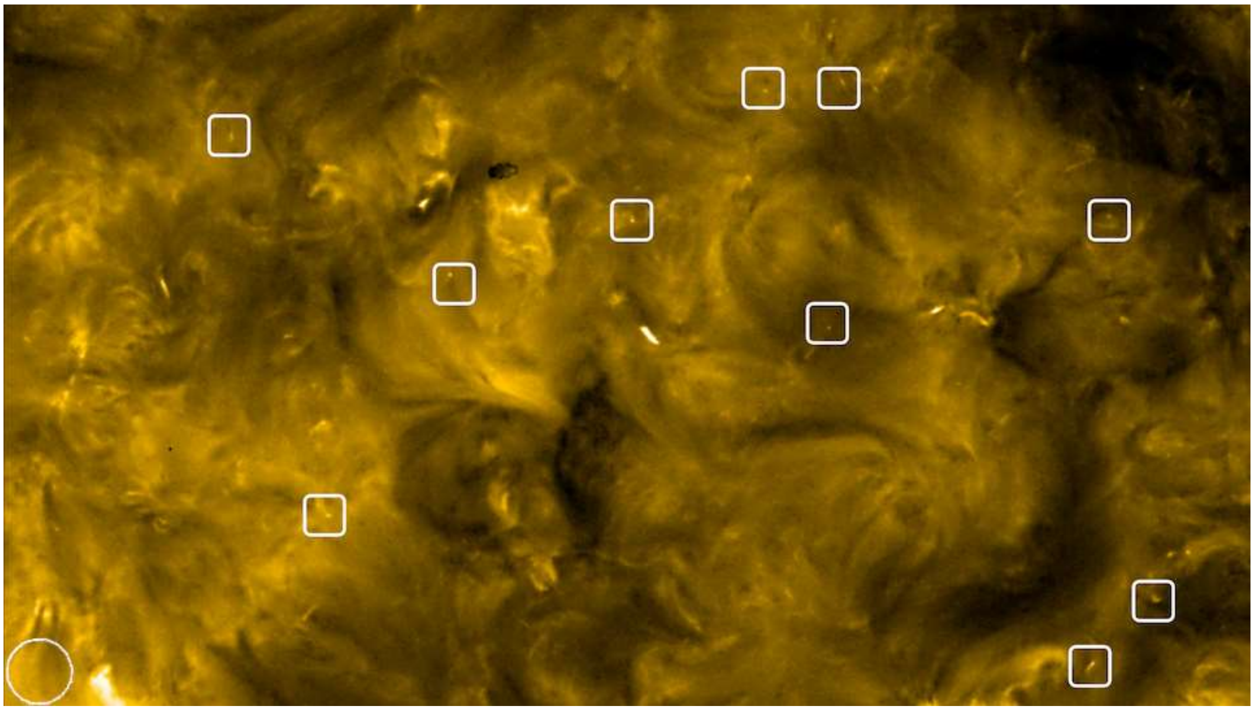

Figure 21: Image from the High Resolution EUV Imager of EUI taken on May 30, 2020. The squares indicate examples of little campfires. The circle bottom left illustrates the size of the Earth for comparison.

On May 30, 2020, Solar Orbiter was roughly halfway between the Earth and the Sun, meaning that it was closer to the Sun than any other solar telescope has ever been. This allowed the EUI telescopes to see features in the solar corona of only 400 km across.

Figure 21 shows a small part of the solar atmosphere observed on May 30, 2020. The sequence of images taken on that day shows an unexpected multitude of small loops, bright spots and dark, moving fibrils. The tiny brightening dots and loops sparked immediate excitement in the EUI team as they show up remarkably sharp and contrasted, ubiquitously all over the so-called quiet Sun where nothing seemed to happen in older data. Only now, looking at the Sun with the unprecedented high resolution of EUI, we see very tiny flashes of light almost everywhere. These flashes of light were named ‘campfires’ by the EUI scientists. They might contribute to the high temperatures of the solar corona and to the origin of the solar wind, possibly answering the question that solar physicists have been tackling for decades.

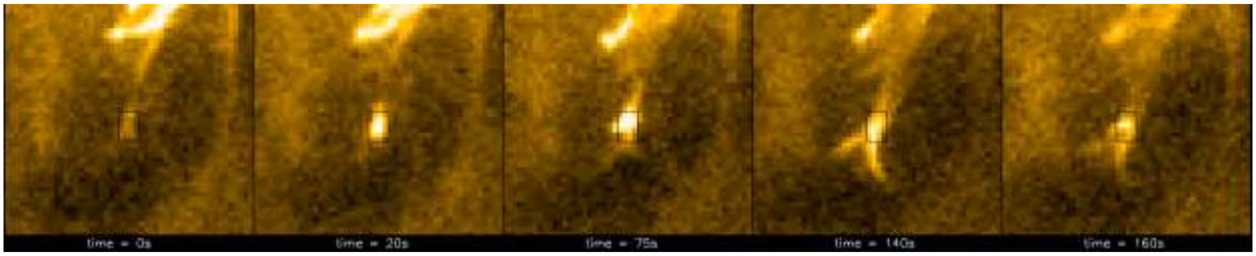

Figure 22: A zoom-in on a campfire lasting less than three minutes. The campfire appearance suggests the interaction of two small coronal loops. The interaction region (the black square) is roughly 800x1200km.

It is well known that the solar atmosphere produces flares, sudden flashes of light that release magnetic energy. The biggest solar flares can impact the Earth, and its technologies in a process called space weather. The campfires that EUI discovered are their little nephews, typically a billion times smaller than common flares (Figure 22). They are totally insignificant each by themselves, but, summing up their effect all over the Sun, they might be the dominant heating contribution of the solar corona. This idea (‘nanoflare heating’) has been proposed a long time ago by Eugene Parker (indeed, the scientist after whom the Parker Solar Probe is named). Further research will be needed to find out whether the campfires are indeed just miniature versions of the big flares or whether they are different in some way. We will also need to collect statistics on campfires and compare with other instruments (such as the SPICE spectrograph) to determine the significance of their heat output.

As the mission continues, Solar Orbiter will go closer to the Sun and this will increase the instrument’s resolving power by a factor of two at closest approach, allowing it to see small features of only a few 100 km in size. The whole team is looking forward to this new data. However, contrary to previous missions in which the EUI team members have participated in, the distance between the Sun and the spacecraft is continuously changing. They will have to get used to the fact that the images that EUI makes are continually changing, as EUI takes pictures of the Sun from a different angle and distance day after day. The EUI team is excited to calibrate, analyse and interpret the new images. New science is on the way!

A Modern Reconstruction of Richard Carrington's Observations (1853-1861)

In 2020, in the framework of the ongoing recalibration of the 400-year-long sunspot number series undertaken in 2015 by the World Data Center SILSO, we focus on the 19th century to revisit original data that were under-exploited in a period when sunspot data are much sparser than in the 20th and 21st centuries. The ultimate goal of our work is to ensure the homogeneity of our longest record of solar activity over the past centuries. A key observer over the years 1853–1861 was Richard Carrington, a prominent solar scientist who measured the solar differential rotation and defined the heliographic coordinate system still in use nowadays.

With the help of Thomas Teague (UK), an active observer from the SILSO worldwide sunspot network, we carried out a full recounting from the original historical drawings and logbooks, preserved at the Royal Astronomical Society (see Figure 23) in England. Indeed, until now, the only numbers at our disposal came from Rudolf Wolf, the initiator of the sunspot number in the 19th century. However, the way Wolf derived those numbers was indirect and poorly documented. With our new recounting, we can now fully assess Wolf's counting method and shed light on the quality of the sunspot number series over that period.

Figure 23: Carrington's original drawing for the Sun of July 7,1860.

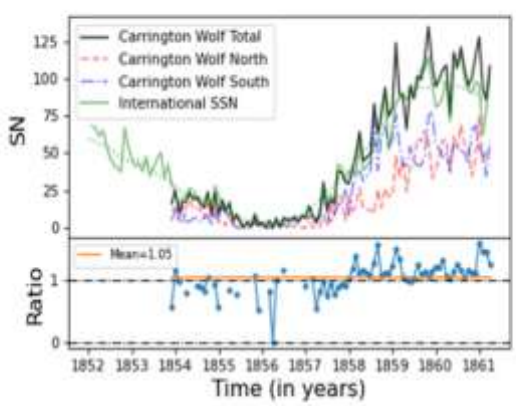

Figure 24: Comparison of recounts by Teague's and Wolf's observations on overlapping days.

Our study shows that the new recounts by Teague closely match the counts by Wolf, the inventor of the sunspot number, on their overlapping days of observation (see Figure 24), which means that the observers from the SILSO network today have a similar way of counting as the creator of the sunspot number series. This testifies to its homogeneity over the past 200 years. From our analysis, we can tell with confidence that Wolf counted sunspots directly from Carrington's original drawings over 1859–1860, but that, afterwards, he used instead an indirect conversion from lists of sunspot areas provided by Carrington in his correspondence.

Moreover, we also identified the cause of an unexplained constant 7° longitude shift of the sunspot positions in Carrington's tables, as reported in previous studies. We found that, in his groundbreaking work, Carrington simply adopted slightly different coordinate references than those used nowadays, and we can now confirm the very high accuracy of his work.

The resulting recounted 1853–1861 Carrington sunspot number series has now been added to the data accessible on the SILSO Web portal. The corresponding article was submitted to Solar Physics in early 2021 (manuscript: https://arxiv.org/pdf/2103.05353.pdf).

Helmet Streamers in the Solar Corona and their Oscillations

Bieke Decraemer started her PhD in 2016, when she was awarded a PhD grant from ORB-KSB. Her PhD project was made jointly at ORB-KSB and at KU Leuven. Bieke's thesis is dedicated to the study of coronal helmet streamers. Streamers are the largest structures observed in the corona, and they are its true building blocks, especially during solar maximum. In the lower solar corona, helmet streamers consist of closed magnetic loop-like arcades connecting to the solar surface. In the outer solar corona, they extend to a radial stalk connecting to the outflowing solar wind. The radial stalk is actually a plasma sheet seen edge-on.

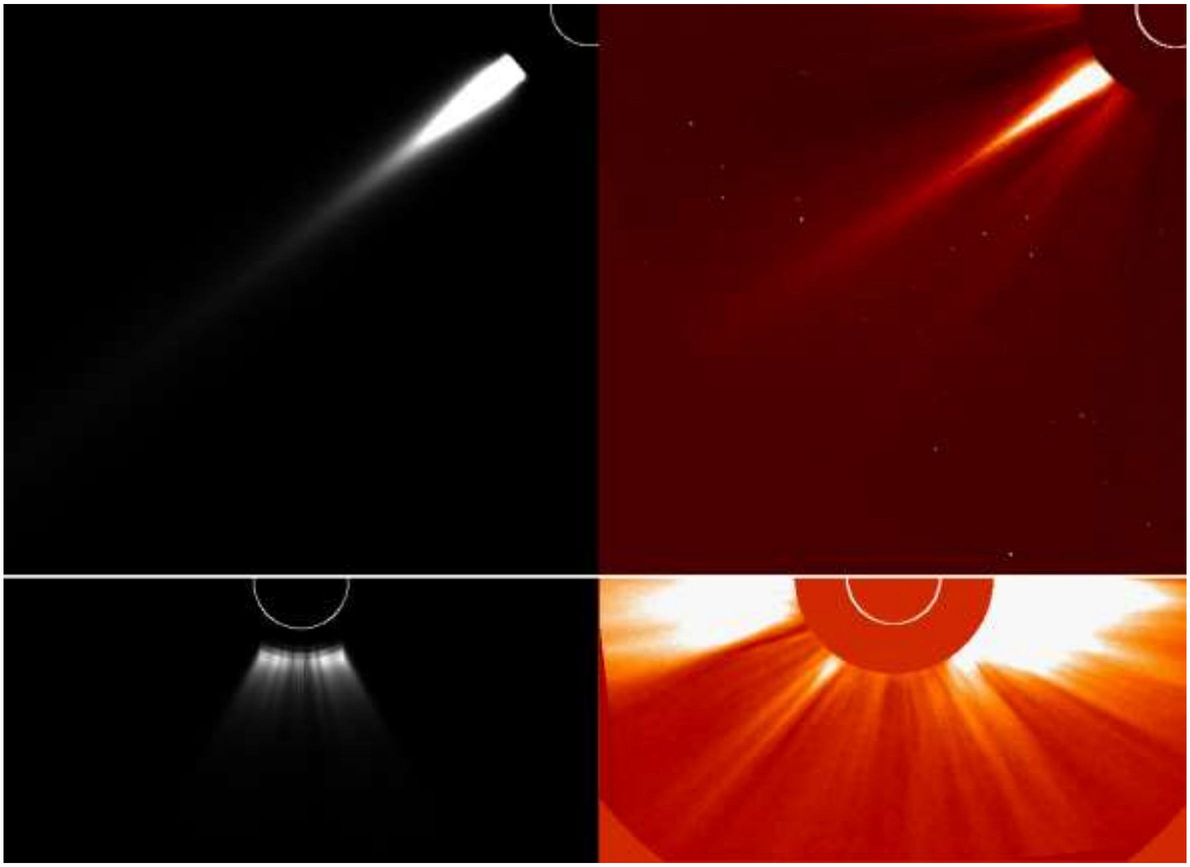

Figure 25: Two views of the same coronal streamer. Left panels show the modelled corona compared with observed corona shown in right panels. STEREO A COR2 images are on top, and SOHO/LASCO images are at bottom.

One of the best ways to study coronal structure is to observe it with two widely separated telescopes, like LASCO onboard the SOHO spacecraft and COR2 onboard the STEREO A spacecraft. This works like the human vision with two eyes providing a better idea about the three-dimensional structure of an object than the information given by one eye only. Bieke combined the data taken by two coronagraphs to derive the first quantitative three-dimensional streamer density model consistent not with one but with both COR2 and LASCO images (see Figure 25).

Sometimes, streamers are perturbed by coronal mass ejections (CMEs) propagating in the corona. They may start to oscillate, with the oscillations propagating outwards like waves (Figure 26). These waves are important as they enable us to derive the plasma parameters in the solar corona, similarly to seismic waves used to derive the properties of Earth's interior. This technique is called 'coronal seismology'. It allowed Bieke to determine the solar wind speed in streamers, a quantity notoriously difficult to measure (Figure 27).

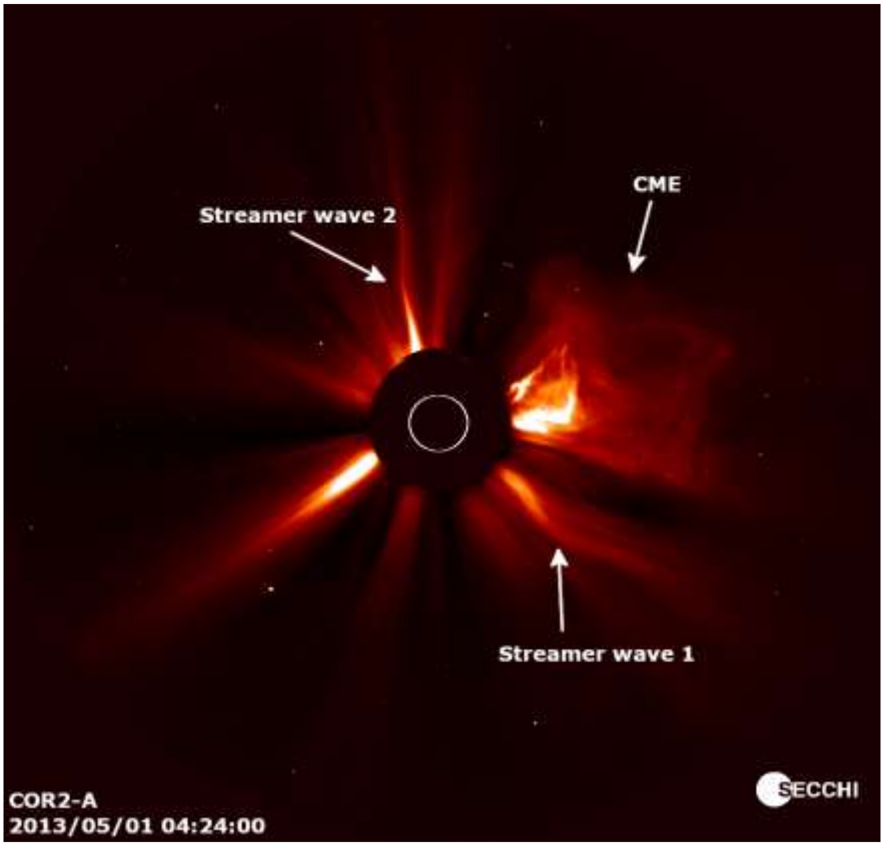

Figure 26: A coronal mass ejection (CME) going towards the right of the image perturbs two streamers and triggers their oscillations that start propagating radially outwards as waves.

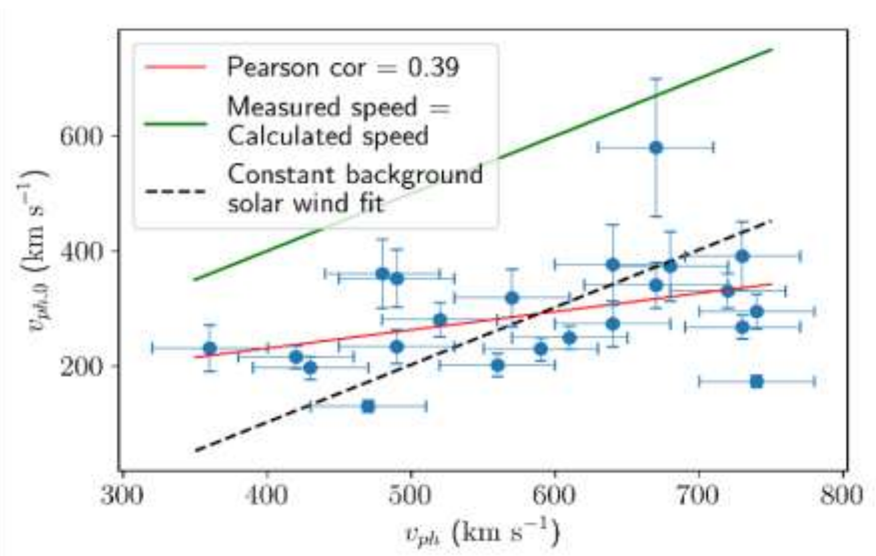

Figure 27: The blue dots with error bars show the streamer wave speeds derived by two independent methods (shown along horizontal and vertical axes). For comparison, the green line is derived from a theory that does not take into account the solar wind propagation in streamers. It is clear that it does not describe well the observed data points. The dashed black line represents the same theoretical fit, but corrected for the solar wind speed of around 300 km/s. This line approximates the observed data points much better.

After having successfully defended her PhD in October 2020, Bieke decided to leave science and start a new job in industry, for which we wish her all the best of luck. We will miss you, Bieke!

Evolution of Coronal Mass Ejections in the Heliosphere

Camilla Scolini started her PhD in 2016, when she was awarded an ORB-KSB PhD grant. She executed her job jointly at ORB-KSB and at KU Leuven (KUL). Her thesis is based on a very relevant and lively topic in space weather and solar physics: the propagation of Coronal Mass Ejections (CMEs) in the heliosphere and their geoeffectiveness upon arrival at the Earth. Furthermore, she also studied how they affected other locations of the heliosphere. In this way, the term geoeffectiveness had to be broadened, and thus helioeffectiveness came to life. So, Camilla's PhD work, apart from interesting scientific results, also created new words! The main tool Camilla used was a newly developed 3D heliospheric MHD model: the EUropean Heliospheric FORecasting Information Asset, EUHFORIA, shown in Figure 28.

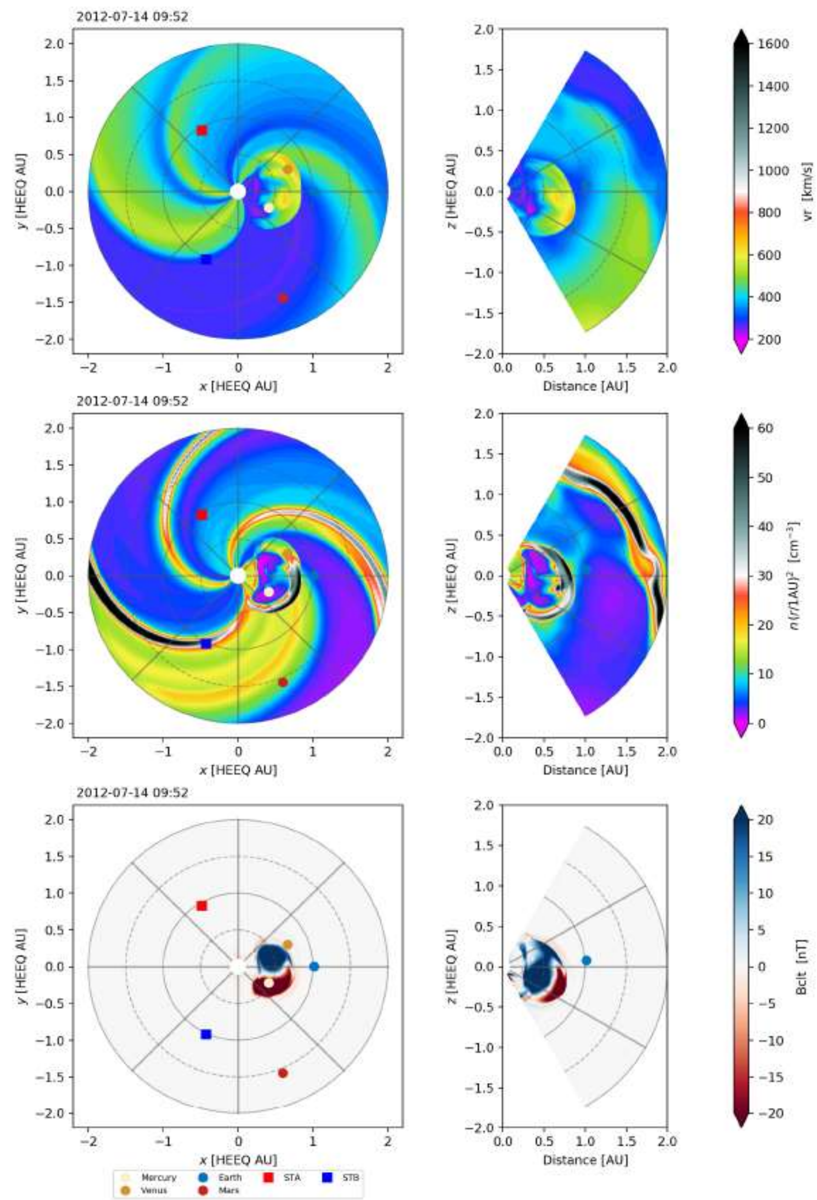

Figure 28: Snapshot of a EUHFORIA run, showing a CME simulation in July 2012. Top panels show the speed, middle ones present the density and the bottom ones depict the magnetic field within the CME.

Camilla developed innovative techniques that are now being used by other researchers. For example, she included the possibility to simulate data at the locations of all the current and new space missions (e.g. Parker Solar Probe and Solar Orbiter) and, more generally, at any location in the heliosphere with the use of virtual spacecraft (Figure 29). She also implemented a clever way to separate the radial and expansion speed of CMEs (a long-standing problem in CME research) in order to be used directly by the model.

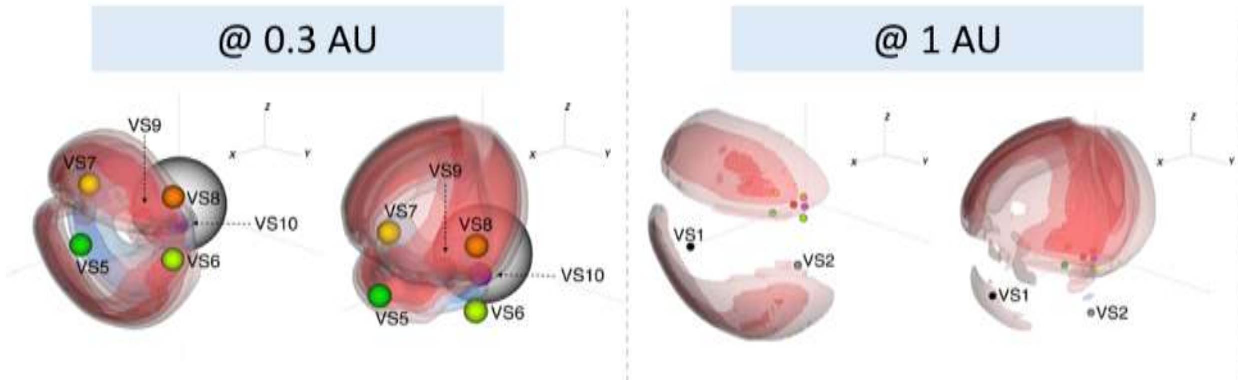

Figure 29: Contour plots showing speed at different locations in the heliosphere, and for different virtual spacecraft (VSx).

She also made critical updates to the model, including the propagation of CMEs with an internal magnetic field configuration (see Figure 30), which is now the state of the art model for CMEs. Camilla helped with the inclusion of EUHFORIA into the space weather Regional Warning Centre in Brussels, where it is currently being validated in order to be used as a forecasting tool. She also coupled EUHFORIA with magnetospheric models, some of these couplings are currently being used in the Virtual Space Weather Modelling Centre (VSWMC, an ESA project currently being developed by a consortium led by KU Leuven, with the participation of ORB-KSB).

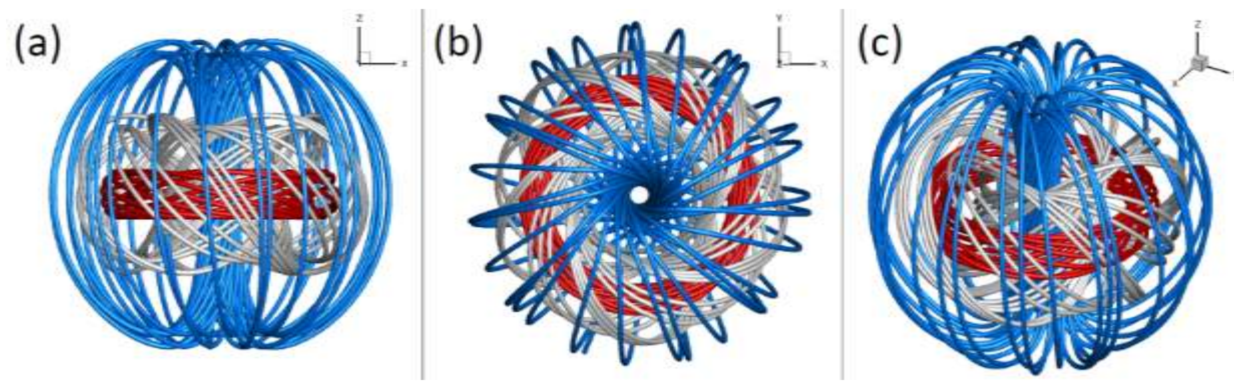

Figure 30: The internal magnetic field configuration of CMEs. Based on a 3D linear force-free spheromak. Different colours mark field lines characterised by different morphologies. (a): side view. (b): top view. (c): angled view.

By the end of her PhD, Camilla had more than 10 published papers in recognised international journals and numerous invited talks given at international conferences. She successfully defended her thesis in May 2020, a copy can be found here http://publi2-as.oma.be/record/5332.

In 2021, the European Solar Physics Division (ESPD) awarded her their 'PhD Thesis Prize', for significant contributions on numerical modelling and observational analyses of the propagation of coronal mass ejections. Camilla has recently received the prestigious Jack Eddy Postdoctoral Fellowship, awarded by the

NASA Living With a Star (LWS) programme, that she will carry out at the University of New Hampshire, continuing space weather research. We definitely expect to hear more from her!

PROBA 2 Data for the Complete Mission Updated

In June 2020, the PROBA2 team reached another milestone in the mission's lifetime. After having celebrated the 10th anniversary of the launch of the satellite in 2019, we completed a full reprocessing of all data from this successful mission in 2020.

PROBA2 is a micro-satellite that was launched in 2009 and that carries 2 solar instruments for which ORB-KSB holds the principal investigator responsibility. LYRA (**L**arge **Y**ield **RA**diometer) measures the ultraviolet solar irradiance in four wavelengths. SWAP (**S**un **W**atcher using **A**ctive Pixel System detector and Image **P**rocessing) takes pictures of the solar corona in ultraviolet. Both instruments are important assets for the space weather services of ORB-KSB: they keep a close and continuous eye on the solar activity.

	Number of files	Amount of data
SWAP level 0 files	> 2 662 000	> 5.2 TB
SWAP level 1 files	> 2 411 000	> 4.7 TB
SWAP movies	> 11 000	> 245 GB
LYRA level 1 files	> 26 000	> 335 GB
LYRA level 2&3 files	> 8000	> 305 GB

Table 1: Amount of data collected by the LYRA and SWAP instruments onboard PROBA2, as well as the derived products, measured at the time of writing, in April 2021.

In 2017, we embarked on the massive project of reprocessing our complete data set, which contains over 10 years of SWAP images and LYRA measurements (see Table 1). This reprocessing served two purposes. Firstly, it allowed us to update all data files to the latest calibration. Indeed, our understanding of the instruments continuously evolves and also the performance of the instruments themselves changes over time (for example due to degradation or faulty pixels). The PROBA2 team therefore continuously works on improving the LYRA and SWAP data: the calibration routines for both instruments are updated regularly, and the latest version is always available, for example through IDL SolarSoft. However, the higher-level data provided through our website and through the SolarSoft IDL routines has been processed with the version of the calibration software that was available at the time of acquisition or processing. Therefore, the most recent improvements were not included in older files. The newly reprocessed data is now calibrated according to our most recent understanding of the instruments. An example image taken by SWAP is shown in Figure 31.

Figure 31: A reprocessed and stacked SWAP image picturing the active solar corona at 174 nm. The stacking of several SWAP images, taken closely together in time, allows us to bring out the faint features in the outer corona.

Figure 32: The old servers used for the PROBA2 pipeline. After 10 years of continuous use, this hardware needed to be replaced by newer servers.

The second purpose of the reprocessing was a major update of the hardware and software that is used to produce all types of PROBA2 data (various levels of FITS files, Quicklook images, movies, etc.). One of the main goals was to get rid of deprecated functions used in the software. The core of the PROBA2 software was written before the launch of the satellite and is thus more than 10 years old. Updating the software while keeping at the same time the running system to process incoming data is not always evident. Therefore, for the reprocessing, we recreated the complete PROBA2 system on new servers (shown in Figure 32), updated all software on them and ran thorough tests. We then performed the reprocessing on the new hardware, and, once it was completed, we migrated the operational tasks to this new server and continued on it.

This transfer to the new servers was performed in June 2020. Due to the measures taken to manage the COVID-19 pandemic, this was not easy to coordinate. Only a few of the PROBA2 colleagues were allowed to come on site together, but after a very long working day the migration was complete and the PROBA2 pipelines were up and running again, with the newly calibrated data online. Afterwards also the remote archive at the ESAC facility in Spain was updated with the newest data.

Astronomy and Astrophysics

The Large Sky Area Multi-Object Fiber Spectroscopic Telescope

The Large Sky Area Multi-Object Fiber Spectroscopic Telescope (LAMOST) is a National Major Scientific Project undertaken by the Chinese Academy of Science that started about a decade ago. This unique instrument is located at the Xinglong station, situated south of the main peak of the Yanshan mountains in the Hebei province of China (Figure 33). It combines a large aperture (4 m telescope) with a wide field of view (circular region with a diameter of 5 degrees on the sky) that is covered with 4000 optical fibres. These fibres are connected with 16 spectrographs (250 fibres each), making this instrument the ideal tool to obtain spectroscopic observations for a large number of objects in a homogeneous and efficient way.

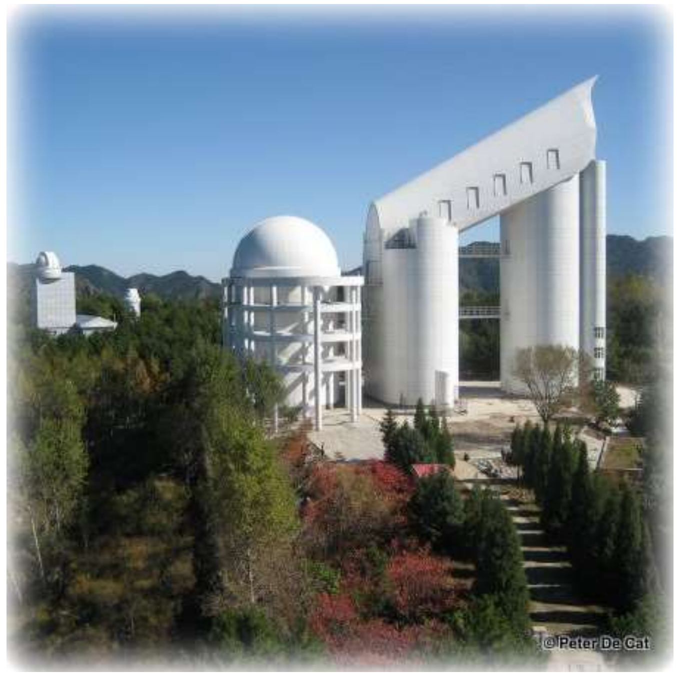

Figure 33: View on LAMOST, located at the Xinglong station in China.

The LAMOST Extra-GAlactic Survey (LEGAS) and the LAMOST Experiment for Galactic Understanding and Exploration (LEGUE) were the two initial scientific driving forces for the LAMOST project. At that time, the space mission Kepler was collecting continuous light curves with an unprecedented precision for objects in a fixed field of view in the constellations Lyra and Cygnus. This was done with the aim to detect Earth-like planets around solar-type stars using the transit method. It was soon realised that the observation of the so-called Kepler field with LAMOST would be a pure scientific goldmine, being a win-win opportunity for both communities: it would provide the Kepler community with the data needed for a homogeneous spectroscopic determination of stellar parameters for objects observed by the Kepler mission while the LAMOST community could benefit from high-precision results derived from data obtained elsewhere for Kepler objects to calibrate the LAMOST results. Therefore, the proposal of the LAMOST-Kepler (LK) project, initiated by P. De Cat from ORB-KSB, was well received in 2010. The project unites one Belgian (ORB-KSB), two Chinese (BNU, NAOC), one Italian (INAF-Catania), one Polish (University of Wrocław), and two American (Steward Observatory, Appalachian State University) partner institutes and is subdivided into a European, Asian, and American team. The members of these groups use independent methods to analyse the spectra collected as part of the LK project. The collaboration celebrated its 10th anniversary in 2020. A general overview of the LK project is given by Fu et al. (2020). In what follows, we highlight the main contributions linked to ORB-KSB research and activities.

Low-Resolution Spectra

The first observations for the LK project were already done during the test phase of LAMOST in early 2011. The scientific observations of the so-called pilot survey began on 24/10/2011 while the first phase, the ‘regular survey', started about one year later on September 28, 2012. In this five-year period, only single-shot low-resolution spectra (LRS) with a spectral resolution of about 1800 covering optical wavelengths ranging from 370 nm to 900 nm were gathered.

Kepler Field

De Cat et al. (2015) give a detailed description of the LK project. They published the first version of the database of LRS spectra that were obtained in this context after the completion of the first round of observations. By the end of 2014, the 14 partly overlapping LAMOST footprints, that were selected to fully cover the Kepler Field (LK footprints; blue dotted circles on Figure 34) all had been observed at least once under good meteorological conditions. At that time, the database consisted of 101,086 pipeline-reduced LRS gathered for 80,447 unique objects, including 42,209 for which observations from the Kepler mission are available (21.1% of the full Kepler sample). For 17,114 objects, more than one LRS was ready-to-use, making it possible to check the internal consistency of the results of the analysis methods of the different groups of the LK collaboration.

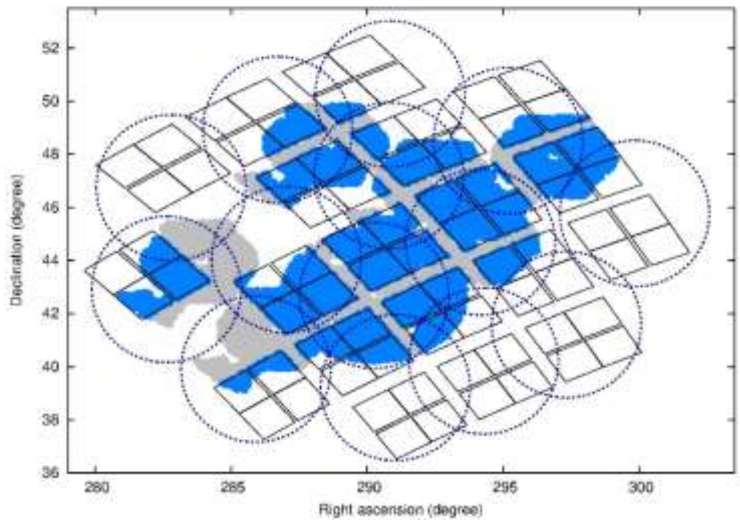

Figure 34: Visualisation of the Kepler field. The areas surrounded by a full black line indicate the position of the Kepler CCDs on the sky. The 14 LAMOST footprints used to gather LRS are represented by blue dotted circles. The stars that have been observed during the testing phase of the medium-resolution spectrographs on plates that have overlap with Kepler CCDs are given with dots (light blue for stars on Kepler CCDs).

The Asian team used the LAMOST Stellar Parameters pipeline (LASP) to analyse spectra from the LK database. With this technique, they derived values for atmospheric parameters (effective temperature T_{eff}, surface gravity log *g*, metallicity [Fe/H]) and the heliocentric radial velocity v_{rad} from 61,226 LK-LRS of 51,406 stars. The external calibration of the LASP results was done by comparing them to literature values obtained from high-resolution spectra or with asteroseismic techniques for stars in common. The mean errors on T_{eff}, log *g*, [Fe/H] and v_{rad} were found to be 2.8%, 0.22 dex, 0.15 dex, and 18 km s^{-1}, respectively. A statistical analysis of the stellar parameters led to the discovery of a sample of stars of interest, including nine very metal-poor candidate stars ([Fe/H] < -2.0 dex), and 18 high-velocity candidate stars ($|v_{rad}| > 300$ km s^{-1}).

The European team adapted the code ROTFIT to the specifications of the LK-LRS for the determination of stellar parameters by exploiting a homogeneous collection of more than 1000 real star spectra (Frasca et al. 2016). Stellar parameters could be determined for 51,385 stars from 61,753 LK-LRS. Their overall accuracy was estimated to be 3.5% for T_{eff}, 0.3 dex for log g, 0.2 dex for [Fe/H], and 14 km s^{-1} for v_{rad}, comparable to those found with LASP. On top of these parameters, they also provide an estimate of the projected rotational velocity v_{sini} for fast rotating stars (v_{sini} > 120 km s^{-1}). They found 442 chromospherically active stars in the sample based on the detection of line filling or emission in their H□and/or CaII IRT profiles. One of them, the K1V star KIC8749284, is believed to be an accreting star.

The American team presented MK spectral classifications determined from LK-LRS with the automatic classification code MKCLASS, that was developed specifically for this purpose (Gray et al. 2016). It is based on the classification procedures that are followed by humans. MKCLASS enables to classify in the temperature dimension with the precision of 0.6 spectral subclass, and in the luminosity dimension with the precision of about 0.5 luminosity class. The identifier was successfully applied to 81,171 LK-MRS. They found that 34.6% of the stars with spectral types between A4 and F1 in their sample are classified as Am stars (chemically peculiar stars showing an under-abundance of certain light elements and an excess of metals). This is in excellent agreement with previous studies. Furthermore, they identified 32 new candidate barium dwarfs (FGK-type dwarfs showing enhanced abundances of s-process elements) and 132 λ Bootis stars (chemically peculiar stars showing unusual low abundances of iron peak elements).

Zong et al. (2018) updated the database of LK-LRS after the completion of the second round of observations, coinciding with the end of the first phase of the regular survey (June 2017). By that time, all the LK footprints were observed at least twice. The number of available spectra more than doubled to 227,870 LK-LRS for 156,390 individual objects, permitting determining spectral parameters for 32.8% of the Kepler sample.

K2 Fields

After about four years of operation, a second reaction wheel of the Kepler mission failed on 11/05/2013. The telescope could no longer continue to point ultra-precisely towards the original Kepler field. The mission was therefore redefined: it received the name K2 and started to observe fields of the same size along the ecliptic plane in campaigns of typically 80 days. Observations were performed in 20 campaigns (C0-C19) before the spacecraft ran out of fuel on 30/10/2018, leading to the retirement of the mission.

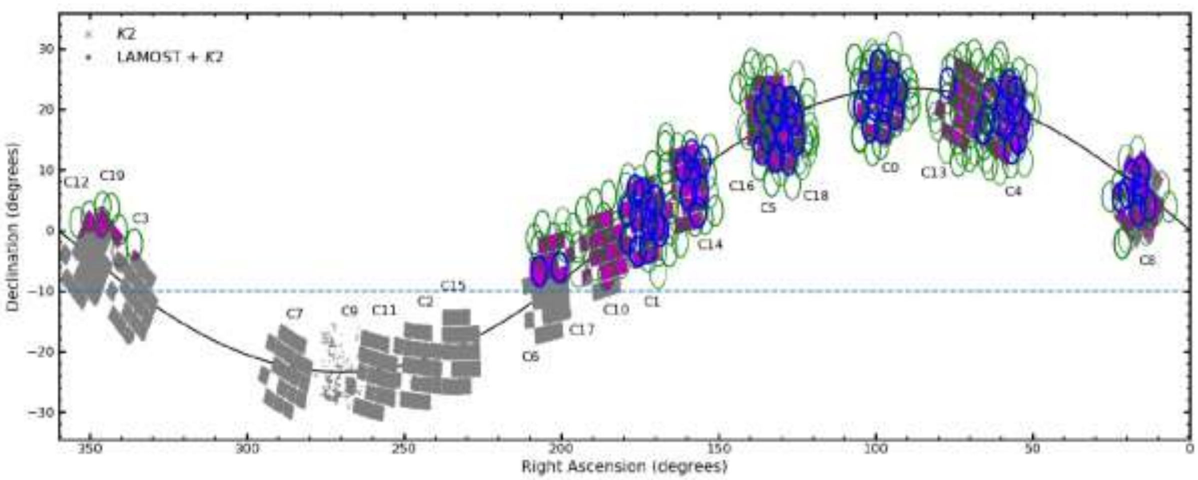

Figure 35: Sky distribution of K2 targets (grey) and LAMOST sources (magenta) in the 20 campaigns of the K2 mission for which LRS are available in DR6. The sky coverage of the footprints observed in the LK2 project and LAMOST general survey within the K2 fields are indicated by blue and green circles, respectively. The solid line represents the ecliptic plane. The cyan dashed line at -10° indicates the declination limit for LAMOST observations. (Figure from Wang et al. 2020)

In 2015, the LK project has been extended to also include targets within the K2 fields. This part of the project is referred to as the LAMOST-K2 (LK2) project. By the end of 2018, a total of 126 LK2 plates were observed (Figure 35; Wang et al., 2020). After cross-matching with the catalogue of 6th data release of LAMOST (DR6), 160,619 usable spectra of 84,012 objects were found, most of which had been observed more than once. The standard LAMOST pipeline (LASP) was successful in deriving values for $T_{eff,}$ log g, [Fe/H] and v_{rad} from 129,974 spectra of 70,895 objects. The internal uncertainties were estimated to be 81 K, 0.15 dex, 0.09 dex, and 5 km s^{-1}, respectively, when derived from a LAMOST LRS with a signal-to-noise ratio in the Sloan g-band (SNRg) of 10. The external accuracy was assessed by comparing the parameters of targets in common with the Apache Point Observatory Galactic Evolution Experiment (APOGEE) and Gaia surveys. In general, the comparisons reveal linear dependencies in the differences. A final calibration is derived, combining external and internal uncertainties for giants and dwarfs separately.

Medium-Resolution Spectra

After a testing phase of one year, also medium-resolution spectrographs both in single-shot and time-series mode are included in the standard observation schedule since the start of the second phase of the regular survey of LAMOST in September 2018. The corresponding medium-resolution spectra (MRS) have a spectral resolution of about 7500 and are obtained in a blue and red arm covering the wavelength ranges 510–540 nm and 830–890 nm, respectively. The increased spectral resolution allows to additionally infer individual abundances of several individual elements observed in the spectra.

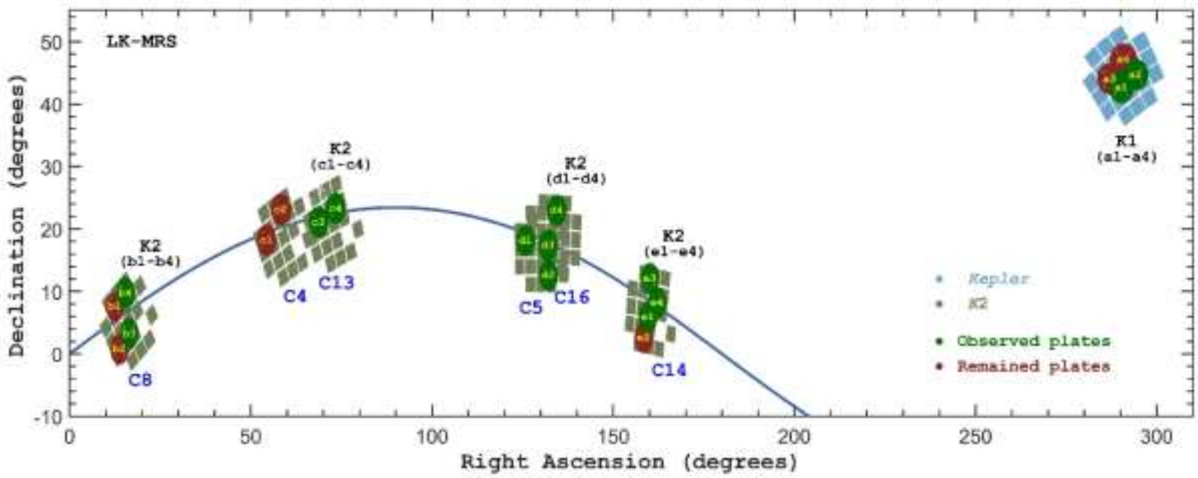

Figure 36: Sky coverage of the footprints of the LK-MRS project (a1-4, b1-4, c1-4, d1-4, e1-4; green for observed and red for unobserved) on top of the targets observed by campaigns of Kepler (K1; light blue) and K2 (C8, C4+C13, C5+C16, C14; grey) campaigns. The solid line represents the ecliptic plane. (Figure from Zong et al. 2020).

We started using the medium-resolution spectrographs to create time series of typically 60 LAMOST MRS in a time span of five observing seasons (September 2018 to June 2023) for more than 50,000 stars. These targets are within 20 LAMOST footprints distributed across the Kepler field and six northern K2 campaigns, with each plate containing up to 3000 targets (Figure 36). During the first year of observations, already 13 plates were visited 223 times during 40 individual nights (Zong et al., 2020). In total, 281,300 spectra of high-quality were analysed by the members of the Asian team. The standard LAMOST pipeline (LASP) was successful in deriving values for T_{eff}, log *g*, [Fe/H] and v_{rad} for 258,797 spectra of 21,053 targets. Their internal uncertainties are found to be 100 K, 0.15 dex, 0.09 dex, and 1 km s^{-1}, respectively, when derived from a LAMOST MRS with SNRg = 10. Compared to results obtained with LK-LRS spectra, it is clear that the v_{rad} determination benefits from the increased spectral resolution while the accuracy of the atmospheric parameters remains similar due to the limited wavelength coverage of the LAMOST MRS. The sample of studied objects has ~70%, ~95%, and ~7.2% targets in common with the LAMOST LRS survey, Gaia, and APOGEE, respectively. In general, the parameters derived from the LK-MRS are consistent with those obtained from the LK-LRS and APOGEE spectra, but the scatter increases for decreasing log *g* when compared with the measurements from APOGEE. For a small fraction of objects, a large discrepancy is found with the Gaia values of Teff that seems to be linked to large values of the line-of-sight extinction (AG > 0.8 mag). Comparisons of the v_{rad} values with those of LK-LRS, Gaia, and APOGEE show nearly Gaussian distributions with mean values of -3.50 km s^{-1}, 1.10 km s^{-1} and 0.73 km s^{-1}, respectively.

In 2020, the members of the European team started working on the LAMOST MRS that are available in DR6 for stars that are observed during the testing phase of the medium-resolution spectrographs with plates that have overlaps with the position of the Kepler CCDs (dots on Figure 34). They are being analysed with an adapted version of ROTFIT (Frasca et al., in preparation).

Network Activities

The success of the LAMOST-Kepler project is partly thanks to the financial help of both the Belgian Science Policy (BELSPO) and the ASBL-v.z.w. for the organisation of network activities. Such activities are crucial to optimise scientific achievements. Indeed, work visits permit to work efficiently on scientific data and to gain hands-on experience with the analysis methods of collaborators while scientific meetings create the opportunity to advertise results and to get inspired by the work of others.

Figure 37: Logo of the Belgo-Chinese project "LAMOST Observations in the Kepler field", financed by BELSPO (BL/33/FWI20).

BELSPO financed the Belgo-Chinese project 'LAMOST observations in the Kepler Field' (LOK) in the period 2016–2018 (BL/33/FWI20; Figure 37). It allowed the ORB-KSB to host the second international LAMOST-Kepler's workshop in the summer of 2017 (31/07/2017-03/08/2017), uniting 46 registered participants originating from 15 different countries. They gave a total of 36 oral presentations spread over 5 scientific sessions. The LOK project also sponsored the work visits of P. De Cat to Beijing (08–22/12/2018) - where he received the title 'LAMOST invited professor of 2018' to honour him for his large contribution to the global success of LAMOST -, and of Y. Pan and J.T. Wang to Europe (18/10/2018-06/12/2018). These PhD students of the Chinese collaborator J.N. Fu stayed in Brussels for 5 weeks and visited the Polish collaborator J. Molenda in Wrocław for 2 weeks.

The financial help of the ASBL/VZW made it possible for three other students of J.N. Fu to stay at the ORB-KSB for a research visit of up to 3 months (Xiaohu Yang: 08/11/2010-07/12/2010 and 08/05/2012-03/08/2012; Zhihua Huang: 10/09/2013-10/11/2013; Ren Anbing: 15/09/2015-10/12/2015).

Publications:

'Lamost Observations in the Kepler Field. I. Database of Low-resolution Spectra', De Cat, Fu, Ren and 34 co-authors, 2015, ApJS 220, 19 (https://publi2-as.oma.be/record/2101)

'LAMOST Observations in the Kepler Field. Analysis of the Stellar Parameters Measured with LASP Based on Low-resolution Spectra', Ren, Fu, De Cat and 12 co-authors, 2016, ApJS 225, 28 (https://publi2-as.oma.be/record/2918)

'Activity indicators and stellar parameters of the Kepler targets. An application of the ROTFIT pipeline to LAMOST-Kepler stellar spectra', Frasca, Molenda-Żakowicz, De Cat and 7 co-authors, 2016, A&A 594, A39 (https://publi2-as.oma.be/record/3408)

'LAMOST Observations in the Kepler Field: Spectral Classification with the MKCLASS Code', Gray, Corbally, De Cat and 11 co-authors, 2016, AJ 151, 13 (https://publi2-as.oma.be/record/2092)

'LAMOST Observations in the Kepler Field. II. Database of the Low-resolution Spectra from the Five-year Regular Survey', Zong, Fu, De Cat and 19 co-authors, 2018, ApJS 23, 30 (https://publi2-as.oma.be/record/3957)

'Phase II of the LAMOST-Kepler/K2 Survey. I. Time Series of Medium-resolution Spectroscopic Observations', Zong, Fu, De Cat and 20 co-authors, 2020, ApJS 251, 15 (https://publi2-as.oma.be/record/5283)

'LAMOST Observations in 15 K2 Campaigns. I. Low-resolution Spectra from LAMOST DR6', Wang, Fu, Zong and 12 co-authors (including De Cat), 2020, ApJS 251, 27 (https://publi2-as.oma.be/record/5283)

'Overview of the LAMOST-Kepler project', Fu, De Cat, Zong and 9 co-authors, 2020, RAA 20, 167 (https://publi2-as.oma.be/record/5284)

The Flux-Weighted Gravity-Luminosity Relation in Classical Cepheids

Defining the Flux-Weighted Gravity-Luminosity Relation

The gravitational acceleration is defined as $g = GM/R^2$ where M is the mass of the object and R its radius and its mean value for the Earth is the well-known value of about 9.81 m/s². This formula applies to all bodies and, for the Sun, it is about 274 m/s². Astronomers often use cm as the unit for this quantity and take the $_{10}$log of its value, and so you will often see for the Sun a value of log g = 4.44 in the literature.

In 2003, Kudritzki et al. remarked that certain classes of stars (the so-called blue supergiants) during certain phases in their evolution evolved at nearly constant mass and luminosity (L). As luminosity is related to stellar parameters according to the Stefan-Boltzmann law, $L \propto R^2\ T_{eff}^4$, it follows that the quantity $g_F \stackrel{def}{=} g/T_{eff}^4$ is also constant, and they called it the 'flux-weighted gravity'.

As stellar evolution theory predicts that more massive stars are more luminous as $L \propto M_\alpha$ and with the definition of the bolometric magnitude M_{bol} = -2.5 log (L) + *constant*, it follows that one expects a relation of the form $-M_{bol} = a \log (g_F) + b$ to hold, where a and b are constants, and they called this the 'flux-weighted gravity-luminosity' relation (FWGLR). If this relation can be calibrated from known objects, one has a method to determine distances. This is so as gravity and effective temperature (and thus g_F) can be determined by observation from high-resolution spectra that are being analysed with model atmospheres. From the by-observation determined g_F value, one gets the absolute magnitude. If one has a measure of the observed luminosity m_{bol}, then the distance follows from $m_{bol} - M_{bol} = 5 \log d - 5$, where the distance d is in parsec. The concept of the FWGLR was explored in Kudritzki et al. (2003, 2008, 2016).

The Potential of the Flux-Weighted Gravity-Luminosity Relation for Classical Cepheids

Classical Cepheids (CCs) are the cornerstone of the distance ladder in the Universe. They are bright and through the period-luminosity (PL) relation they tie the distance scale in the nearby universe and that further out via those galaxies that contain both Cepheids and Supernova of type Ia (see Riess et al. 2019) .

Anderson et al. (2016) demonstrated for the first time that theoretical pulsation models for CCs also followed a tight FWGLR, which is in fact tighter than the PL relation, and that there was a good correspondence between observed g_F and pulsation period for a sample of CCs.

The potential of the FWGLR for CCs was explored in Groenewegen (2020b). To apply the FWGLR one needs gravity, effective temperatures and luminosities. The topic of bolometric luminosities in CCs was discussed in Groenewegen (2020a), based on the sample introduced in Groenewegen (2018).

Photometry from the ultraviolet to the far infrared was collected from the literature for over 450 CCs. The resulting spectral energy distribution was then fitted with a model atmosphere to derive the photometric effective temperature and luminosity. Interstellar reddening was taken from the literature and the distance was as much as possible taken from the Second Data Release of Gaia (Gaia Collaboration 2018).

Figure 38 shows examples of model fits where there is not only available photometry (the circles in the top panels) but also mid-IR spectra (the bottom panels). The fits are extremely good, and the error in luminosity is entirely determined by the error in the adopted distance or parallax.

Model atmospheres have been fitted to high-resolution optical spectra for hundreds of CCs. Such fitting results in the determination of the effective temperature, the gravity and the metallicity. CCs with metallicity determinations were collected by Groenewegen (2018) and the corresponding values for log g and T_{eff} were collected from the literature in Groenewegen (2020b).

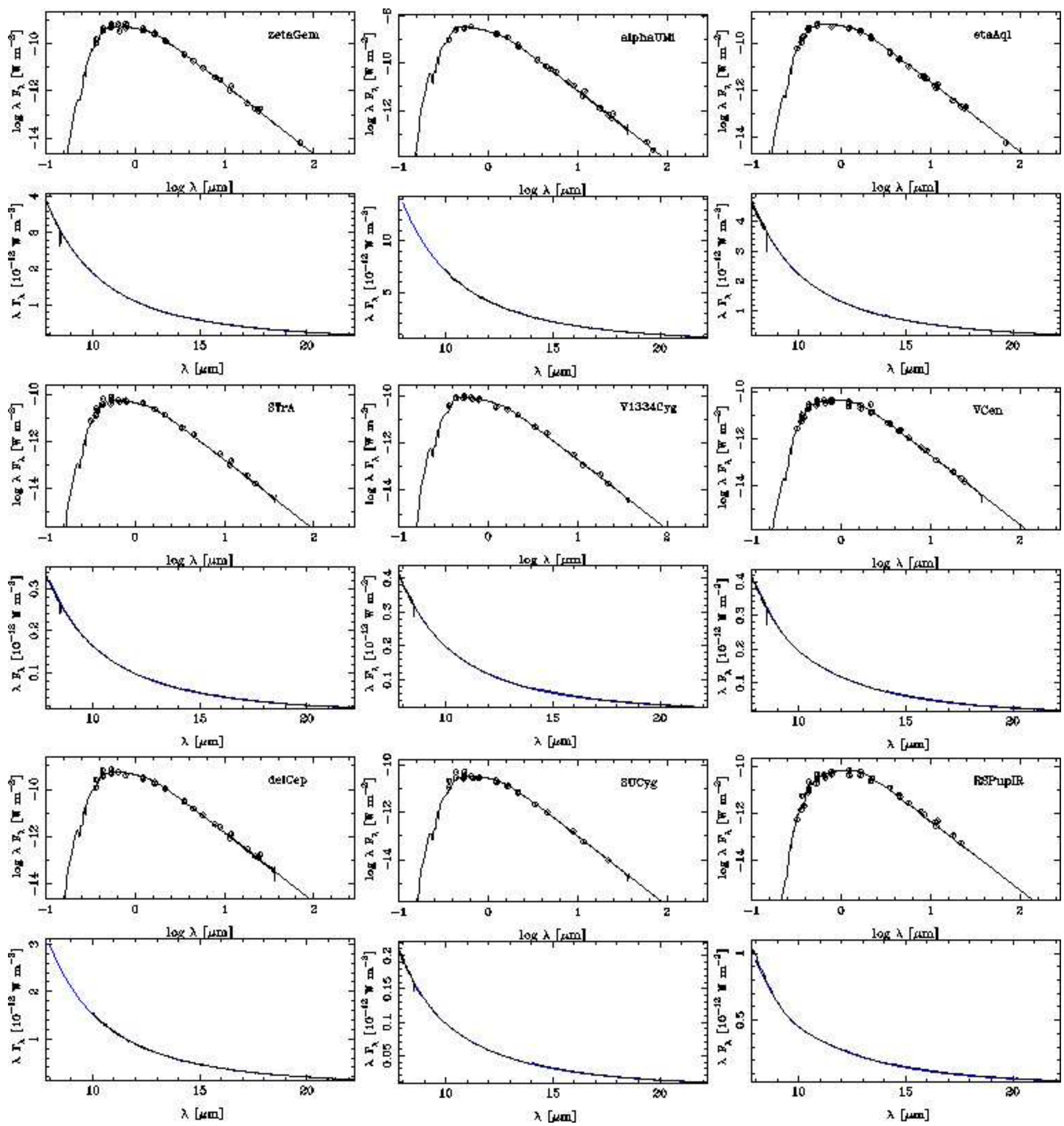

Figure 38: Model fits (the solid lines) to the spectral energy distribution (top panel) and mid-infrared spectra of some CCs. From Groenewegen (2020a).

Figure 39 illustrates the theoretical picture in the top panels: the tight correlation between M_{bol} and g_F, and g_F and period, based on the models of Anderson et al. (2016).

The best fits are: $M_{bol} = (3.35 \pm 0.02) (\log g_F - 3.0) + (-2.975 \pm 0.012)$ with a rms scatter of 0.16 mag, and $\log g_F = (-0.834 \pm 0.011) \log P_0 + (3.402 \pm 0.011)$ with a rms of 0.09 dex, shown as the green lines in Figure 39. The fundamental period in days is represented by P_0.

The latter relation can serve in several ways: to give a first guess for log *g* in spectroscopic analysis based on the pulsation period and an estimate of the effective temperature, or as a posteriori check on published log g values.

The bottom panels of Figure 39 show the observational picture. The left-hand panel confirms the general trend of the theory but also that there are quite some outliers. Most of them are linked to a single paper, who derived very low log *g* values for some objects (see Groenewegen 2020b for details). The best fit is $\log g_F = (-0.80 \pm 0.03) \log P_0 + (3.43 \pm 0.03)$ with a rms of 0.16 dex, in very good agreement with the theoretically predicted relation.

The bottom right-hand panel shows the FWGLR. The best fit is

$M_{bol} = (2.93 \pm 0.13) (\log g_F - 2.5) + (-4.23 \pm 0.06)$

with a rms of 0.54 mag using 170 stars and is shown as the blue line in the figure. This is currently the best observational determination of the FWGLR for CCs.

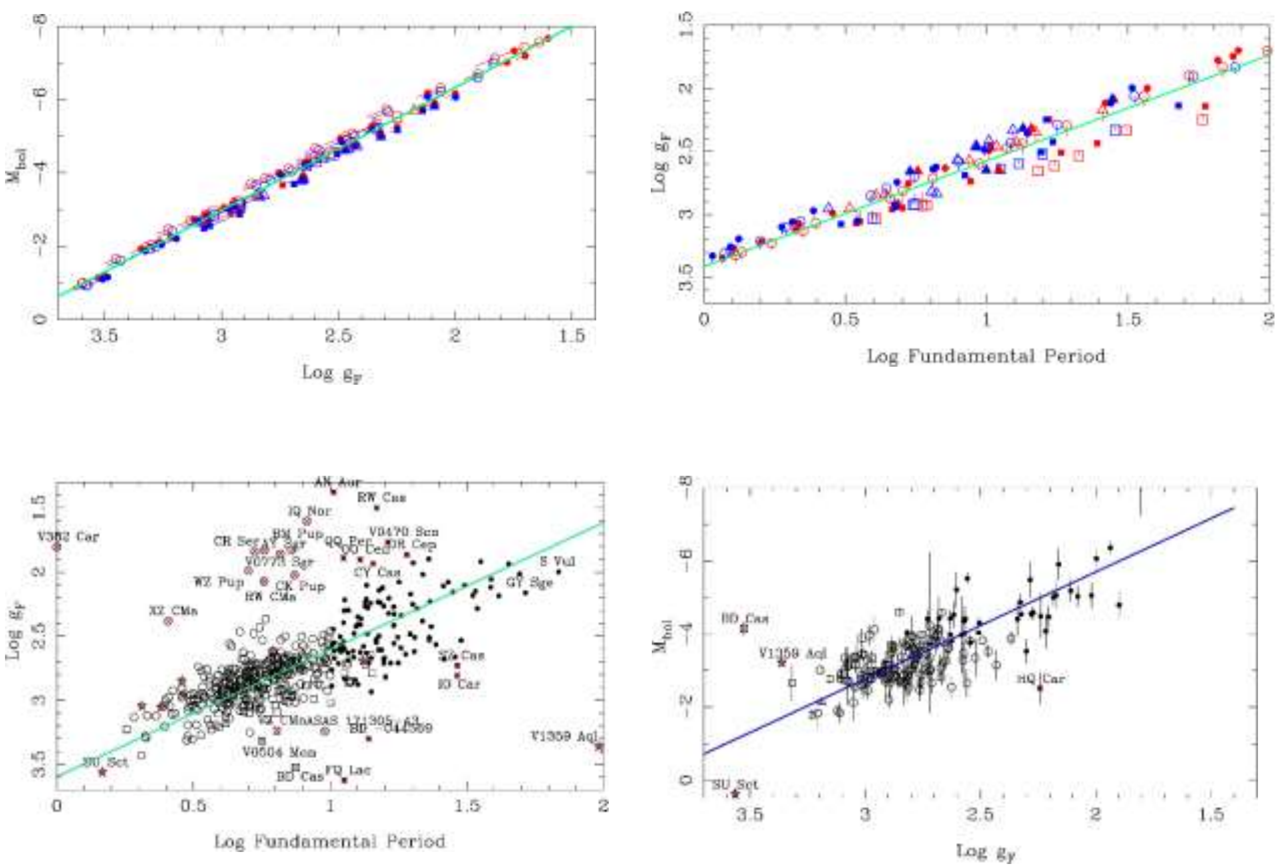

Figure 39: Top panels. The relation between M_{bol} and log g_F (left), and log g_F and fundamental period (right) based on the theoretical models of Anderson et al. (2016). The bottom panels show the relations based on observational data. Some outliers have been marked. See Groenewegen (2020b) for details.

The FWGLR has the potential to be an alternative to the classical PL relation in distance determination for CCs. In its current empirically best calibrated version, it is not. The scatter of 0.54 mag is larger than the 0.40 mag in the bolometric PL relation determined in Groenewegen (2020a) using the identical sample of stars, distances, and luminosities.

Future Gaia releases will provide several improvements (better distances, hence, bolometric magnitudes) and uniformly derived stellar parameters (from the Bp, Rp and RVS spectra) so that the FWGLR could prove to become an extremely powerful tool in Cepheid studies in the future.

References:

Anderson R.I., Saio H., Ekström S., Georgy C., and Meynet G. 2016, A&A 591, A8
Gaia Collaboration (Brown, A. G. A.) 2018, A&A 616, A1
Groenewegen M.A.T. 2018, A&A 619, A8 (https://publi2-as.oma.be/record/3775)
Groenewegen M.A.T. 2020a, A&A 635, A33 (https://publi2-as.oma.be/record/5042)
Groenewegen M.A.T. 2020b, A&A 640, A113 (https://publi2-as.oma.be/record/5043)
Kudritzki R.P., Bresolin F., and Przybilla N. 2003, ApJ 582, L83
Kudritzki R.-P., Urbaneja M.A., Bresolin F., et al. 2008, ApJ 681, 269
Kudritzki R.-P., Castro N., Urbaneja M.A., et al. 2016, ApJ 829, 70
Riess A.G., Casertano S., Yuan W., Macri L.M., and Scolnic D. 2019, ApJ 876, 85

COBRaS – The Cyg OB2 Radio Survey

COBRaS is a survey that uses the e-MERLIN radio telescopes to make a high-resolution map of the radio sources in the Cyg OB2 stellar association. This stellar association is of special interest as it is one of the most massive ones in our Milky Way, containing many young and massive stars. Cyg OB2 also contains a lot of interstellar dust that prevents us from penetrating deeply in the association at optical or infrared wavelengths. Radio observations, however, do not suffer from this extinction and therefore provide us an unprecedented look at this intriguing association.

Cyg OB2

The Cygnus X region (Figure 40) is one of the richest stellar nurseries in our Milky Way. It contains numerous young open clusters, compact H II regions and star formation regions, as well as a supernova remnant, and a super-bubble blown by the combined stellar winds of the massive stars. At the core of Cygnus X, and located behind the 'Great Cygnus Rift', lies Cyg OB2, one of the most massive stellar associations in our Milky Way. The stars in this association are, astronomically speaking, very young with ages ranging between 1 and 7 million years. Cyg OB2 contains both lower-mass stars as well as a large number of the hottest, most massive and most luminous stars – those of spectral type O and B.

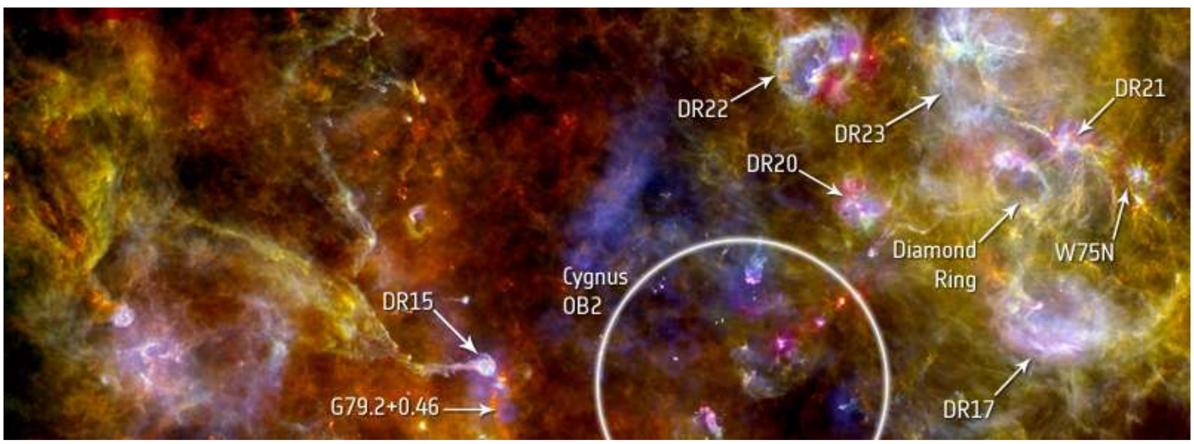

Figure 40: An infrared view of the Cygnus X region with, at its heart, the Cyg OB2 association.

The energy and momentum of the combined stellar winds of these hot stars shape the interstellar material around them. By compressing this material they can stimulate more stars to be born, or by blowing away the material they can actually hinder further star birth. Clusters and associations like Cyg OB2 therefore play an important role in the ecology of our Milky Way.

Because of its exceptional nature, Cyg OB2 and the wider area around it has been the object of a number of surveys, going from X-rays through infrared to radio wavelengths. The main problem with observing Cyg OB2 is that it has a high visual extinction, due to the large amounts of interstellar dust. By observing at longer wavelengths, the effect of this extinction is reduced. At radio wavelengths, the extinction is even negligible, making radio observations ideal for studying Cyg OB2.

e-MERLIN

e-MERLIN is an array of seven linked radio telescopes across the UK (Figure 41), operated by the University of Manchester on behalf of the UK Science and Technology Facilities Council. e-MERLIN is an upgrade of MERLIN (Multi-Element Radio Linked Interferometer Network).

The angular resolution of a single radio telescope is quite bad, but, by combining a number of radio telescopes in an array, the resolution is improved. Using this interferometric technique the resolution becomes that of a virtual telescope that has a diameter equal to the largest baseline between two telescopes in the array. A huge amount of data needs to be exchanged and processed for this interferometric technique to work, and the old microwave connections of MERLIN were therefore replaced by optical fibre links. The detectors on each of the telescopes were also upgraded, leading to a factor 30 increase in sensitivity.

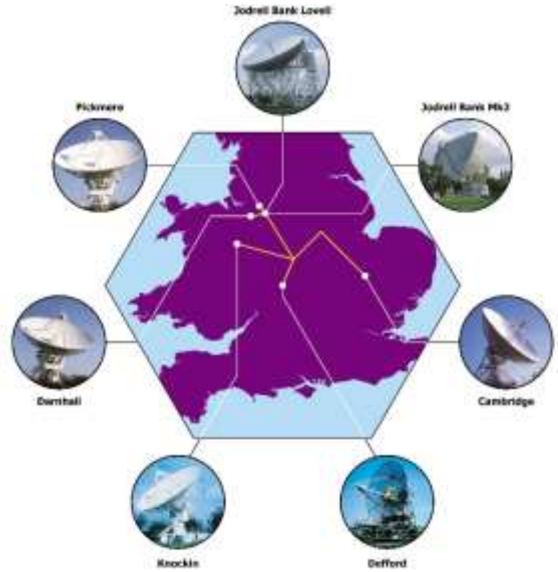

Figure 41: The locations of the seven radio telescopes making up the e-MERLIN radio interferometer. Credit: University of Manchester.

COBRaS

The Cyg OB2 Radio Survey (COBRaS) is a Legacy project that uses e-MERLIN to do an extensive radio survey of the central region of the Cyg OB2 association. It collects observations at L-band (20 cm; 1.5 GHz) and at C-band (6 cm; 5 GHz). It provides a radio survey of this region that goes substantially deeper than the previous radio surveys and provides a higher angular resolution. As a Legacy project, it was awarded 294 hours of observing time. The Survey is a collaboration between scientists from 18 different institutes, most of them in the UK, including the Royal Observatory of Belgium.

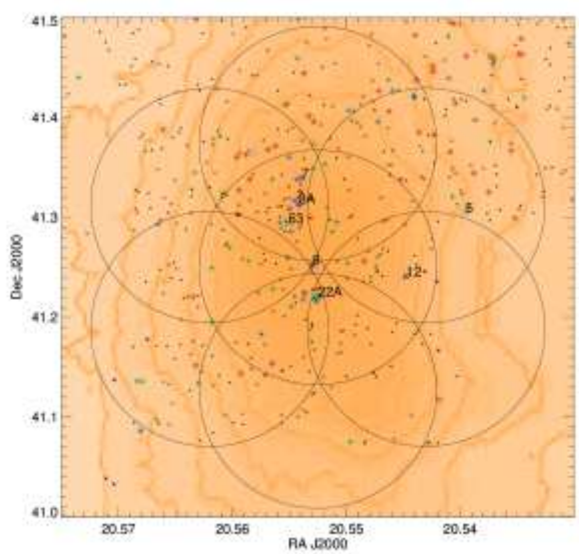

Figure 42: The area on the sky covered by the L-band observations of COBRaS. The background colour figure is the stellar density distribution from the infrared 2MASS survey. Various symbols indicate known stars from different catalogues.

The Survey was a long-term effort. The planning began in 2008, and the first data were collected in 2014. Figure 42 shows the seven pointings that were used to cover the inner part of Cyg OB2. The data reduction of the 42 hours of L-band observations took a considerable effort, as 940 GB of data had to be processed. Specific software was developed for the flux measurements. A first publication, limited to a few O and B-type stars was out in 2016, and the first full-Survey paper appeared in 2020.

The Survey reaches a noise level of 21 µJy and an angular resolution of 180 milliarcsec. Of the 61 sources detected, 27 can be associated with sources in other catalogues.

Among them, there are a number of colliding-wind binaries. The very luminous stars in Cyg OB2 have such a high luminosity that they blow away their surface layers by the radiation pressure, thus creating a stellar wind.

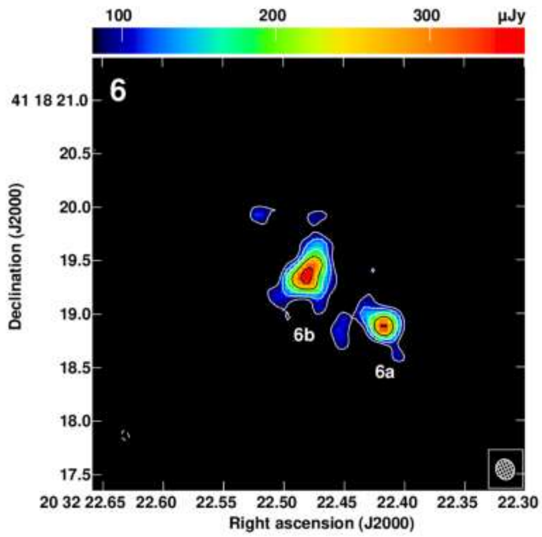

Figure 43: Cyg OB2#5 is a multiple-star system. Although we cannot detect the individual stars, we see the radio emission of two colliding-wind regions (Morford et al. 2020, A&A 637, A64).

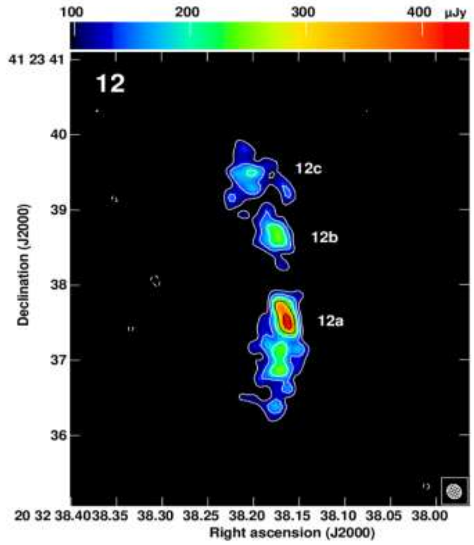

Figure 44: The morphology of this source strongly suggests that it is an Active Galactic Nucleus (AGN), far beyond our Milky Way (Morford et al. 2020, A&A 637, A64).

When two such stars are in a binary system, their winds must collide at a certain point. Around the collision shocks, electrons are accelerated to relativistic speeds and emit synchrotron radiation. In this way, we can detect these colliding-wind binaries. The most spectacular case is the system Cyg OB2 #5, which consists of four stars. On Figure 43, two of the colliding-wind regions in this system can be seen.

Another interesting detection is that of Cyg OB2 #12. This is a candidate Luminous Blue Variable (LBV) star. LBVs are massive stars that show variability in a range of amplitudes on different timescales. This variability can profoundly affect the mass loss of these stars. Cyg OB2 #12 emits radiation at radio wavelengths because of the free-free emission in its ionised stellar wind: as an electron passes near an ion, it can lose energy, which is then emitted as radiation at radio wavelengths. The radio flux of Cyg OB2 # 12 is variable, which is suspected to be due to inhomogeneities in its stellar wind.

We also detect two young stellar objects (YSOs), as well as a source that shows a very large change in its L-band flux over the 15-day period between epochs. This suggests a possible flaring event in a pre-main sequence type object or a potential small-period massive star binary system imaged at significantly different orbital phases.

As the absorption at radio wavelengths in negligible, we can actually see through the Milky Way and detect extragalactic objects behind it. Figure 44 shows an example of an Active Galactic Nucleus (AGN). Although the object was not previously catalogued, we can give it this classification based on its morphology: it clearly shows the double-lobed structure (due to jets) around the galaxy in the centre.

Finally, thirty-three sources have been detected for the first time. But, without further information, only a limited number of conclusions can be drawn for these objects.

At the moment, the Survey is far from finished. A much larger amount of observing time will be used to obtain C-band observations of the same area of Cyg OB2. With flux information at two wavelengths, we will be better able to classify the sources that have been detected, and we will undoubtedly detect new ones as well.

The Belgian Repository of Fundamental Atomic Data and Stellar Spectra

Brain-be BRASS project

Accurate atomic line transition data are fundamental input parameters in astrophysics. Spectrum synthesis calculations are of central importance for the development of complex models that describe, analyse and explain stars and planets, their internal structures, atmospheres, and evolution in relation to their environments. Uncertainties and errors in adopted fundamental atomic data may systematically propagate throughout all fields of astrophysics, from star-planet formation to large-scale galactic evolution. It is very difficult to obtain accurate fundamental atomic data of astrophysical interest from laboratory measurements. There are only a limited number of repositories that offer these important atomic data values. The atomic repositories are often complementary rather than redundant, and can provide incomplete or inaccurate information. Important quality assessments of the provided atomic data values are scarce (and mostly absent), which very much complicates the validation of results that follow from their application.

The BRASS project was a large scientific collaboration (The BRASS Team 2015–2020) on astrophysics research of the Royal Observatory of Belgium (ORB-KSB), the University of Leuven (KULeuven), the European Southern Observatory (ESO) at Paranal, Chile, and the Université Libre de Bruxelles (ULB), the University of Antwerp (UA), and the Vereniging voor Sterrenkunde (VVS).

Science goals

The main objective of BRASS was to properly assess the quality of input atomic data required in astrophysics research. In particular, atomic line transition data are fundamental parameters for quantitative stellar spectroscopy. Emphasis was set on the development and application of new methods for removing and reducing systematic errors in atomic datasets offered in the literature and the largest on-line repositories by comparing very high-quality observed stellar spectra with state-of-the-art theoretical spectra.

The objective of BRASS was to provide the largest systematic and homogeneous quality assessment of fundamental atomic data to date in terms of wavelengths and atomic species. The BRASS Team has combined very high-quality stellar spectra, observed with modern high-resolution spectrographs, with carefully selected fundamental atomic data required for computing accurate theoretical stellar spectra. The research has compared observed and theoretical spectra in detail, on a line-by-line basis, to assess the validity and quality of the selected atomic input data. The theoretical spectra were computed with advanced radiative transfer codes that use modern atmosphere models of stars of the K, G, F, A and B stellar spectral types.

An important goal of BRASS also was to deliver an open dynamic data platform with standardised data presentations allowing user interaction with the integrated (hyperlinked) investigated atomic data, in combination with advanced graphics display tools that offer powerful new functionalities for stellar spectroscopic research (see Figure 45).

Figure 45: BRASS Spectral Data Interface (SBDI) showing the solar spectrum (central top panel) and the BRASS benchmark HERMES spectrum of solar-like star 51 Peg (central bottom panel). The red and blue interactive labels mark identified absorption lines with atomic and line property data tables shown in the right-hand sub-panels. Atomic quality assessment pages are displayed under the central Atomic Data Quality tab by clicking on the 'View data quality' link in the red or green line data tables.

To achieve these goals, the following questions were addressed:

1. Can fundamental atomic data required for astrophysical spectroscopic research, but scattered across a large variety of online data repositories and in the scientific literature, be combined in a single open access database? What methods are required for uniformly combining these datasets? This goal has been accomplished by developing two methods for ordering atomic line data according to the traditional cross-matching method using transition wavelengths, and a more advanced novel approach that can account for unique electronic transition configuration information (see Figure 46 and Figure 47).

2. Can fundamental atomic data available in the repositories and literature combined in BRASS be quality-assessed as they are mainly produced in laboratory measurements and/or theoretical atomic structure and transition probability calculations with limited accuracy inherent to these (historical) production methods? This goal has been accomplished by offering atomic line data the BRASS Team thoroughly tested by comparing theoretical and observed stellar spectra. Extensive quality assessments of the selected atomic input data were performed using advanced radiative transfer spectrum synthesis calculations that were compared in detail to high-resolution Mercator-HERMES and KPNO-FTS spectra of FGK-type stars observed with very large signal-to-noise ratios (see Figure 48 and Figure 49).

3. Can the quality analysis results of tested atomic data comprehensively be provided in a user-friendly open access way? This goal has been accomplished with the development of advanced online access infrastructure offering the quality assessment results together with all input data. The validated datasets, combined with the observed and theoretical spectra, are interactively offered at http://brass.sdf.org. The combination of stellar spectra and atomic line data is a novel approach for its development providing a universal reference for advanced stellar spectroscopic research.

Results

The detailed comparisons of line transition data (or log(g_f)-values) retrieved from various atomic data repositories and the literature revealed remarkably large differences of up to 3 dex or more. The values can considerably change over time, sometimes within a few years, showing the importance of providing an external assessment of their accuracy (quality) by comparing to values obtained from contemporary high-quality astrophysical spectroscopic observations (Figure 46 and Figure 47).

By combining the atomic and spectroscopic data analyses of BRASS (i.e. using spectral line lists and high-quality benchmark stars) the project compiled an extensive list of reference spectral lines suitable for the quality assessment of the retrieved atomic datasets. The results of these complementary analysis methods determined the reliability of the atomic line data. In case the methods produced similar values within errors, the retrieved atomic data were considered reliable. Otherwise, one or more complicating factors could exclude them from further analysis.

Figure 46: The online BRASS Data Interface query page.

Figure 47: BRASS query results page for spectral lines sorted by transition wavelengths. The line data are cross-matched in BRASS using various atomic databases and the corresponding literature. References are also offered.

The objectives of the project were accomplished by performing a systematic analysis of the selected spectral lines in each FGK benchmark star. It resulted in the final list of 1091 spectral lines that were scrutinised and quantitatively compared between the various atomic data repositories and the observed stellar benchmark spectra. A subset of 845 atomic lines was retained having log(g_f)-values internally consistent with the astrophysical selection criteria. The ‘astrophysical’ values therefore have been used as benchmark values for quality assessing against those retrieved from the repositories and literature. In case the latter values were in agreement with the benchmark values they are recommended as reliable for advanced spectroscopic research.

The BRASS project has produced important new results with the development of novel methods for the quality assessment of atomic line data of central importance in modern astrophysical spectroscopic research. It provided accuracy assessment results of atomic log(g_f)-values required for theoretical modelling of high-resolution stellar spectra using seven FGK-type benchmark stars including the Sun. Astrophysical log(g_f)-values have been calculated for 1091 carefully selected unblended line transitions between 420 nm and 680 nm using two different methods. The agreement between both methods selected 845 lines suitable for the atomic quality assessments. An investigation of mean Δlog(g_f)-values (difference between literature and BRASS astrophysical log(g_f)-values) revealed large differences for lines with limited atomic data quality offered in the literature for $-3 \le \log(g_f) \le -0.5$ (Figure 48 and Figure 49).

Figure 48: An example of BRASS online page with the atomic data quality assessment results of the Ni I λ6598 line observed in seven BRASS benchmark spectra. The SBDI pages offer an overview of all atomic data quality results for each investigated line, including observed and theoretical line equivalent width values.

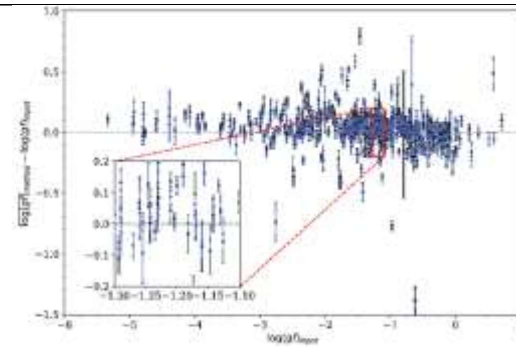

Figure 49: Mean Δlog(g_f)-values determined in BRASS plotted against literature log(g_f)-values. The difference values of astrophysical log(g_f)-values for 408 analysis-independent lines are calculated with the GRID (blue symbols) and COG (black symbols) atomic data quality assessment methods developed in BRASS.

The BRASS results showed that ∼53% of the quality-assessable lines have at least one literature log(g_f)-value in agreement with astrophysical values, while values for other lines can differ by more than 0.5 dex. Only ∼38% of the investigated Fe I lines have sufficiently accurate literature log(g_f)-values, while ∼70%-75% for other Fe-group element lines. The large percentage of theoretical Fe I log(g_f)-values with low quality offered in the literature mainly results from medium-strong and weak lines in atomic multiplets having lower transition levels above 4 eV, likely due to strong level mixing and inaccurate/incomplete energy levels. The results also revealed that the majority of Δλ-values are below ±0.01 Å, comparable to the high accuracy of the HERMES spectra wavelength scale.

The cross-matched atomic line datasets and the observed and theoretical stellar spectra have been incorporated in the online BRASS Data Interface (BDI). Users of the BRASS repository can query the Lines and Spectra BDI for atomic data downloading, including the corresponding literature references, with interactive display of dynamic plots for comparisons of database log(g_f)-values. The Spectra BDI offers interactive display tools for the (observed and theoretical) benchmark spectra, combined with line identification and atomic data values and line properties for user downloading. The BDI offers interactive atomic data quality assessment pages for the 1091 investigated spectral lines. It also offers tools for interactive line equivalent width measurements and comprehensive help pages and tutorial videos to its users.

Acknowledgments: The research for the present results has been subsidised by the Belgian Federal Science Policy Office under contract No. BR/143/A2/BRASS.

Outreach and Communication

Since March 16, due to the COVID-19 pandemics, the majority of the ORB-KSB staff are teleworking at 100%. Some events at the Observatory, such as the ASGARD balloon launch day, which was scheduled to take place at the Uccle site on April 23, 2020, were cancelled. As most of the ORB-KSB services, activities of the Communication and Information Service remained operational.

Calendar 2021 of the Royal Observatory of Belgium

Figure 50: Cover page of the 2021 calendar of the Royal Observatory of Belgium

At the end of December 2020, the Calendar 2021 of the Royal Observatory of Belgium (ORB-KSB) was published in the Planetarium shop. The purposes of the calendar are

- To present ORB-KSB to the public, with pictures related to the institute and its activities. A short text in French and Dutch describes each picture;
- To give to the public a list of astronomical events visible to the naked eye. This list is selected from the Yearbook of the Observatory.

The remaining copies of the 2021 Calendar (about one hundred copies) were given to Jean-Pierre Grootaerd, a member of the IAU outreach group.

Virtual exhibition at the Royal Palace 2020

Due to the COVID-19 pandemics, the 2020 edition of Science & Culture at the Royal Palace did not take place in situ, but online on the website http://www.royalbelspo.be/. The theme of this year was 'Birth'. The exhibition is a collaboration of the Federal Scientific Institutes, including ORB-KSB, which are joined by SCIENSANO, CINEMATEK, the National Geographic Institute (IGN) and the coordination unit of the BCCM Consortium (Belgian Co-ordinated Collections of Micro-organisms) of BELSPO.

Figure 51: Georges Lemaître visiting the Royal Observatory of Belgium with his students.

ORB-KSB shared media related to the birth of the universe and to George Lemaître, one of the founders of the Big Bang theory. In the 1950s, Georges Lemaître, as a professor of astronomy at the Université catholique de Louvain, visited the ORB-KSB telescopes every year with his students. During these visits, he gave a practical lecture in front of the Double Astrograph, the telescope with which several comets and asteroids were discovered.

Information to the Public, Website, News and Press releases

In 2020, the Communication and Information service replied to questions from authorities, public and the media sent by email (489, with 290 in French, 160 in Dutch and 39 in English), by telephone (191), by letter or fax (21), and on the social media of ORB-KSB (Facebook and Twitter, 27), hence 618 replies in total. 57 questions came from authorities (courts, police…) or particulars such as lawyers, with 41 in Dutch and 16 in French. As usual, most questions were about sunset and sunrise, astronomical phenomena, calendars and time, satellite and space station flybys and the history of ORB-KSB. Questions related to other fields of expertise such as seismology or space weather were forwarded to the respective services. Due to lockdown and COVID-19 safety measurements (put in place since March 12, 2020), visits were restricted and strongly discouraged.

In April 2020, there was a surge of questions and requests from the public related to the passing of Starlink satellites and to the planet Venus, which was particularly visible at night during this period. This surge of questions was probably related to the good weather at this moment (no rain for several months, not much clouds), and to the first lockdown period which gave more opportunities for people to observe the sky at night.

In 2020, the main website of ORB-KSB (https://www.astro.oma.be) got 397,423 visits on the main website (comprising the information service website) and a mean duration of 1 min 27 s per visit. 14 topics were published in the 'News' section of the ORB-KSB's website (always in three languages: NL/FR/EN), including 7 press releases. The most important news of this year was related to the launch, first light and first images of Solar Orbiter (see the highlights on page 12 and page 30) and to the participation of ORB-KSB to the ESA Hera mission with the instrument GRACE (see the highlight on page 14).

Social Media

On 31 December 2020, the ORB-KSB Facebook webpage had 1054 likes (with 256 new likes since end 2019), and the ORB-KSB Twitter account had 917 followers (311 new followers since end 2019). The themes of the published posts and videos are related to all services of the institutes, comprising shared posts from the Planetarium Facebook page, from the Seismologie.be Facebook page and Twitter account, from the EUI Twitter account and also from the Royal Belgian Institute for Space Aeronomy and the Royal Meteorological Institute.

The most successful ORB-KSB Facebook post of the year is related to the passing of the ISS in front of the Sun (see the highlight on page 9). On Twitter, it was an interview of Dirk Frimout on the occasion of Hubble's 30th anniversary of the year.

Some social media accounts linked to ORB-KSB gained a significant increase of views, likes and engagements in 2020. In March 2020, the Seismology and Gravimetry's Facebook page and Twitter account published a post which showed the significant decrease of seismic noise due to the COVID-19 lockdown (see highlight on page 20). This post got viral in the public and the media worldwide. The Planetarium's Facebook page also page got a significant increase of impressions, engagements and page likes from March 2020, which peaked in May, June and July 2020 (see highlight on page 61). This is related to an increase of educational and astronomical information posts on the page since the first COVID-19 lockdown, during which the Planetarium was closed.

The Planetarium

Daily Activities

The COVID-19 pandemic and the lockdown periods obviously had a significant impact on the activities and visitor numbers in the Planetarium in 2020. The Planetarium was closed to the public from mid-March to the end of June and again from mid-October to the end of November. In total, the Planetarium was open to the public for two and a half months at the beginning of the year under normal conditions (from January to mid-March), and then for four and a half months (from July to mid-October and then December) under reduced room capacity (often at 20% of the total capacity).

Only 20,383 paying visitors were welcomed. It should be noted, however, that the family public was largely present during the summer months and during the month of December, but this success was, of course, unable to compensate for the absence of school groups in the autumn and the months of complete closure.

A total of 828 sessions were given, divided between 83 school group courses, 6 workshops and 739 film screenings (individual visits, families, tourists). These figures, compared to a normal year such as 2019 (1657 sessions including 222 school group courses, 40 workshops and 1395 film screenings), give a clear idea of the impact of the school closure and lockdown periods on the Planetarium's daily activities.

The Facebook page continued its upward curve as the year 2020 ended with 2963 followers (+945 over the year) and 2846 likes (+899).

Special Activities

The number of science promotion, educational and cultural events that traditionally complemented the daily activities throughout the year was consequently much reduced in 2020. Nevertheless, the following can be listed:

- Educational posts on the Planetarium's Facebook: from March 27 to June 27, an educational post (e.g. create your own folding solar system) was posted almost daily (55 posts in total) on the Facebook, keeping in touch with the public, especially the younger ones.
- The *Facebook Watch Party* organised by the ESA/Hubble Public Information Office on the occasion of the Hubble Anniversary on April 24. The Planetarium actively participated by posting the filmed testimonies of Dirk Frimout, two scientists from ORB-KSB (Peter Van Hoof and Alex Lobel) and two amateur astronomers (Francis Meeus and Raoul Lannoy).
- The co-organisation of the *Brussels Planetarium Poetry Festival* on 11 and September 12.
- The online coordination of the ASGARD competition on 23–26 September.
- The special *Come-Back Musea* evenings organised by the Brussels Council of Museums on October 1 and 2.
- Participation in the Night of Darkness (*Nuit de l'Obscurité/Nacht van de Duisternis*) on 10 October 2020.
- Creation of online content for the *Dag van de Wetenschap* on November 22.
- <u>Room rental</u> (projection room or auditorium) on September 15 (Geography Olympiad) and October 17 (Astrophotography Fair).
- <u>Media interviews</u>: RTL-TVI (March 4), Bel-RTL (April 24), Radio-Vivacité (June 30), RTBF (December 21)

Annex 1: Publications

Publications with peer review

[1] Arnous, Ahmad ; Zeckra, Martin ; Venerdini, Agostina ; Alvarado, Patricia ; Arrowsmith, Ramon ; Guillemoteau, Julien ; Landgraf, Angela ; Gutierrez, Antonio ; Strecker, Manfred
Neotectonic Activity in the Low-Strain Broken Foreland (Santa Bárbara System) of the North-Western Argentinean Andes (26°S)
Lithosphere, 2020 issue 1, pp. 1-25 (2020). https://doi.org/10.2113/2020/8888588

[2] Auchere, F. ; Andretta, V. ; Antonucci, E. ; ManyOtherAuthors, X. ; Berghmans, D. ; Mampaey, B. ; Parenti, S. ; Verbeeck, C. ; Zhukov, A.N.
Coordination Within the Remote Sensing Payload on the Solar Orbiter Mission
Astronomy and Astrophysics, 642, pp. A6 (2020). http://dx.doi.org/https://doi.org/10.1051/0004-6361/201937032

[3] Baland, R-M ; Yseboodt, M ; Le Maistre, S ; Rivoldini, A ; Van Hoolst, T ; Dehant, V
The precession and nutations of a rigid Mars
Celestial Mechanics and Dynamical Astronomy, 132 issue 47, pp. 1-52 (2020). http://dx.doi.org/10.1007/s10569-020-09986-0

[4] Banerdt, W.B. ; Smrekar, S. ; Banfield, D. ; Giardini, D. ; Golombek, M. ; Johnson, C. ; Lognonné, P. ; Spiga, A. ; Spohn, T. ; Perrin, C. ; Stähler, S. ; Antonangeli, D. ; Asmar, S. ; Beghein, C. ; Bowles, N. ; Bozdag, E. ; Chi, P. ; Christensen, U. ; Clinton, J. ; Collins, G. ; Daubar, I. ; Dehant, V. ; Drilleau, M. ; Fillingim, M. ; Folkner, W. ; Garcia, R. ; Garvin, J. ; Grant, J. ; Grott, M. ; Grygorczuk, J. ; Hudson, T. ; Irving, J. ; Kargl, G. ; Kawamura, T. ; Kedar, S. ; King, S. ; Knapmeyer-Endrun, B. ; Knapmeyer, M. ; Lemmon, M. ; Lorenz, R. ; Maki, J. ; Margerin, L. ; McLennan, S. ; Michaut, C. ; Mimoun, D. ; Mittelholz, A. ; Mocquet, A. ; Morgan, P. ; Mueller, N. ; Murdoch, N. ; Nagihara, S. ; Newman, C. ; Nimmo, F. ; Panning, M. ; Pike, W. ; Plesa, A.C. ; Rodriguez, S.R. ; odriguez-Manfredi, J. ; Russell, C. ; Schmerr, N. ; Siegler, M. ; Stanley, S. ; Stutzmann, E. ; Teanby, N. ; Tromp, J. ; van Driel, M. ; Warner, N. ; Weber, R. ; Wieczorek, M.
Initial results from the InSight mission on Mars
Nature Geoscience, 13, pp. 183-189 (2020). http://dx.doi.org/10.1038/s41561-020-0544-y

[5] Banfield, Don ; Spiga, Aymeric ; Newman, Claire ; Forget, Fran√ßois ; Lemmon, Mark ; Lorenz, Ralph ; Murdoch, Naomi ; Viudez-Moreiras, Daniel ; Pla-Garcia, Jorge ; Garcia, Rapha√´l F. ; Lognonn√©, Philippe ; Karatekin, Ozgur ; Perrin, Cl√©ment ; Martire, L√©o ; Teanby, Nicholas ; Hove, Bart Van ; Maki, Justin N. ; Kenda, Balthasar ; Mueller, Nils T. ; Rodriguez, S√©bastien ; Kawamura, Taichi ; McClean, John B. ; Stott, Alexander E. ; Charalambous, Constantinos ; Millour, Ehouarn ; Johnson, Catherine L. ; Mittelholz, Anna ; M√§√§tt√§nen, Anni ; Lewis, Stephen R. ; Clinton, John ; St√§hler, Simon C. ; Ceylan, Savas ; Giardini, Domenico ; Warren, Tristram ; Pike, William T. ; Daubar, Ingrid ; Golombek, Matthew ; Rolland, Lucie ; Widmer-Schnidrig, Rudolf ; Mimoun, David ; Beucler, √âric ; Jacob, Alice ; Lucas, Antoine ; Baker, Mariah ; Ansan, V√©ronique ; Hurst, Kenneth ; Mora-Sotomayor, Luis ; Navarro, Sara ; Torres, Josefina ; Lepinette, Alain ; Molina, Antonio ; Marin-Jimenez, Mercedes ; Gomez-Elvira, Javier ; Peinado, Veronica ; Rodriguez-Manfredi, Jose-Antonio ; Carcich, Brian T. ; Sackett, Stephen ; Russell, Christopher T. ; Spohn, Tilman ; Smrekar, Suzanne E. ; Banerdt, W. Bruce
The atmosphere of Mars as observed by InSight
Nature Geoscience, 13, pp. 190-198 (2020). http://dx.doi.org/10.1038/s41561-020-0534-0

[6] Barnes, D. ; Davies, J. ; Harrison, R. ; Byrne, J. ; Perry, C. ; Bothmer, V. ; Eastwood, J. ; Gallagher, P. ; Kilpua, E. ; Moestl, C. ; Rodriguez, L. ; Rouillard, A. ; Odstrcil, D.

CMEs in the Heliosphere: III. A Statistical Analysis of the Kinematic Properties Derived from Stereoscopic Geometrical Modelling Techniques Applied to CMEs Detected in the Heliosphere from 2008 to 2014 by STEREO/HI-1
Solar Physics 295, 150 (2020). https://doi.org/10.1007/s11207-020-01717-w

[7] Beerten, Koen ; Verbeeck, Koen ; Laloy, Eric ; Vanacker, Veerle ; Vandenberghe, Dimitri ; Christl, Marcus ; De Grave, Johan ; Wouters, Laurent
Electron spin resonance (ESR), optically stimulated luminescence (OSL) and terrestrial cosmogenic radionuclide (TCN) dating of quartz from a Plio-Pleistocene sandy formation in the Campine area, NE Belgium
Quaternary International, 556, pp. 144-158 (2020). http://dx.doi.org/10.1016/j.quaint.2020.06.011

[8] Bernauer, F. ; Garcia, R.F. ; Murdoch, N. ; Dehant, V. ; Sollberger, D. ; Schmelzbach, C. ; Wassermann, J. ; Cadu, A. ; Mimoun, D. ; Ritter, B. ; Filice, V. ; Karatekin, Ö. ; Ferraioli, L. ; Robertsson, J.O.A. ; Giardini, D. ; Lecamp, G. ; Guattari, F. ; Bonnefois, J.-J. ; de Raucourt, S.
Exploring Planets and Asteroids with 6DoF Sensors - Utopia and Realism
Earth, Planets and Space, 72, pp. 191 (2020). http://dx.doi.org/10.1186/s40623-020-01333-9

[9] Berthier, J. ; Descamps, P. ; Vachier, F. ; Normand, J. ; Maquet, L. ; Deleflie, F. ; Colas, F. ; Klotz, A. ; Teng-Chuen-Yu, J.-P. ; Peyrot, A. ; Braga-Ribas, F. ; Marchis, F. ; Leroy, A. ; Bouley, S. ; Dubos, G. ; Pollock, J. ; Pauwels, T. ; Vingerhoets, P. ; Farrell, J. A. ; Sada, P. V. ; Reddy, V. ; Archer, K. ; Hamanowa, H. H.
Physical characterization of double asteroid (617) Patroclus from 2007/2012 mutual events observations
Icarus, 352 issue 113990 (2020). http://dx.doi.org/10.1016/j.icarus.2020.113990

[10] Bertrand, Bruno ; Defraigne, Pascale
Fundamental physics tests using the propagation of GNSS signals
Advances in Space Reasearch, 66 issue 12, pp. 2764-2772 (2020).
http://dx.doi.org/10.1016/j.asr.2020.06.033

[11] Beuthe, Mikael
Comment on `Heating of Enceladus due to the dissipation of ocean tides' by R. Tyler
Icarus, 350 issue 113934 (2020). http://dx.doi.org/10.1016/j.icarus.2020.113934

[12] Beuthe, Mikael ; Charlier, Bernard ; Namur, Olivier ; Rivoldini, Attilio ; Van Hoolst, Tim
Mercury's Crustal Thickness Correlates With Lateral Variations in Mantle Melt Production
Geophysical Research Letters, 47 issue e2020GL087261, pp. 1-9 (2020).
http://dx.doi.org/10.1029/2020GL087261

[13] Blanc, M ; including, also ; Van Hoolst, T
Joint Europa Mission (JEM): a multi-scale study of Europa to characterize its habitability and search for extant life
Planetary and Space Sciences , 193, pp. 104960 (2020). http://dx.doi.org/10.1016/j.pss.2020.104960

[14] Brenguier, F. ; Courbis, R. ; Mordret, A. ; Campman, X. ; Boué, P. ; Chmiel, M. ; Takano, T. ; Lecocq, T. ; Van der Veen, W. ; Postif, S. ; Hollis, D.
Noise-based ballistic wave passive seismic monitoring. Part 1: body waves
Geophysical Journal International, pp. 683–691 (2020). http://dx.doi.org/10.1093/gji/ggz440

[15] Camelbeeck, Thierry ; Vanneste, Kris ; Lecocq, Thomas
Natural and Man-induced Destructive Earthquakes in Stable Continental Regions
Bulletin of the Royal Academy for Overseas Sciences, 63, pp. 321-340 (2020).
http://dx.doi.org/10.5281/zenodo.3894460

[16] Camelbeeck, Thierry ; Vanneste, Kris ; Verbeeck, Koen ; Garcia-Moreno, David ; Van Noten, Koen ; Lecocq, Thomas
How well does known seismicity between the Lower Rhine Graben and southern North Sea reflect future earthquake activity?
Historical Earthquakes, Paleoseismology, Neotectonics and Seismic Hazard: New Insights and Suggested Procedures, DGEB-Publikation Nr. 18, pp. 53-72 (2020).
http://dx.doi.org/10.23689/fidgeo-3860

[17] Caspi, A. ; Seaton, D. B. ; Tsang, C. C. C. ; DeForest, C. E. ; Bryans, P. ; DeLuca, E. E. ; Tomczyk, S. ; Burkepile, J. T. ; Casey, T. ; Collier, J. ; Darrow, D. ; Del Rosso, D. ; Durda, D. D. ; Gallagher, P. T. ; Golub, L. ; Jacyna, M. ; Johnson, D. ; Judge, P. G. ; Klemm, C. ; Laurent, G. T. ; Lewis, J. ; Mallini, C. J. ; Parent, T. ; Propp, T. ; Steffl, A. J. ; Warner, J. ; West, M. J. ; Wiseman, J. ; Yates, M. ; Zhukov, A. N.
A New Facility for Airborne Solar Astronomy: NASA's WB-57 at the 2017 Total Solar Eclipse
Astrophysical Journal, 895, pp. 131 (2020). http://dx.doi.org/10.3847/1538-4357/ab89a8

[18] Cécere, M. ; Sieyra, M. V. ; Cremades, H. ; Mierla, M. ; Sahade, A. ; Stenborg, G. ; Costa, A. ; West, M. J. ; D'Huys, E.
Large non-radial propagation of a coronal mass ejection on 2011 January 24
Advances in Space Research, 65 issue 6 (2020). https://doi.org/10.1016/j.asr.2019.08.043

[19] Cochetti, Y. R. ; Zorec, J. ; Cidale, L. S. ; Arias, M. L. ; Aidelman, Y. ; Torres, A. F. ; Frémat, Y. ; Granada, A.
Be and Bn stars: Balmer discontinuity and stellar-class relationship
Astronomy & Astrophysics, 634, pp. A18 (2020). http://dx.doi.org/10.1051/0004-6361/201936444

[20] Cremonese, G ; including, also ; Van Hoolst, T
SIMBIO-SYS: cameras and spectrometer for the BepiColombo mission
Space Science Reviews, 216 issue 75, pp. 1-78 (2020). http://dx.doi.org/10.1007/s11214-020-00704-8

[21] Decraemer, Bieke ; Zhukov, Andrei ; Van Doorsselaere, Tom
Properties of Streamer Wave Events Observed during the STEREO Era
Astrophysical Journal, 893, pp. 78 (2020). http://dx.doi.org/10.3847/1538-4357/ab8194

[22] Dehant, V. ; Le Maistre, S. ; Baland, R.M. ; Bergeot, N. ; Karatekin, O. ; Peters, M.J. ; Rivoldini, A. ; Ruiz Lozano, L. ; Temel, O. ; Van Hoolst, T. ; Yseboodt, M. ; Mitrovic, M. ; Kosov, A. ; Valenta, V. ; Thomassen, L. ; Karki, S. ; Al Khalifeh, K. ; Craeye, C. ; Gurvits, L. ; Marty, J.C. ; Asmar, S. ; Folkner, W. ; LaRa Team, and the
The radioscience LaRa instrument onboard ExoMars 2020 to investigate the rotation and interior of Mars
Planetary and Space Science, 180, pp. 104776 (2020).
http://dx.doi.org/doi.org/10.1016/j.pss.2019.104776

[23] Delforge, D ; Vanclooster, M ; Van Camp, M ; Muñoz-Carpena, R
A Parsimonious Empirical Approach to Streamflow Recession Analysis and Forecasting
Water Resources Research, 56 issue 2 (2020). http://dx.doi.org/10.1029/2019WR025771

[24] Drilleau, Mélanie ; Beucler, Éric ; Lognonné, Philippe ; Panning, Mark P. ; Knapmeyer-Endrun, Brigitte ; Banerdt, W. Bruce ; Beghein, Caroline ; Ceylan, Savas ; van Driel, Martin ; Joshi, Rakshit ; Kawamura, Taichi ; Khan, Amir ; Menina, Sabrina ; Rivoldini, Attilio ; Samuel, Henri ; Stähler, Simon ; Xu, Haotian ; Bonnin, Mickaël ; Clinton, John ; Giardini, Domenico ; Kenda, Balthasar ; Lekic, Vedran ; Mocquet, Antoine ; Murdoch, Naomi ; Schimmel, Martin ; Smrekar, Suzanne E. ; Stutzmann, Éléonore ; Tauzin, Benoit ; Tharimena, Saikiran
MSS1: Single-Station and Single-Event Marsquake Inversion
Earth and Space Science, 7 issue 12 (2020). http://dx.doi.org/10.1029/2020EA001118

[25] Emel'yanov, N. V. ; Arlot, J.-E. ; Zhang, X. L. ; Bradshaw, J. ; De Cat, P. ; Han, X. L. ; Ivantsov, A. ; Jindra, J. ; Maigurova, N. ; Manek, J. ; Pauwels, T. ; Pomazan, A. ; Vingerhoets, P.
Astrometric Results for Observations of Jupiter's Galilean Satellites During Mutual Occultations and Eclipses in 2009 and 2014–2015
Solar System Research, 53, pp. 436–442 (2019) (Published on February 18, 2020).
http://dx.doi.org/10.1134/S0038094619060017

[26] Falk, R ; Pálinkáš, V ; Wziontek, H ; Rülke, A ; Val'ko, M ; Ullrich, C ; Butta, H ; Kostelecký, J ; Bilker-Koivula, M ; Näränen, J ; Prato, A ; Mazzoleni, F ; Kirbaş, C ; Coşkun, İ ; Van Camp, M ; Castelein, S ; Bernard, J D ; Lothhammer, A ; Schilling, M ; Timmen, L ; Iacovone, D ; Nettis, G ; Greco, F ; Messina, A A ; Reudink, R ; Petrini, M ; Dykowski, P ; Sękowski, M ; Janák, J ; Papčo, J ; Engfeldt, A ; Steffen, H
Final report of EURAMET.M.G-K3 regional comparison of absolute gravimeters
Metrologia, 57 issue 1A (2020). http://dx.doi.org/10.1088/0026-1394/57/1A/07019

[27] Fu, J.N. ; De Cat, P. ; Zong, W.K. ; Frasca, A. ; Gray, R.O. ; Ren, A.-B. ; Molenda-Żakowicz, J. ; Corbally, C.J. ; Catanzaro, G. ; Shi, J.R. ; Luo, A.L. ; Zhang, H.T.
Overview of the LAMOST-Kepler project
Research in Astronomy and Astrophysics, 20 issue 10, pp. id.167, 10 pp. (2020).
http://dx.doi.org/10.1088/1674-4527/20/10/167

[28] Gaia Collaboration, including Blomme, R., Frémat, Y., Lobel A. and Pauwels, T.
Gaia Data Release 2. The kinematics of globular clusters and dwarf galaxies around the Milky Way (Corrigendum)
Astronomy & Astrophysics, 642 issue id.C1 (2020). http://dx.doi.org/10.1051/0004-6361/202039217

[29] Gaia Collaboration, including Blomme, R., Frémat, Y., Lobel A. and Pauwels, T.
Gaia Data Release 2. Kinematics of globular clusters and dwarf galaxies around the Milky Way (Corrigendum)
Astronomy & Astrophysics, 637 issue id.C3 (2020). http://dx.doi.org/10.1051/0004-6361/201832698e

[30] Gaia Collaboration, Luri X., including Blomme R., Frémat Y., Lobel A. and Pauwels, T.
VizieR Online Data Catalog: MC structure and properties
Astronomy & Astrophysics, 649, issue id.A7 (2020).
https://ui.adsabs.harvard.edu/abs/2020yCat..36490007G/abstract

[31] Giardini, D. ; Lognonné, P. ; Banerdt, W. B. ; Pike, W. T. ; Christensen, U. ; Ceylan, S. ; Clinton, J. F. ; van Driel, M. ; Stähler, S. C. ; Böse, M. ; Garcia, R. F. ; Khan, A. ; Panning, M. ; Perrin, C. ; Banfield, D. ; Beucler, E. ; Charalambous, C. ; Euchner, F. ; Horleston, A. ; Jacob, A. ; Kawamura, T. ; Kedar, S. ; Mainsant, G. ; Scholz, J. -R. ; Smrekar, S. E. ; Spiga, A. ; Agard, C. ; Antonangeli, D. ; Barkaoui, S. ; Barrett, E. ; Combes, P. ; Conejero, V. ; Daubar, I. ; Drilleau, M. ; Ferrier, C. ; Gabsi, T. ; Gudkova, T. ; Hurst, K. ; Karakostas, F. ; King, S. ; Knapmeyer, M. ; Knapmeyer-Endrun, B. ; Llorca-Cejudo, R. ; Lucas, A. ; Luno, L. ; Margerin, L. ; McClean, J. B. ; Mimoun, D. ; Murdoch, N. ; Nimmo, F. ; Nonon, M. ; Pardo, C. ; Rivoldini, A. ; Manfredi, J. A. Rodriguez ; Samuel, H. ; Schimmel, M. ; Stott, A. E. ; Stutzmann, E. ; Teanby, N. ; Warren, T. ; Weber, R. C. ; Wieczorek, M. ; Yana, C.
The seismicity of Mars
Nature Geoscience, 13 issue 3 (2020). http://dx.doi.org/10.1038/s41561-020-0539-8

[32] Gillmann, C. ; Golabek, G. ; Raymond, S. ; Schonbachler, M. ; Tackley, P. ; Dehant, V. ; Debaille, V.
Dry Late Accretion inferred from Venus' coupled atmosphere and internal evolution
Nature Geoscience, 13, pp. 265-269 (2020). http://dx.doi.org/10.1038/s41561-020-0561-x

[33] Golombek, M.; Warner, N.H.; Grant, J.A.; Hauber, E.; Ansan, V.; Weitz, C.M.; Williams, N.; Charalambous, C.; Wilson, S.A.; DeMott, A.; Kopp, M.; Lethcoe-Wilson, H.; Berger, L.; Hausmann, R.; Marteau, E.; Vrettos, C.; Trussell, A.; Folkner, W.; Le, Maistre, S.; Mueller, N.; Grott, M.; Spohn, T.; Piqueux, S.; Millour, E.; Forget, F.; Daubar, I.; Murdoch, N.; Lognonné, P.; Perrin, C.; Rodriguez, S.; Pike, W.T.; Parker, T.; Maki, J.; Abarca, H.; Deen, R.; Hall, J.; Andres, P.; Ruoff, N.; Calef, F.; Smrekar, S.; Baker, M.M.; Banks, M.; Spiga, A.; Banfield, D.; Garvin, J.; Newman, C.E.; Banerdt, W.B.
Geology of the InSight Landing Site on Mars
Nature Communications volume 11, Article number: 1014 (2020).
http://dx.doi.org/10.1038/s41467-020-14679-1

[34] Gomez Casajus, L ; Modenini, D ; Tortora, P ; Zannoni, M ; Nimmo, F ; Van Hoolst, T ; Buccino, D ; Oudrhiri, K
Updated Europa gravity field and interior structure from a reanalsysis of Galileo tracking data
Icarus (2020). http://dx.doi.org/10.1016/j.icarus.2020.114187

[35] Groenewegen, M.A.T.
Analysing the spectral energy distributions of Galactic classical Cepheids
Astronomy and Astrophysics, 635, pp. A33 (2020). https://doi.org/%2010.1051/0004-6361/201937060

[36] Groenewegen, M.A.T.
The flux-weighted gravity-luminosity relation of Galactic classical cepheids
Astronomy and Astrophysics, 640, pp. A113 (2020). https://doi.org/10.1051/0004-6361/202038292

[37] Groenewegen, M.A.T. ; Nanni, A. ; Cioni, M.-R.L. ; Girardi, L. ; de Grijs, R. ; Ivanov, V.D. ; Marconi, M. ; Moretti, M.-J. ; Oliveira, J.M. ; Petr-Gotzens, M.G. ; Ripepi, V. ; van Loon, J.Th.
The VMC Survey - XXXVII. Pulsation periods of dust enshrouded AGB stars in the Magellanic Clouds
Astronomy & Astrophysics, 636, pp. A48 (2020). https://doi.org/10.1051/0004-6361/201937271

[38] Hayakawa, Hisashi ; Clette, Frédéric ; Horaguchi, Toshihiro ; Iju, Tomoya ; Knipp, Delores J. ; Liu, Huixin ; Nakajima, Takashi
Sunspot observations by Hisako Koyama: 1945-1996
Monthly Notices of the Royal Astronomical Society, 492 issue 3, pp. 4513-4527 (2020).
http://dx.doi.org/10.1093/mnras/stz3345

[39] Hofmeister, Stefan J. ; Veronig, Astrid M. ; Poedts, Stefaan ; Samara, Evangelia ; Magdalenic, Jasmina
On the Dependency between the Peak Velocity of High-speed Solar Wind Streams near Earth and the Area of Their Solar Source Coronal Holes
The Astrophysical Journal Letters, Volume 897, Issue 1, id.L17 (2020).
https://doi.org/10.3847/2041-8213/ab9d19

[40] Journaux, B. ; Kalousová, K. ; Sotin, C. ; Tobie, G. ; Vance, S. ; Saur, J. ; Bollengier, O. ; Noack, L. ; Rückriemen-Bez, T. ; Van Hoolst, T. ; Soderlund, K. ; Brown, J.M.
Large ocean worlds with high-pressure ices
Space Science Reviews, 217 issue 7 (2020). http://dx.doi.org/10.1007/s11214-019-0633-7

[41] Konopliv, A ; Park, RS ; Rivoldini, A ; Baland, R-M ; Le Maistre, S ; Van Hoolst, T ; Yseboodt, M ; Dehant, V
Detection of the Mars Chandler Wobble from Mars Orbiting Spacecraft
Geophysical Research Letters, 47, pp. e2020GL090568 (2020).
https://doi.org/10.1029/2020GL090568

[42] Koukras, Alexandros ; Marqué, Christophe ; Downs, Cooper ; Dolla, Laurent

Analyzing the propagation of EUV waves and their connection with type II radio bursts by combining numerical simulations and multi-instrument observations
Astronomy & Astrophysics, 644 (2020). http://dx.doi.org/10.1051/0004-6361/202038699

[43] Labadie-Bartz, J. ; Handler, G. ; Pepper, J. ; Balona, L. ; De Cat, P. ; Stevens, D. J. ; Lund, M. B. ; Stassun, K. G. ; Rodriguez, J. E. ; Siverd, R. J. ; James, D. J. ; Kuhn, R. B.
New Beta Cephei stars with KELT
The Astronomical Journal, 160 issue 1, pp. id.32, 22 pp. (2020). http://dx.doi.org/10.3847/1538-3881/ab952c

[44] Lanabere, V. ; Dasso, S. ; Démoulin, P. ; Janvier, M. ; Rodriguez, L. ; Masías-Meza, J.J.
Magnetic twist profile inside magnetic clouds derived with a superposed epoch analysis
Astronomy & Astrophysics, Volume 635, Issue A85, 13 pp. (2020). https://doi.org/10.1051/0004-6361/201937404

[45] Le Maistre, Sébastien
Martian Lander Radio Science Data Calibration for Mars Troposphere
Radio Science (2020). https://doi.org/10.1029/2020RS007155

[46] Le Maistre, S. ; Péters, M.-J. ; Marty, J.-C. ; Dehant, V.
On the impact of the operational and technical characteristics of the LaRa experiment on the determination of Mars' nutation
Planetary and Space Science, 180, pp. 104766 (2020). http://dx.doi.org/10.1016/j.pss.2019.104766

[47] Lecocq, T. ; Ardhuin, F. ; Collin, F. ; Camelbeeck, T.
On the Extraction of Microseismic Ground Motion from Analog Seismograms for the Validation of Oceanic-Climatic Models
Seismological Research Letters, 91 (3): 1518–1530 (2020). http://dx.doi.org/10.1785/0220190276

[48] Lecocq, T. ; Hicks, S.P. ; Van Noten, Koen ; van Wijk, K. ; Koelemeijer, P. ; De Plaen, R.S.M. ; Massin, F. ; Hillers, G. ; Anthony, R.E. ; Apoloner, M.-T. ; Arroyo-Solórzano, M. ; Assink, J.D. ; Büyükakpinar, P. ; Cannata, A. ; Cannavo, F. ; Carrasco, S. ; Caudron, C. ; Chaves, E.J. ; Cornwell, D.G. ; Craig, D. ; den Ouden, O.F.C. ; Diaz, J. ; Donner, S. ; Evangelidis, C.P. ; Evers, L. ; Fauville, B. ; Fernandez, G.A. ; Giannopoulos, D. ; Gibbons, S.J. ; Girona, T. ; Grecu, B. ; Grunberg, M. ; Hetényi, G. ; Horleston, A. ; Inza, A. ; Irving, J.C.E. ; Jamalreyhani, M. ; Kafka, A. ; Koymans, M.R. ; Labedz, C.R. ; Larose, E. ; Lindsey, N.J. ; McKinnon, M. ; Megies, T. ; Miller, M.S. ; Minarik, W. ; Moresi, L. ; Márquez-Ramírez, V.H. ; Möllhoff, M. ; Nesbitt, I.M. ; Niyogi, S. ; Ojeda, J. ; Oth, A. ; Proud, S. ; Pulli, J. ; Retailleau, L. ; Rintamäki, A.E. ; Satriano, C. ; Savage, M.K. ; Shani-Kadmiel, S. ; Sleeman, R. ; Sokos, E. ; Stammler, K. ; Stott, A.E. ; Subedi, S. ; Sørensen, M.B. ; Taira, T. ; Tapia, M. ; Turhan, F. ; van der Pluijm, B. ; Vanstone, M. ; Vergne, J. ; Vuorinen, T.A.T. ; Warren, T. ; Wassermann, J. ; Xiao, H.
Global quieting of high-frequency seismic noise due to COVID-19 pandemic lockdown measures
Science, Vol. 369, Issue 6509, pp. 1338-1343 (2020). http://dx.doi.org/10.1126/science.abd2438

[49] Lindsey, N.J. ; Yuan, S. ; Lellouch, A. ; Gualtieri, L. ; Lecocq, T. ; Biondi, B.
City-scale dark fiber DAS measurements of infrastructure use during the COVID-19 pandemic
Geophysical Research Letters, 47 issue 16, pp. e2020GL089931 (2020). http://dx.doi.org/10.1029/2020GL089931

[50] Lobel, A. ; Royer, P. ; Martayan, C. ; Laverick, M. ; van Hoof, P.A.M. ; Merle, T. ; Van der Swaelmen, M. ; David, M. ; Hensberge, H. ; Thienpont, E.
The Belgian Repository of fundamental Atomic data and Stellar Spectra. Final Report
Belgian Science Policy Office 2020 (BRAIN-be - Belgian Research Action through Interdisciplinary Networks), 2012-2017, pp. 1-57 (2020). https://www.belspo.be/belspo/brain-be/themes_2_GeoUniClim_nl.stm#BRASS

[51] Lobel A., Royer P., Martayan C., Laverick M., van Hoof P.A.M., Merle T., Van der Swaelmen M., David M., Hensberge H., Thienpont E
The Belgian Repository of fundamental Atomic data and Stellar Spectra: Samenvatting (NL), Résumé (FR), Summary (EN) – 4 p
Belgian Science Policy Office 2020 (BRAIN-be - Belgian Research Action through Interdisciplinary Networks) (2020). https://www.belspo.be/belspo/brain-be/projects/FinalReports/BRASS_summ_nl.pdf https://www.belspo.be/belspo/brain-be/projects/FinalReports/BRASS_summ_fr.pdf https://www.belspo.be/belspo/brain-be/projects/FinalReports/BRASS_summ_en.pdf

[52] Magdalenic, J. ; Marque, C. ; Fallows, R. A. ; Mann, G. ; Vocks, C. ; Zucca, P. ; Dabrowski, B. P. ; Krankowski, A. ; Melnik, V.
Fine Structure of a Solar Type II Radio Burst Observed by LOFAR
The Astrophysical Journal Letters, 897 (2020). http://dx.doi.org/10.3847/2041-8213/ab9abc

[53] Mandea, M. ; Dehant, V. ; Cazenave, A.
GRACE Satellite Gravimetry for deep interior
Remote Sensing, 12 issue 24, pp. 4198 (2020). http://dx.doi.org/10.3390/rs12244186

[54] Marini, E. ; Dell'Agli, F. ; Di Criscienzo, M. ; Garcia-Hernandez, D.A. ; Ventura, P. ; Groenewegen, M.A.T. ; Mattsson, L. ; Kamath, D. ; Puccetti, S. ; Tailo, M. ; Villaver, E.
Characterization of M-stars in the LMC in the JWST era
Monthly Notices of the Royal Astronomical Society, 493, pp. 2996-3012 (2020). https://doi.org/10.1093/mnras/staa353

[55] Martin, Aurélie ; Lecocq, Thomas ; Hinzen, Klaus-G. ; Camelbeeck, Thierry ; Quinif, Yves ; Fagel, Nathalie
Characterizing Stalagmites' Eigenfrequencies by Combining In Situ Vibration Measurements and Finite Element Modeling Based on 3D Scans
Geosciences, 10 issue 10 (2020). http://dx.doi.org/10.3390/geosciences10100418

[56] Matsuyama, I. ; Keane, J.T. ; Trinh, A. ; Beuthe, M. ; Watters, T.R.
Global tectonic patterns of the Moon
Icarus issue 114202 (2020). http://dx.doi.org/10.1016/j.icarus.2020.114202

[57] Mayer, P. ; Harmanec, P. ; Zasche, P. ; Catalan-Hurtado, R. ; Barlow, B. N. ; Frémat, Y. ; Wolf, M. ; Drechsel, H. ; Chini, R. ; Nasseri, A. ; Christie, G. W. ; Walker, W. S. G. ; Henden, A. A. ; Bohlsen, T. ; Božić, H.
Improved physical properties of the quadruple sub-system with the eclipsing binary QZ Carinae
Contributions of the Astronomical Observatory Skalnate Pleso, 50 issue 2, pp. 580-584 (2020). http://dx.doi.org/10.31577/caosp.2020.50.2.580

[58] Mecina, M. ; Aringer, B. ; Nowotny, W. ; Groenewegen, M.A.T. ; Kerschbaum, F. ; Brunner, M. ; Gail, H.-P.
Extended view on the dust shells around two carbon stars
Astronomy and Astrophysics, 644, pp. A66 (2020). https://doi.org/10.1051/0004-6361/202039178

[59] Merle, T. ; Van der Swaelmen, M. ; Van Eck, S. ; Jorissen, A. ; Jackson, R. J. ; Traven, G. ; Zwitter, T. ; Pourbaix, D. ; Klutsch, A. ; Sacco, G. ; Blomme, R. ; Masseron, T. ; Gilmore, G. ; Randich, S. ; Badenes, C. ; Bayo, A. ; Bensby, T. ; Bergemann, M. ; Biazzo, K. ; Damiani, F. ; Feuillet, D. ; Frasca, A. ; Gonneau, A. ; Jeffries, R. D. ; Jofré, P. ; Morbidelli, L. ; Mowlavi, N. ; Pancino, E. ; Prisinzano, L.
The Gaia-ESO Survey: detection and characterisation of single-line spectroscopic binaries
Astronomy & Astrophysics, 635, pp. A155 (2020). http://dx.doi.org/10.1051/0004-6361/201935819

[60] Meyer, Karen A. ; Mackay, Duncan H. ; Talpeanu, Dana-Camelia ; Upton, Lisa A. ; West, Matthew J.

Investigation of the Middle Corona with SWAP and a Data-Driven Non-Potential Coronal Magnetic Field Model
Solar Physics, 295 issue 7, pp. 26 (2020). http://dx.doi.org/10.1007/s11207-020-01668-2

[61] Micera, A. ; Boella, E. ; Zhukov, A. N. ; Shaaban, S. M. ; Lazar, M. ; Lapenta, G.
Particle-in-Cell simulations of the parallel proton firehose instability influenced by the electron temperature anisotropy in solar wind conditions
Astrophysical Journal, 893, pp. 130 (2020). http://dx.doi.org/10.3847/1538-4357/ab7faa

[62] Micera, A. ; Zhukov, A. N. ; López, R. A. ; Innocenti, M. E. ; Lazar, M. ; Boella, E. ; Lapenta, G.
Particle-in-cell Simulation of Whistler Heat-flux Instabilities in the Solar Wind: Heat-flux Regulation and Electron Halo Formation
Astrophysical Journal Letters, 903, pp. L23 (2020). http://dx.doi.org/10.3847/2041-8213/abc0e8

[63] Mierla, Marilena ; Janssens, Jan ; D'Huys, Elke ; Wauters, Laurence ; West, Matthew J. ; Seaton, Daniel B. ; Berghmans, David ; Podladchikova, Elena
Long-term Evolution of the Solar Corona Using PROBA2 Data
Solar Physics, 295 issue 66 (2020). http://dx.doi.org/https://doi.org/10.1007/s11207-020-01635-x

[64] Mordret, A. ; Courbis, R. ; Brenguier, F. ; Chmiel, M. ; Garambois, S. ; Mao, S. ; Boué, P. ; Campman, X. ; Lecocq, T. ; Van der Veen, W. ; Hollis, D.
Noise-based ballistic wave passive seismic monitoring – Part 2: surface waves
Geophysical Journal International, 221, pp. 692–705 (2020). http://dx.doi.org/10.1093/gji/ggaa016

[65] Morford, J. C. ; Fenech, D. M. ; Prinja, R. K. ; Blomme, R. ; Yates, J. A. ; Drake, J. J. ; Eyres, S. P. S. ; Richards, A. M. S. ; Stevens, I. R. ; Wright, N. J. ; Clark, J. S. ; Dougherty, S. ; Pittard, J. M. ; Smith, H. A. ; Vink, J. S.
COBRaS: The e-MERLIN 21 cm Legacy survey of Cygnus OB2
Astronomy & Astrophysics, 637, pp. A64 (2020). http://dx.doi.org/10.1051/0004-6361/201731379

[66] Morosan, D. E.; ; Palmerio, E.; ; Rasanen, J. E.; ; Kilpua, E. K. J.; ; Magdalenic, J.; ; Lynch, B. J.; ; Kumari, A.; ; Pomoell, J.; ; Palmroth, M.
Electron acceleration and radio emission following the early interaction of two coronal mass ejections
Astronomy & Astrophysics, 642, issue A151, 13 pp. (2020). http://dx.doi.org/%2010.1051/0004-6361/202038801

[67] Müller, D. ; St. Cyr, O. C. ; Zouganelis, I. ; Gilbert, H. R. ; Marsden, R. ; Nieves-Chinchilla, T. ; Antonucci, E. ; Auchère, F. ; Berghmans, D. ; ManyOtherAuthors, X.
The Solar Orbiter mission. Science overview
Astronomy and Astrophysics, 642 issue A1 (2020). http://dx.doi.org/https://doi.org/10.1051/0004-6361/202038467

[68] Mumford, S J ; Freij, N ; Christe, S ; Ireland, J ; Mayer, F ; Hughit, V K ; Shih, A Y ; Chakraborty, P ; Vishnunarayan, K ; Inglis, A ; Patnaik, P ; Sipőcz, B ; Sharma, R ; Leonard, A ; Stansby, D ; Hewet, R ; Hamilton, A ; Hayes, L ; Panda, A ; Earnshaw, M ; Choudhary, N ; Kumar, A ; Chanda, P ; Haque, M A ; Kirk, M S ; Mueler, M ; Konge, S ; Srivastava, R ; Jain, Y ; Benet, S ; Baruah, A ; Barnes, W ; Charlton, M ; Maloney, S ; Chorley, N ; Himanshu, A ; Modi, S ; Mason, J P ; Naman, A ; Campos Rozo, J I ; Manley, L ; Chaterje, A ; Evans, J ; Malocha, M ; Bobra, M G ; Ghosh, S ; Stańczak, D ; De Vischer, R ; Verma, S ; Agrawal, A ; Budhika, D ; Sharma, S ; Park, J ; Bates, M ; Goel, D ; Taylor, G ; Cetusic, G ; Inchaurandieta, M ; Dacie, S ; Dubey, S ; Sharma, D ; Bray, E M ; Rideout, J R ; Zahniy, S ; Meszaros, T ; Bose, A ; Chicrala, A ; Ankit, A ; Guenou, C ; D'Avela, D ; Wiliams, D ; Balew, J ; Murphy, N ; Lodha, P ; Robitaile, T ; Krishan, Y ; Hil, A ; Eigenbrot, A ; Mampaey, B ; Wiedeman, B M ; Molina, C ; Keşkek, D ; Habib, I ; Lets, J ; Bazán, J ; Arbolante, Q ; Reid Gomilion, R ; Yash Kothari, Y ; Yash Sharma, Y ; Stevens, A L ; Price-Whelan, A ; Mehrotra, A ; Kustov, A ; Stone, B ; Kien nil Dang,

T ; Arias, E ; Mackenzie Dover, F ; Verstringe, F ; Kumar, G ; Mathur, H ; Babuschkin, I ; Wimbish, J ; Buitrago-Casas, J C ; Krishna, K ; Hiware, K ; Mangaonkar, M ; Mendero, M ; Schoentgen, M ; Gyenge, N G ; Streicher, O ; Mekala, R R ; Mishra, R ; Srikanth, S ; Jain, S ; Yadav, T ; Wilkinson, T D ; Pereira, T M D ; Agrawal, Y ; Jamescalixto, A ; Yasintoda, A ; Muray, S A
SunPy: A Python package for Solar Physics
Journal of Open Source Software, 5 issue 46, pp. 1832-1836 (2020).
https://doi.org/10.21105/joss.01832

[69] Nunn, Ceri ; Garcia, Raphael F. ; Nakamura, Yosio ; Marusiak, Angela G. ; Kawamura, Taichi ; Sun, Daoyuan ; Margerin, Ludovic ; Weber, Renee ; Drilleau, Mélanie ; Wieczorek, Mark A. ; Khan, Amir ; Rivoldini, Attilio ; Lognonné, Philippe ; Zhu, Peimin
Lunar Seismology: A Data and Instrumentation Review
Space Science Reviews, 216 issue 5 (2020). http://dx.doi.org/10.1007/s11214-020-00709-3

[70] Park, Sung-Hong ; Leka, KD ; Kusano, Kanya ; Andries, Jesse ; Barnes, Graham ; Bingham, Suzy ; Bloomfield, Shaun ; McCloskey, Aiofe ; Delouille, Veronique ; Falconer, David ; Gallagher, Peter ; Georgoulis, Manolis ; Kubo, Yuki ; Lee, Kangjin ; Lee, Sangwoo ; Lobzin, Vasily ; Mun, Jun-Chul ; Murray, Sophie ; Nagem, Tarek.A.M.Hamad ; Qahwaji, Rami ; Sharpe, Michael ; Steenburgh, Rob ; Steward, Graham ; Terkildsen, Mike
A Comparison of Flare Forecasting Methods. IV. Evaluating Consecutive-Day Forecasting Patterns
The Astrophysical Journal, Volume 890, Issue 2, id.124, 22 pp. (2020).
https://ui.adsabs.harvard.edu/link_gateway/2020ApJ...890..124P/doi:10.3847/1538-4357/ab65f0

[71] Pastorelli, G. ; Marigo, P. ; Girardi, L. ; Aringer, B. ; Chen, Y. ; Rubele, S. ; Trabucchi, M. ; Bladh, S. ; Boyer, M.L. ; Bressan, A. ; Dalcanton, J. ; Groenewegen, M.A.T. ; Lebzelter, T. ; Mowlavi, N. ; Chubb, K. L. ; Cioni, M.-R.L. ; de Grijs, R. ; Ivanov, V.D. ; Nanni, A. ; van Loon, J.Th. ; Zaggia, S.
Constraining the thermally-pulsing asymptotic giant branch phase with resolved stellar populations in the Large Magellanic Cloud
Monthly Notices of the Royal Astronomical Society, 498, pp. 3283--3301 (2020).
https://ui.adsabs.harvard.edu/link_gateway/2020MNRAS.498.3283P/doi:10.1093/mnras/staa2565

[72] Peters, M.J. ; Le Maistre, S. ; Yseboodt, M. ; Marty, J.C. ; Rivoldini, A. ; Van Hoolst, T. ; Dehant, V.
LaRa after RISE: Expected improvement in the Mars rotation and interior models
Planetary and Space Science, 180, pp. 104745 (2020). http://dx.doi.org/10.1016/j.pss.2019.104745

[73] Pick, M. ; Magdalenic, J. ; Cornilleau-Wehrlin, N. ; Grison, B. ; Schmieder, B. ; Bocchialini, K.
Role of the Coronal Environment in the Formation of Four Shocks Observed without Coronal Mass Ejections at Earth's Lagrangian Point L1
The Astrophysical Journal, 895, 144 (2020). http://dx.doi.org/10.3847/1538-4357/ab8fae

[74] Pieres, A. ; Girardi, L. ; Balbinot, E. ; Santiago, B. ; da Costa, L. N. ; Carnero Rosell, A. ; Pace, A. B. ; Bechtol, K. ; Groenewegen, M. A. T. ; Drlica-Wagner, A. ; Li, T. S. ; Maia, M.A.G. ; Ogando, R.L.C. ; dal Ponte, M. ; Diehl, H.T. ; Amara, A. ; Avila, S. ; Bertin, E. ; Brooks, D. ; Burke, D. L. ; Carrasco Kind, M. ; Carretero, J. ; De Vicente, J. ; Desai, S. ; Eifler, T.F. ; Flaugher, B. ; Fosalba, P. ; Frieman, J. ; Garcia-Bellido, J. ; Gaztanaga, E. ; Gerdes, D. W. ; Gruen, D. ; Gruendl, R.A. ; Gschwend, J. ; Gutierrez, G. ; Hollowood, D.L. ; Honscheid, K. ; James, D.J. ; Kuehn, K. ; Kuropatkin, N. ; Marshall, J.L. ; Miquel, R. ; Plazas, A.A. ; Sanchez, E. ; Serrano, S. ; Sevilla-Noarbe, I. ; Sheldon, E. ; Smith, M. ; Soares-Santos, M. ; Sobreira, F. ; Suchyta, E. ; Swanson, M.E.C. ; Tarle, G. ; Thomas, D. ; Vikram, V. ; Walker, A.R.
Modelling the Milky Way. I - Method and first results fitting the thick disk and halo with DES-Y3 data
Monthly Notices of the Royal Astronomical Society, 497, pp. 1547--1562 (2020).
https://doi.org/10.1093/mnras/staa1980

[75] Poedts, S. ; Kochanov, A. ; Lani, A. ; Scolini, C. ; Verbeke, C. ; Hosteaux, S. ; Chané, E. ; Deconinck, H. ; Mihalache, N. ; Diet, F. ; Heynderickx, D. ; De Keyser, J. ; De Donder, E ; Crosby, N. B. ; Echim, M. ; Rodriguez, L. ; Vansintjan, R. ; Verstringe, F. ; Mampaey, B. ; Horne, R. ; Glauert, S. ; Jiggens, P. ; Keil, R. ; Glover, A. ; Deprez, G. ; Luntama, J.-P.
The Virtual Space Weather Modelling Centre
Journal of Space Weather and Space Climate, Volume 10, Article 14, 23 pp. (2020).
https://doi.org/10.1051/swsc/2020012

[76] Poedts, S. ; Lani, A. ; Scolini, C. ; Verbeke, C. ; Wijsen, N. ; Lapenta, G. ; Chané, E. ; Van der Linden, R. ; Rodriguez, L. ; Vanlommel, P. ; Vainio, R. ; Afanasiev, A. ; Kilpua, E. ; Pomoell, J. ; Aran, A. ; Clarke, E., ; Thomson, A. ; Rouilard, A. ; Pinto, R. ; Marchaudon, A. ; Heber, B. ; Kochanov, A. ; Raeder, J. ; Depauw, J.
EUropean Heliospheric FORecasting Information Asset 2.0
Journal of Space Weather and Space Climate, Volume 10, id.57, 14 pp. (2020).
https://ui.adsabs.harvard.edu/link_gateway/2020JSWSC..10...57P/doi:10.1051/swsc/2020055

[77] Ramjatan, Sahade ; Lani, A. ; Boccelli, S. ; Van Hove, B. ; Karatekin, O. ; Magin, T. ; Thoemel, J.
Blackout analysis of Martian reentry missions
Journal of Fluid Mechanics, 904, A26 (2020). http://dx.doi.org/doi:10.1017/jfm.2020.714

[78] Ramstedt, S. ; Vlemmings, W. H. T. ; Doan, L. ; Danilovich, T. ; Lindqvist, M. ; Saberi, M. ; Olofsson, H. ; De Beck, E. ; Groenewegen, M.A.T. ; Höfner, S. ; Kastner, J. H. ; Kerschbaum, F. ; Khouri, T. ; Maercker, M. ; Montez, R. ; Quintana-Lacaci, G. ; Sahai, R. ; Tafoya, D. ; Zijlstra, A.
DEATHSTAR: Nearby AGB stars with the Atacama Compact Array I. CO envelope sizes and asymmetries: A new hope for accurate mass-loss-rate estimates
Astronomy & Astrophysics, Volume 640, id.A133, 28 pp. (2020).
https://ui.adsabs.harvard.edu/link_gateway/2020A&A...640A.133R/doi:10.1051/0004-6361/201936874

[79] Rekier, Jeremy ; Triana, Santiago Andres ; Trinh, Antony ; Dehant, Veronique
Inertial modes of a freely rotating ellipsoidal planet and their relation to nutations
The Planetary Science Journal, 1 issue 20, pp. 1-11 (2020). http://dx.doi.org/10.3847/PSJ/ab93c8

[80] Rochus, P. ; Auchere, F. ; Berghmans, D. ; Harra, L. ; Schmutz, W. ; Schühle, U. ; Addison, P. ; Appourchaux, T. ; Aznar Cuadrado, R. ; Baker, D. ; Barbay, J. ; Bates, D. ; BenMoussa, A. ; Bergmann, M. ; Beurthe, C. ; Borgo, B. ; Bonte, K. ; Bouzit, M. ; Bradley, L. ; Büchel, V. ; Buchlin, E. ; Büchner, J. ; Cabé, F. ; Cadiergues, L. ; Chaigneau, M. ; Chares, B. ; Choque Cortez, C. ; Coker, P. ; Condamin, M. ; Coumar, S. ; Curdt, W. ; Cutler, J. ; Davies, D. ; Davison, G. ; Defise, J.-M. ; Del Zanna, G. ; Delmotte, F. ; Delouille, V. ; Dolla, L. ; Dumesnil, C. ; Dürig, F. ; Enge, R. ; François, S. ; Fourmond, J.-J. ; Gillis, J.-M. ; Giordanengo, B. ; Gissot, S. ; Green, L. ; Guerreiro, N. ; Guilbaud, A. ; Gyo, M. ; Haberreiter, M. ; Hafiz, A. ; Hailey, M. ; Halain, J.-P. ; Hansotte, J. ; Hecquet, C. ; Heerlein, K. ; Hellin, M.-L. ; Hemsley, S. ; Hermans, A. ; Hervier, V. ; Hochedez, J.-F. ; Houbrechts, Y. ; Ihsan, K. ; Jacques, L. ; Jérôme, A. ; Jones, J. ; Kahle, M. ; Kennedy, T. ; Klaproth, M. ; Kolleck, M. ; Koller, S. ; Kotsialos, E. ; Kraaikamp, E. ; Langer, P. ; Lawrenson, A. ; Le Clech', J.-C. ; Lenaerts, C. ; Liebecq, S. ; Linder, D. ; Long, D. M. ; Mampaey, B. ; Markiewicz-Innes, D. ; Marquet, B. ; Marsch, E. ; Matthews, S. ; Mazy, E. ; Mazzoli, A. ; Meining, S. ; Meltchakov, E. ; Mercier, R. ; Meyer, S. ; Monecke, M. ; Monfort, F. ; Morinaud, G. ; Moron, F. ; Mountney, L. ; Müller, R. ; Nicula, B. ; Parenti, S. ; Peter, H. ; Pfiffner, D. ; Philippon, A. ; Phillips, I. ; Plesseria, J.-Y. ; Pylyser, E. ; Rabecki, F. ; Ravet-Krill, M.-F. ; Rebellato, J. ; Renotte, E. ; Rodriguez, L. ; Roose, S. ; Rosin, J. ; Rossi, L. ; Roth, P. ; Rouesnel, F. ; Roulliay, M. ; Rousseau, A. ; Ruane, K. ; Scanlan, J. ; Schlatter , P. ; Seaton, D. B. ; Silliman, K. ; Smit, S. ; Smith, P.J. ; Solanki, S.K. ; Spescha, M. ; Spencer, A. ; Stegen, K. ; Stockman, Y. ; Szwec, N. ; Tamiatto, C. ; Tandy, J. ; Teriaca, L. ; Theobald, C. ; Tychon, I. ; van Driel-Gesztelyi, L. ; Verbeeck, C. ;

Vial, J.-C. ; Werner, S. ; West, M. J. ; Westwood, D. ; Wiegelmann, T. ; Willis, G. ; Winter, B. ; Zerr, A. ; Zhang, X. ; Zhukov, A. N.
The Solar Orbiter EUI instrument: The Extreme Ultraviolet Imager
Astronomy & Astrophysics, 642, pp. A8 (2020). http://dx.doi.org/https://doi.org/10.1051/0004-6361/201936663

[81] Rodriguez, L. ; Scolini, C. ; Mierla, M. ; Zhukov, A. ; West, M.
Space weather monitor at the L5 point: a case study of a CME observed with STEREO B
Space Weather, 18, pp. e2020SW002533 (2020). http://dx.doi.org/10.1029/2020SW002533

[82] Rouillard, A.P. ; Pinto, R.F. ; Vourlidas, A. ; De Groof, A. ; ManyOtherAuthors, X. ; Berghmans, D. ; Nicula, B. ; Kraaikamp, E. ; Parenti, S. ; Rodriguez, L. ; Verbeeck, C. ; Zhukov, A.N.
Models and data analysis tools for the Solar Orbiter mission
Astronomy & Astrophysics, 642, pp. A2 (2020). http://dx.doi.org/10.1051/0004-6361/201935305

[83] Samadi-Ghadim, A. ; Lampens, P. ; Jassur, D. M. ; Jofré, P.
KIC 8975515: A fast-rotating (gamma Dor - delta Sct) hybrid star with Rossby modes and a slower delta Sct companion in a long-period orbit
Astronomy & Astrophysics, 638, pp. A57 (2020). http://dx.doi.org/10.1051/0004-6361/201936555

[84] Schmidt, Th. ; Cioni, M.-R. L. ; Niederhofer, F. ; Bekki, K. ; Bell, C.P.M. ; de Grijs, R. ; Diaz, J. ; El Youssoufi, D. ; Emerson, J. ; Groenewegen, M.A.T. ; Ivanov, V.D. ; Matijevic, G. ; Oliveira, J.M. ; Petr-Gotzens, M.G. ; Queiroz, A.B.A. ; Ripepi, V. ; van Loon, J.Th.
The VMC survey XXXVIII. Proper motion of the Magellanic Bridge
Astronomy & Astrophysics, 641, pp. A134 (2020). https://doi.org/10.1051/0004-6361/202037478

[85] Scolini, C. ; Chané, E. ; Pomoell, J. ; Rodriguez, L. ; Poedts, S.
Improving predictions of high-latitude Coronal Mass Ejections throughout the heliosphere
Space Weather, Volume18, Issue 3 (2020). https://doi.org/10.1029/2019SW002246

[86] Scolini, C. ; Chané, E. ; Temmer, M. ; Kilpua, E. ; Dissauer, K. ; Veronig, A. ; Palmerio, E. ; Pomoell, J. ; Dumbovic, M. ; Guo, J. ; Rodriguez, L. ; Poedts, S.
CME-CME Interactions as Sources of CME Geo-effectiveness: The Formation of the Complex Ejecta and Intense Geomagnetic Storm in Early September 2017
The Astrophysical Journal Supplement Series, 247:21, 27 pp. (2020). https://doi.org/10.3847/1538-4365/ab6216

[87] Sieyra, M. Valeria ; Cécere, Mariana ; Cremades, Hebe ; Iglesias, Francisco A. ; Sahade, Abril ; Mierla, Marilena ; Stenborg, Guillermo ; Costa, Andrea ; West, Matthew J. ; D'Huys, Elke
Analysis of Large Deflections of Prominence-CME Events during the Rising Phase of Solar Cycle 24
Solar Physics, 295 issue 9 (2020).
https://ui.adsabs.harvard.edu/link_gateway/2020SoPh..295..126S/doi:10.1007/s11207-020-01694-0

[88] Soderlund, K.M. ; Kalousová, K. ; Buffo, J.J. ; Glein, C.R. ; Goodman, J.C. ; Mitri, G. ; Patterson, G.W. ; Postberg, F. ; Rovira-Navarro, M. ; Rückriemen, T. ; Saur, J. ; Schmidt, B.E. ; Sotin, C. ; Spohn, T. ; Tobie, G. ; Van Hoolst, Tim ; Vance, S.D. ; Vermeersen, B.
Ice-Ocean Exchange Processes in the Jovian and Saturnian Satellites
Space Science Reviews, 216 issue 5, pp. 80 (2020). http://dx.doi.org/10.1007/s11214-020-00706-6

[89] Sorsa, Liisa-Ida ; Takala, Mika ; Bambach, Patrick ; Deller, Jakob ; Vilenius, Esa ; Agarwal, Jessica ; Carroll, Kieran A. ; Karatekin, Ozgur ; Pursiainen, Sampsa
Tomographic inversion of gravity gradient field for a synthetic Itokawa model
Icarus, 336, 113425 (2020). http://dx.doi.org/DOI:%2010.1016/j.icarus.2019.113425

[90] Steinbrügge, G. ; Dumberry, M. ; Rivoldini, A. ; Schubert, G. ; Cao, H. ; Schroeder, D. M. ; Soderlund, K. M.
Challenges on Mercury's interior structure posed by the new measurements of its obliquity and tides
Geophysical Research Letters (2020). http://dx.doi.org/10.1029/2020GL089895

[91] Talpeanu, Dana-Camelia ; Chané, Emmanuel ; Poedts, Stefaan ; D'Huys, Elke ; Mierla, Marilena ; Roussev, Ilia ; Hosteaux, Skralan
Numerical Simulations of Shear-Induced Consecutive Coronal Mass Ejections
Astronomy & Astrophysics, 637, A77, 10 pp. (2020). http://dx.doi.org/10.1051/0004-6361/202037477

[92] Taubner, Ruth-Sophie ; Olsson-Francis, Karen ; Vance, Steven D. ; Ramkissoon, Nisha K. ; Postberg, Frank ; de Vera, Jean-Pierre ; Antunes, Andre ; Camprubi Casas, Eloi ; Sekine, Yasuhito ; Noack, Lena ; Barge, Laura ; Goodman, Jason ; Jebbar, Mohamed ; Journaux, Baptiste ; Karatekin, Ozgur ; Klenner, Fabian ; Rabbow, Elke ; Rettberg, Petra ; Rackriemen-Bez, Tina ; Saur, Joachim ; Shibuya, Takazo ; Soderlund, Krista M.
Experimental and Simulation Efforts in the Astrobiological Exploration of Exooceans
Space Science Reviews, 216, Article number: 9 (2020). http://dx.doi.org/10.1007/s11214-020-0635-5

[93] Trust, O. ; Jurua, E. ; De Cat, P. ; Joshi, S.
Rotation and spots in normal A and Am/Fm stars
Monthly Notices of the Royal Astronomical Society, 492 issue 3, pp. 3143-3155 (2020). http://dx.doi.org/10.1093/mnras/stz3623

[94] Turbet, M.; Gillmann, C.; Forget, F.; Baudin, B.; Palumbo, A.; Head, J.; Karatekin, Ö.
The environmental effects of very large bolide impacts on early Mars explored with a hierarchy of numerical models
Icarus, 335, Article Id. 113419, (2020). http://dx.doi.org/10.1016/j.icarus.2019.113419

[95] Van Hoolst, T ; Baland, R-M ; Trinh, A ; Yseboodt, M ; Nimmo, F
The librations, and interior structure of Io
Journal of Geophysical Research Planets, 125, pp. e2020JE006473 (2020). http://dx.doi.org/doi.org/10.1029/2020JE006473

[96] Van Malderen, R. ; Pottiaux, E. ; Klos, A. ; Domonkos, P. ; Elias, M. ; Ning, T. ; Bock, O. ; Guijarro, J. ; Alshawaf, F. ; Hoseini, M. ; Quarello, A. ; Lebarbier, E. ; Chimani, B. ; Tornatore, V. ; Zengin Kazancı, S. ; Bogusz, J.
Homogenizing GPS Integrated Water Vapor Time Series: Benchmarking Break Detection Methods on Synthetic Data Sets
Earth and Space Science, 7 issue 5 (2020). http://dx.doi.org/10.1029/2020EA001121

[97] Velli, M. ; Harra, L. K. ; Vourlidas, A. ; Schwadron, N. ; Panasenco, O. ; Liewer, P. C. ; Müller, D. ; Zouganelis, I. ; St Cyr, O. C. ; Gilbert, H. ; Nieves-Chinchilla, T. ; Auchère, F. ; Berghmans, D. ; ManyOtherAuthors, X.
Understanding the origins of the heliosphere: integrating observations and measurements from Parker Solar Probe, Solar Orbiter, and other space- and ground-based observatories
Astronomy & Astrophysics, 642 issue A4 (2020). http://dx.doi.org/https://doi.org/10.1051/0004-6361/202038245

[98] Wang, J.T. ; Fu, J.-N. ; Zong, W.K. ; Smith, M.C. ; De Cat, P. ; Shi, J.R. ; Luo, A.L. ; Zhang, H.T. ; Frasca, A. ; Corbally, C. J. ; Molenda-Żakowicz, J. ; Catanzaro, G. ; Gray, R.O. ; Wang, J.X. ; Pan, Y.
LAMOST Observations in 15 K2 Campaigns. I. Low-resolution Spectra from LAMOST DR6
The Astrophysical Journal Supplement Series, 251 issue 2, pp. id.27, 12 pp. (2020). http://dx.doi.org/10.3847/1538-4365/abc1ed

[99] Watlet, A ; Van Camp, M ; Francis, O ; Poulain, A ; Rochez, G ; Hallet, V ; Quinif, Y ; Kaufmann, O
Gravity monitoring of underground flash flood events to study their impact on groundwater recharge and the distribution of karst voids
Water Resources Research, 56 issue 4 (2020). http://dx.doi.org/10.1029/2019WR026673

[100] West, M. J. ; Kintziger, C. ; Haberreiter, M. ; Gyo, M. ; Berghmans, D. ; Gissot, S. ; Büschel, V ; Golub, L. ; Shestov, S. ; Davies, J.
LUCI onboard Lagrange, the Next Generation of EUV Space Weather Monitoring
Journal of Space Weather and Space Climate, 10 issue 49 (2020). http://dx.doi.org/https://doi.org/10.1051/swsc/2020052

[101] Wiegert, J. ; Groenewegen, M.A.T. ; Jorissen, A. ; Decin, L. ; Danilovich, T.
How to disentangle geometry and mass-loss rate from AGB-star spectral energy distributions -- The case of EP Aqr
Astronomy & Astrophysics 642, A142 (2020). https://doi.org/10.1051/0004-6361/202038029

[102] Wijsen, Nicolas ; Samara, Evangelia ; Aran, Angels ; Lario, David ; Pomoell, Jens ; Poedts, Stefaan
A self-consistent simulation of proton acceleration and transport near a high-speedsolar wind stream
The Astrophysical Journal Letters (2020). https://doi.org/10.3847/2041-8213/abe1cb

[103] Yang, Xuan ; Yan, J.G. ; Le Maistre, Sebastien ; Dehant, Veronique ; Ye, M. ; Jin, W.T. ; Li, F.
Mars orientation parameters determination based on direct-to-Earth measurement
SCIENTIA SINICA Physica, Mechanica & Astronomica (2020). http://dx.doi.org/10.1360/SSPMA-2020-0005

[104] Zhang, P.J. ; Zucca, P. ; Wang, C.B. ; Bisi, M. M. ; Dąbrowski, B. ; Fallows, R. A. ; Krankowski, A. ; Magdalenic, J. ; Mann, G. ; Morosan, D. E. ; Vocks, C.
The Frequency Drift and Fine Structures of Solar S-bursts in the High Frequency Band of LOFAR
The Astrophysical Journal, 891, 89 (2020). https://doi.org/10.3847/1538-4357/ab7005

[105] Zhang, PJ. ; Zucca, P. ; Sridhar, S. S. ; Wang, C.B. ; Bisi, M. M. ; Dabrowski, B. ; Krankowski, A. ; Mann, G. ; Magdalenic, J. ; Morosan, D. E. ; Vocks, C.
Interferometric imaging with LOFAR remote baselines of the fine structures of a solar type-IIIb radio burst
Astronomy & Astrophysics, Volume 639, Article Number A115, 5 pp. (2020). https://doi.org/10.1051/0004-6361/202037733

[106] Zharkov, Sergei ; Matthews, Sarah ; Zharkova, Valentina ; Druett, Malcolm ; Inoue, Satoshi ; Dammasch, Ingolf E. ; Macrae, Connor
Sunquake with a second bounce, other sunquakes, and emission associated with the X9.3 flare of 6 September 2017 I. Observations
Astronomy & Astrophysics, 639 issue A78, pp. 1-19 (2020). http://dx.doi.org/10.1051/0004-6361/201936755

[107] Zong, W.K. ; Fu, J.-N. ; De Cat, P. ; Wang, J.X. ; Shi, J.R. ; Luo, A.L. ; Zhang, H.T. ; Frasca, A. ; Molenda-Żakowicz, J. ; Gray, R.O. ; Corbally, C.J. ; Catanzaro, G. ; Cang, T.Q. ; Wang, J.T. ; Chen, J.J. ; Hou, Y.H. ; Liu, J.M. ; Niu, H.B. ; Pan, Y. ; Tian, H. ; Yan, H.L. ; Zhang, Y. ; Zuo, H.
Phase II of the LAMOST-Kepler/K2 Survey. I. Time Series of Medium-resolution Spectroscopic Observations
The Astrophysical Journal Supplement Series, 251 issue 1, pp. id.15, 18 pp. (2020). http://dx.doi.org/10.3847/1538-4365/abbb2d

[108] Zouganelis, I. ; 183-co-authors, ROB-only ; Berghmans, D. ; Dolla, L. ; Gissot, S. ; Rodriguez, L. ; Verbeeck, C. ; Zhukov, A. N.

The Solar Orbiter Science Activity Plan - Translating solar and heliospheric physics questions into action
Astronomy & Astrophysics, 642, id. A3. 19 pp. (2020).
https://ui.adsabs.harvard.edu/link_gateway/2020A&A...642A...3Z/doi:10.1051/0004-6361/202038445

Non-refereed publications

[109] Asmar, S.W. ; Preston, R.A. ; Vergados, P. ; et al, including ; Dehant, V. ; Le Maistre, S.; Yseboodt, M.
Solar System Interiors, Atmospheres, and Surfaces Investigations via Radio Links: Goals for the Next Decade
White Paper for the Planetary Science and Astrobiology Decadal Survey 2023-2032, The National Academies of Sciences, Engineering, and Medicine, pp. 132 (2020).
http://surveygizmoresponseuploads.s3.amazonaws.com/fileuploads/623127/5489366/40-5d91ae36d75ec38a6563158f69d2c85b_AsmarSamiW.pdf

[110] Bergeot, N. ; Alfonsi, L. ; Cilliers, P.J. ; De Franceschi, G. ; Correia, E. ; Enell, C-F ; Engebretson, M.J. ; Häggström, I. ; Heygster, G. ; Kauristie, K. ; Kosch, M. ; Lee, C. ; Macotela, E. ; Marcucci, F. ; Miloch, W. J. ; Morton, J. ; Negusini, M. ; Pottiaux, E. ; Shreedevi, P.R. ; Prikryl, P. ; Spogli, L. ; Stephenson, J.A.E. ; Troshichev, O. ; Van Malderen, R. ; Zou, S.
Polar atmosphere and Geospace: Present knowledge, infrastructures and future research directions
SCAR White Paper (2020). https://www.scar.org/library/science-4/physical-sciences/grape-2/5539-grape-white-paper-2020/file/

[111] Clette, Frédéric ; Vaquero, José M. ; Cruz Gallego, María ; Lefèvre, Laure
Sunspot and Group Number: Recent advances from historical data
Proceedings of the IAU, 14 issue Symposium A30, pp. 156-159 (2020).
http://dx.doi.org/10.1017/S174392131900396X

[112] Debehogne, H. ; Elst, E. ; De Cat, P. ; Pauwels, T.
Minor Planet Observations [012 Uccle]
Minor Planet Circulars (2020).

[113] Dehant, V. ; Triana, S.A. ; Rekier, J. ; Trinh, A. ; Zhu, P. ; Laguerre, R. ; Houliez, A. ; Van Hoolst, T.
Progress in understanding nutations
Proc. Journées Systèmes de Référence Spatio-Temporels 2019, on 'Astrometry, Earth Rotation, and Reference Systems in the GAIA era', Paris, France, JSR2019, pp. 1-4 (2020).
https://syrte.obspm.fr/astro/journees2019/FILES/dehant.pdf

[114] Garcia, R.F. ; Murdoch, N. ; Dehant, V. ; Bernauer, F. ; Schmelzbach, C. ; Igel, H. ; Guattari, F. ; Mimoun, D. ; Lecamp, G. ; Deraucourt, S.
Vibrations and Rotations of Asteroids: Planetary Flyby as an Opportunity for Internal Structure Imaging with 6 Degrees of Freedom Instruments
Proc. Apophis T–9 Years 2020, LPI Contrib., 2242, pp. 2242 (2020).
https://www.hou.usra.edu/meetings/apophis2020/pdf/2017.pdf

[115] Gelenbe, E. ; Brasseur, G. ; Chefneux, L. ; Dehant, V. ; Halloin, V. ; Haton, J.-P. ; Judkiewicz, M. ; Rentier, B. ; Weikmans, R.
Du partage de la connaissance et de la promotion d'une « science ouverte » – Réflexions sur la diffusion des connaissances à travers les grands colloques internationaux, les revues scientifiques, et la communication libre et rapide entre chercheurs et innovateurs dans un contexte de réduction de l'empreinte climatique
Rapports Opinio de l'Académie royale de Belgique, pp. 1-48 (2020).
https://www.academieroyale.be/Academie/documents/Opinio2versionnumerique30529.pdf

[116] Gloesener, E. ; Temel, O. ; Karatekin, Ö. ; Joiret, S. ; Dehant, V.
Destabilization of methane clathrate hydrate by meteorite impacts on present-day Mars
EPSC 2020 Proceedings, 14, pp. EPSC2020-843 (2020).
https://meetingorganizer.copernicus.org/EPSC2020/EPSC2020-843.html

[117] Irrgang, A. ; De Cat, P. ; Pigulski, A. ; Handler, G. ; Tkachenko, A.
The slowly pulsating B-star 18 Peg: A testbed for upper main sequence stellar evolution
Proceedings of the International Conference on Stars and their Variability Observed from Space, pp. 275-280 (2020). https://ui.adsabs.harvard.edu/abs/2020svos.conf..275I/abstract

[118] Jorissen, Alain ; Waelkens, Christoffel ; Groenewegen, Martin ; Decin, Leen ; Escorza, Anna ; Goriely, Stephane ; Rajeev, Manick ; Nicolaes, Dries ; Shetye, Shreeya ; Siess, Lionel ; Van de Steene, Griet ; Van Eck, Sophie ; Van Winckel, Hans
STARLAB Evolved stars and their shells: Laboratories for stellar physics. Final Report
BELSPO (2020). https://www.belspo.be/belspo/brain-be/projects/FinalReports/STARLAB_FinRep_AD.pdf

[119] Kobzar, O. ; Khalack, V. ; Bohlender, D. ; David-Uraz, A. ; Kashko, P. ; Bowman, D.~M. ; Lovekin, C. ; Tvardovskyi, D. ; Perron-Cormier, M. ; Paunzen, E. ; Sikora, J. ; Lampens, P. ; Richard, O.
Study of Slowly Rotating CP Stars Observed with TESS
Proceedings of the Workshop on Stellar Magnetism: A Workshop in Honour of the Career and Contributions of John D. Landstreet, 11 issue nov, pp. 214-218 (2020).
https://ui.adsabs.harvard.edu/abs/2020pase.conf..214K

[120] Lampens, P.
Nouvelles détections d'étoiles doubles et multiples grâce aux missions spatiales explorant les systèmes planétaires. New detections of double and multiple stars thanks to space missions exploring planetary systems
Etoiles Doubles, 1, pp. 2-3 (2020). https://ui.adsabs.harvard.edu/abs/2020ED......1....2L

[121] Lampens, P. ; Vermeylen, L. ; De Cat, P. ; Sodor, A. ; Bognar, Zs. ; Frémat, Y. ; Skarka, M. ; Lehmann, H. ; Samadi, A. ; Fox-Machado, L. ; Joshi, S.
The spectroscopic multiplicity fraction in a sample of A/F-type (candidate) hybrid stars from the Kepler mission
Proceedings of the International Conference on Stars and their Variability Observed from Space, pp. 353-354 (2020). https://ui.adsabs.harvard.edu/abs/2020svos.conf..353L

[122] Lamy, H. ; Anciaux, M. ; Ranvier, S. ; Martínez Picar, A. ; Calders, S. ; Calegaro, A. ; Verbeeck, C.
Calibration of the BRAMS interferometer
Proceedings of the International Meteor Conference 2019, Bollmansruh, Germany, October 3-6, pp. 33-38 (2020).

[123] Lapenta, Giovanni ; Zhukov, Andrei ; van Driel-Gesztelyi, Lidia
Editorial: Solar Wind at the Dawn of the Parker Solar Probe and Solar Orbiter Era
Solar Physics, 295, pp. 103 (2020). http://dx.doi.org/10.1007/s11207-020-01670-8

[124] Laverick M., Lobel A., Royer P., Merle T., Martayan C., van Hoof P., Van der Swaelmen M., Da-vid M., Hensberge H., and Thienpont E.
The Belgian Repository of fundamental Atomic data and Stellar Spectra (BRASS)
in Laboratory Astrophysics: From Observations to Interpretation, held 14-19 April 2019 in Cam-bridge, UK. Edited by F. Salama and H. Linnartz. Proceedings of the International Astronomical Union, 350, 386 (2020). https://doi.org/10.1017/S1743921320000046

[125] Mkrtichian, D. ; Gunsriwiwat, K. ; Engelbrecht, C. ; A-thano, N. ; Lehmann, H. ; Lampens, P. ; Matthews, J. ; Rodriguez, E. ; Kusakin, A.
The pulsation spectrum of a mass-accreting component of AS Eri
Proceedings of the International Conference on Stars and their Variability Observed from Space, pp. 113-114 (2020). https://ui.adsabs.harvard.edu/abs/2020svos.conf..113M

[126] Monier, R. ; Lampens, P.
Rotational Variability in the TESS Light Curve of 21 Com

Research Notes of the American Astronomical Society, 4 issue 7, pp. 121 (2020). http://dx.doi.org/10.3847/2515-5172/abaa41

[127] Rekier, J. ; Triana, S.A. ; Dehant, V.
Planetary inertial modes and their relation to nutations
EPSC 2020 Proceedings, 14, pp. EPSC2020-853 (2020). http://dx.doi.org/10.5194/epsc2020-853

[128] Ruiz Lozano, L. ; Karatekin, Ö. ; Caldiero, A. ; Imbreckx, A.C. ; Temel, O. ; Dehant, V. ; Daerden, F. ; Thomas, I.R. ; Ristic, B. ; Patel, M.R. ; Bellucci, G. ; Lopez-Moreno, J.J. ; Vandaele, A.C.
Use of TGO-NOMAD nadir observations for ices detection
EPSC 2020 Proceedings, 14, pp. EPSC2020-748 (2020). http://dx.doi.org/10.5194/epsc2020-748

[129] Shestov, Sergei V ; Bourgoignie, Bram ; Nicula, Bogdan ; Dolla, Laurent ; Jean, Christophe ; Verstringe, Freek ; Katsiyannis, Athanassios C ; Inhester, Bernd ; Dalmiro, Maia ; Ribeiro, Bruno Miguel Freitas ; Zhukov, Andrei N
Scientific processing pipeline for ASPIICS coronagraph
Proceedings SPIE: Space Telescopes and Instrumentation 2020: Optical, Infrared, and Millimeter Wave, 4 issue 1, pp. 264-279 (2020). http://dx.doi.org/10.1117/12.2560164

[130] Smerkar, S. ; Andrews-Hanna, J. ; Breuer, D. ; et al, including ; Dehant, V.
Geodynamics, Habitability, and the Case for Venus
White Paper for the Planetary Science and Astrobiology Decadal Survey 2023-2032, The National Academies of Sciences, Engineering, and Medicine, pp. 186 (2020).
http://surveygizmoresponseuploads.s3.amazonaws.com/fileuploads/623127/5489366/154-9d3f6ba14e5bf5fb80186587132527ae_SmrekarSuzanneE.pdf

[131] Trust, O. ; Jurua, E. ; De Cat, P. ; Joshi, S.
Starspots and rotation velocities of normal A- and Am- stars
Proceedings of the International Conference on Stars and their Variability Observed from Space, pp. 353-354 (2020), pp. 433-434 (2020). https://ui.adsabs.harvard.edu/abs/2020svos.conf..433T/abstract

[132] Van Camp, Michel ; Van Noten, Koen ; Lecocq, Thomas ; Vanneste, Kris
[NL] Opvolging van seismiciteit in de context van toepassingen in de diepe ondergrond van Vlaanderen [EN] Monitoring seismicity in the context of applications in the deep subsurface of Flanders
Expertise report ROB-VPO 2020-01, pp. 83 (2020). https://archief-algemeen.omgeving.vlaanderen.be/xmlui/handle/acd/261302?show=full

[133] van Hoof, P. A. M. ; Van de Steene, G. C. ; Guzmán, F. ; Dehghanian, M. ; Chatzikos, M. ; Ferland, G. J.
Current and future development of the photoionization code Cloudy
Contributions of the Astronomical Observatory Skalnaté Pleso, 50 issue 1, pp. 32-43 (2020).
http://dx.doi.org/10.31577/caosp.2020.50.1.3

[134] Vanneste, Kris ; Camelbeeck, Thierry
Probabilistic Seismic Hazard Assessment for the Fluxys methane terminal in Zeebrugge
Expertise report, pp. 83 (2020).

[135] Van Noten, Koen ; Burlet, Christian ; Lecocq, Thomas ; Delaby, Serge ; Verheyden, Sophie ; Triantafyllou, Antoine
Résumé de trois missions géophysiques dans la Salle de la Structure et perspectives pour réaliser une étude de géologie structurale de Bruniquel
Rapport Intermédiaire 2020 d'opération archéologique programmée Triennale 2018-20. SRA Occitanie., pp. 117-120 (2020).

[136] Verbeeck, C. ; Lamy, H. ; Calders, S. ; Martínez Picar, A. ; Calegaro, A.
BRAMS forward scatter observations of major meteor showers in 2016–2019

Proceedings of the International Meteor Conference 2019, Bollmansruh, Germany, October 3-6, pp. 27-31 (2020).

[137] Verbeeck, C. ; Lamy, H. ; Calders, S. ; Martínez Picar, A. ; Calegaro, A. ; Anciaux, M.
Year-to-year comparison of BRAMS forward scatter observations of selected meteor showers
WGN, 48 issue 5, pp. 142-145 (2020).

Other publications

[138] Bruyninx, C. ; Brockmann, E. ; Kenyeres, A. ; Legrand, J. ; Liwosz, T. ; Pacione, R. ; Söhne, W. ; Völksen, C
EUREF Permanent Network Technical Report 2019
In Villiger, Arturo; Dach, Rolf (2020). International GNSS Service: Technical Report 2019 IGS Central Bureau and University of Bern Open Publishing (2020). https://boris.unibe.ch/144003/

[139] Bruyninx, C. ; Legrand, J. ; Aerts, W.
GPS, Data Acquisition and Analysis
In: Gupta H. (eds) Encyclopedia of Solid Earth Geophysics. Encyclopedia of Earth Sciences Series. Springer, Cham. https://doi.org/10.1007/978-3-030-10475-7_137-1 (2020).

[140] De Meyer, Cédric
Theoretical model for the analysis of induced seismicity at geothermal projects in the Campine Basin (Belgium)
Bachelor thesis supervised by Sintubin, Manuel (KULeuven); Van Noten, Koen (ROB); Van Baelen, Hervé (NIRAS) (KU Leuven)

[141] Jones, Jonathan ; Guerova, Guergana ; Douša, Jan ; Dick, Galina ; de Haan, Siebren ; Pottiaux, Eric ; Bock, Olivier ; Pacione, Rosa ; van Malderen, Roeland
Advanced Global Navigation Satellite Systems Tropospheric Products for Monitoring Severe Weather Events and Climate : COST Action ES1206 Final Action Dissemination Report
Springer Nature Switzerland AG 2020, Edition Number 1, 563 pp., eBook ISBN 978-3-030-13901-8 (2020). https://doi.org/10.1007/978-3-030-13901-8

[142] Pauwels, T., Bruyninx, C. and Roosbeek, F.
Annuaire de l'Observatoire royal de Belgique – Jaarboek van de Koninklijke Sterrenwacht van België 2021
Fedopress, ISSN-0373-4900 (2020).
https://www.astro.oma.be/common/pdf/ybook/yearbook_2021.pdf

[143] Pottiaux, Eric ; Berckmans, Julie ; de Haan, Siebren ; Bruyninx, Carine
A GNSS-Based Nowcasting Toolbox for Severe Weather in Belgium
In Jones et al., *Advanced Global Navigation Satellite Systems Tropospheric Products for Monitoring Severe Weather Events and Climate : COST Action ES1206 Final Action Dissemination Report*, Springer Nature Switzerland AG 2020, Edition Number 1, 563 pp., eBook ISBN 978-3-030-13901-8 (2020). https://doi.org/10.1007/978-3-030-13901-8

[144] Scolini, Camilla
Magnetised Coronal Mass Ejections: evolution from the Sun to 1 AU and geo-effectiveness
PhD thesis supervised by Poedts, Stefaan; Rodriguez, Luciano (KU Leuven - ROB) (2020).
https://lirias.kuleuven.be/3021444?limo=0

Annex 2: Workforce

Staff statistics

On 31 December 2020, 173 employees are working in ORB-KSB (including people working at the Planetarium). The staff includes two more employees than last year (171 employees on 31 December 2019).

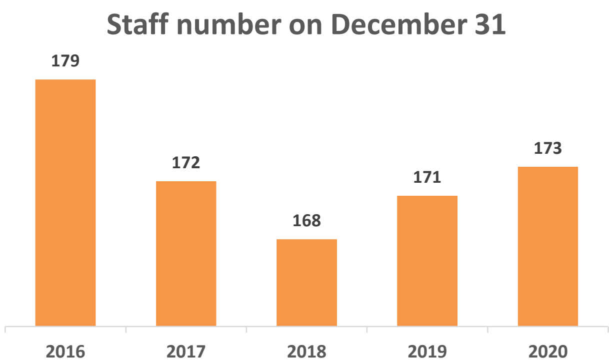

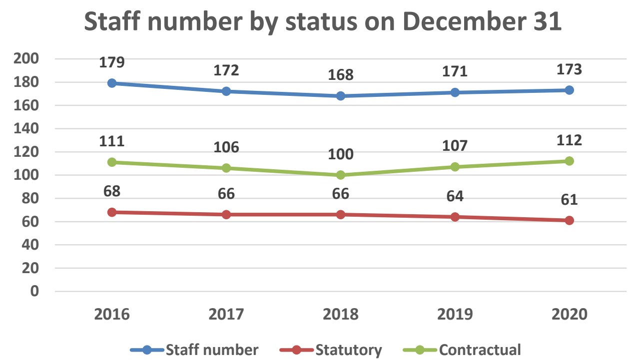

As expected from a research institute, scientists constitute the main part of the personnel (96 agents, or 55% of the staff). This highlights the importance of scientific knowledge and expertise at ORB-KSB.

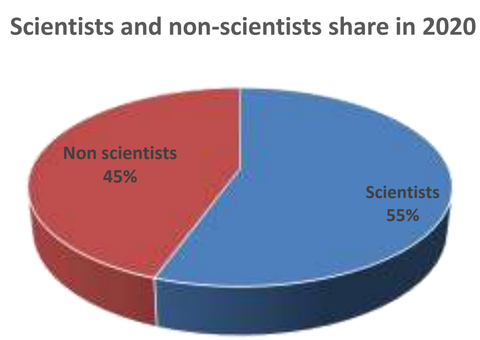

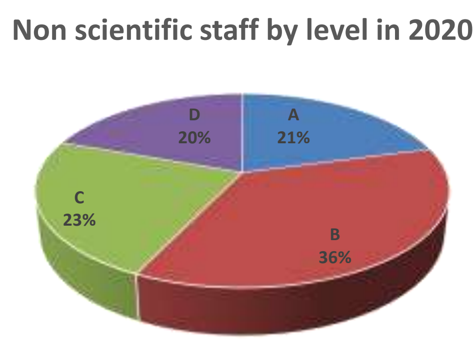

The majority of the staff (65%) are contractual agents. This is particularly true for scientists, in whom 75% are contractual. This is related to the fact that scientific research is more and more funded by external projects while the federal dotation is shrinking. The proportion of contractual to statutory is even higher for employees of level D (93% of them are contractual). Only agents of level B are in the vast majority statutory (82% of level B agents).

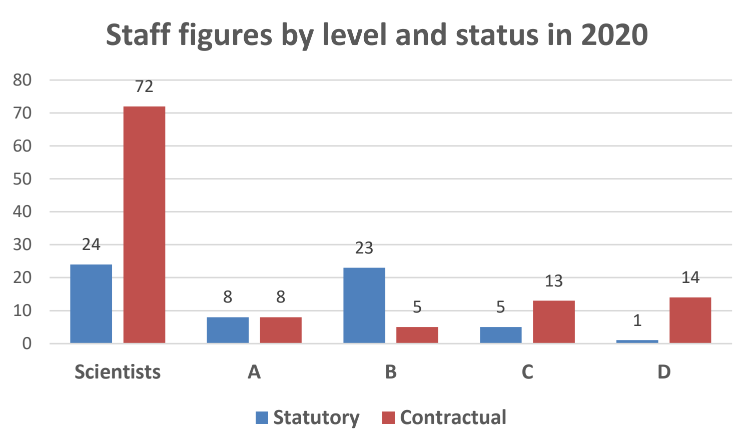

39% of the agents are women (67 women and 106 men), which a bit higher than in 2019. Among statutory agents, the proportion is lower as only 31% of them are women. Actually, 72% of the female employees are contractual, compared to 60% of the male employees. At the scientists' level, the women proportion is slightly lower than the women proportion for the whole staff (with 35% of scientists being women).

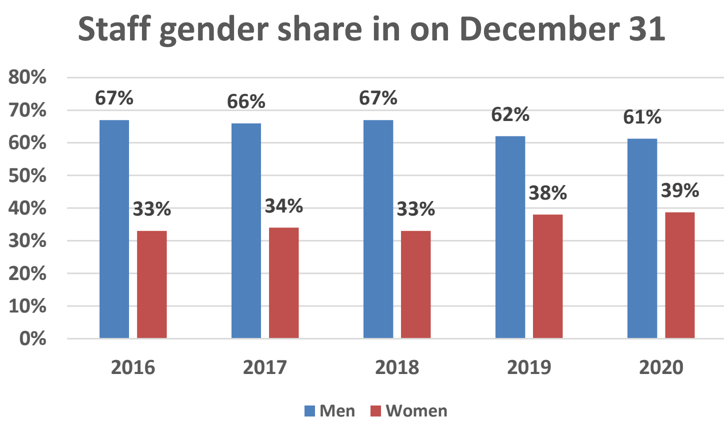

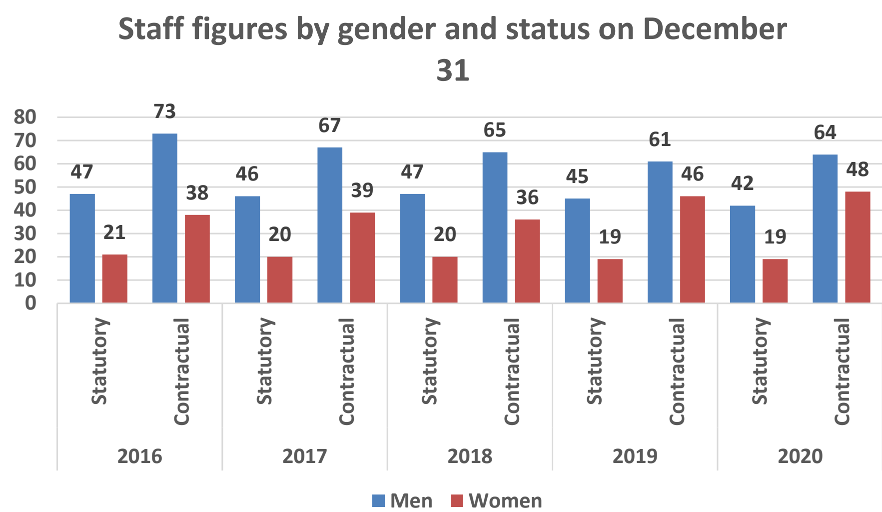

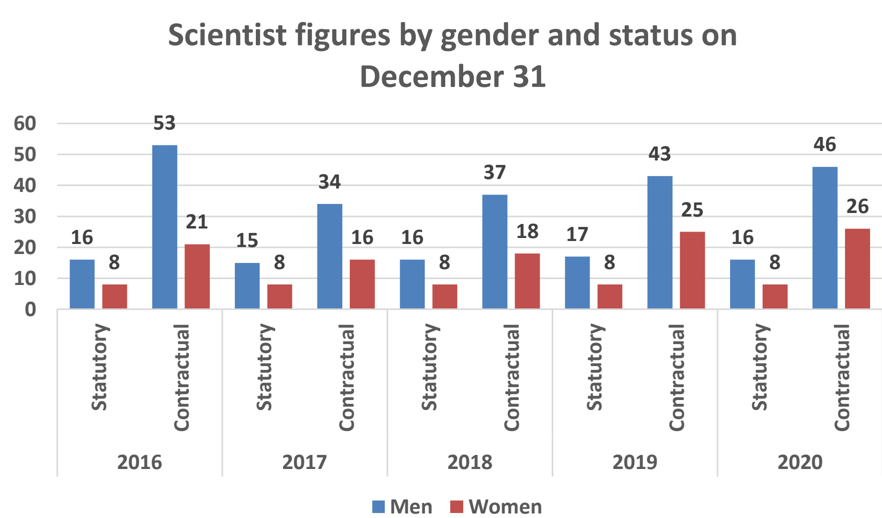

De activiteiten beschreven in dit verslag werden ondersteund door

Les activités décrites dans ce rapport ont été soutenues par

The activities described in this report were supported by

De POD Wetenschapsbeleid
Le SPP Politique Scientifique
The Belgian Science Policy

De Nationale Loterij
La Loterie Nationale
The National Lottery

Het Europees Ruimtevaartagentschap
L'Agence Spatiale Européenne
The European Space Agency

De Europese Gemeenschap
La Communauté Européenne
The European Community

Het Fonds voor Wetenschappelijk Onderzoek – Vlaanderen

Le Fonds de la Recherche Scientifique